

ROTARY ENGINE

by
Kenichi Yamamoto



621.434
Y19
C.2

Published
by
TOYO KOGYO CO., LTD.

ROTARY ENGINE

by
Kenichi Yamamoto

Published
by
TOYO KOGYO CO., LTD.

CONTENTS

1. The concept of the rotary engine	1
1. 1 History of the development of rotary piston engines	1
1. 2 Trochoid	6
1. 2. 1 Peritrochoid	6
1. 2. 2 Epitrochoid	6
1. 2. 3 Hypotrochoid	7
1. 3 Trochoid envelopes and their possible combinations	7
1. 4 The basic structure of a planetary engine and its operation	10
1. 5 Structure and operation of single rotation engines	15
1. 6 Features of the planetary rotation engine	17
2. Basic dimensions	20
2. 1 Geometric analysis of basic dimensions	20
2. 1. 1 Equation of a peritrochoid	20
2. 1. 2 Inner envelope of the peritrochoid	21
2. 1. 3 Leaning angle and the trochoid constant	22
2. 1. 4 Circumferential velocity of the rotor apex	24
2. 2 Volumetric change and working volume of the working chamber ..	24
2. 2. 1 Volumetric change of the working chamber	24
2. 2. 2 Volume of the working chamber	25
2. 3 Basic dimensions and theoretical compression ratio	27
2. 4 Basic dimensions and fundamental construction of the rotary engine	28
2. 4. 1 Basic dimensions and intake and exhaust ports	28
2. 4. 2 Basic dimensions and the construction of the engine output shaft system	29
2. 5 Practical examples of basic dimensions	31

3.	Basic structure	32
3.1	Intake and exhaust systems	32
3.1.1	Intake and exhaust port layout	32
3.1.2	Port timing	35
3.1.3	Examples of intake and exhaust port construction	37
3.2	Housings	39
3.2.1	Essentials of rotor housing design	40
3.2.2	Rotor housing materials	41
3.2.3	Wear resistant treatment of the trochoid surface	42
3.2.4	Wear resistant treatment of the side housing	43
3.3	Rotor	45
3.3.1	Function and structure	45
3.3.2	Rotor materials	47
3.4	Design of the phasing gear	47
3.5	Tooth load	48
3.6	Eccentric shaft and bearing	50
4.	Gas seal	52
4.1	Principal construction	52
4.2	Apex seal	54
4.3	Side seal, corner seal	57
4.4	Notes on designing gas seals	58
4.5	Gas seal and sliding surface materials	60
5.	Cooling	63
5.1	Cooling of housings	63
5.1.1	Methods of cooling housings	63
5.1.2	Housing temperature	65
5.2	Rotor cooling	68

6. Lubrication	70
6. 1 Lubrication methods	70
6. 2 Lubrication system for automobile engine	71
6. 3 Oil seal	76
6. 4 Blow-by gas recirculating system	79
7. Engine vibration	80
7. 1 Engine balance	80
7. 2 Fluctuation of torque	83
8. Ignition system	88
8. 1 Spark plug	88
8. 2 Two-spark plug arrangement and ignition system	89
8. 3 Trend of future ignition system	90
9. Engine performance . combustion	92
9. 1 Power generated by engine	92
9. 2 Engine performance	93
9. 3 Heat balance	98
9. 4 Combustion	99
10. Multi-rotor engines	107
10. 1 Significance of multi-rotor engines	107
10. 2 Operation of multi-rotor engines	108
10. 3 Performance possibility of multi-rotor engines	110
10. 4 Examples of multi-rotor engine construction	112
11. Manufacturing methods	115
11. 1 Machining the trochoidal curve	115

11. 2	Inspection of trochoid	118
11. 3	Machining of inner envelope	119
12.	Examples of rotary engine applications	121
12. 1	Multi-purpose engine	121
12. 2	Automotive engines	125
12. 3	Marine engine	133
12. 4	Aircraft engine	136
13.	Exhaust emission of rotary engines	137
13. 1	Factors affecting emissions	137
13. 2	Secondary air injection system	143

Preface

Only about 20 years have passed since Felix Wankel devised the principle of the Wankel engine, which consists of two-lobe epitrochoid with inner envelope.

Since then, the basic construction has been improved from the DKM to the KKM type, with steady development continuing in the area of mechanical design, such as engine specifications, dimensions and component constructions, as well as in other areas such as materials and manufacturing techniques. Today, Wankel engines are being put to practical use by two companies in Japan and three in Germany.

Historically, the development of prime movers, including the reciprocating engine, has proved to be an extremely difficult task, requiring a great deal of research and experimental work, due to the fact that development of this sort involves a multitude of highly complex, interrelated problems. On top of this, the necessary refinements are extremely time-consuming since they are based on careful observation and evaluation of the various phenomena and test data observed and gathered during actual testing, processes which often involve tedious trial and error methods.

We can see, then, that the present NSU-Wankel engine was put into practical use with a comparatively small amount of research and, at the same time, within a relatively short period of time. It gives every indication of harboring tremendous potential for development and growth. In fact, rotary engines are so attractive, as potential prime moving mechanisms in the next generation, that engineers the world over had been busily putting forth all sorts of ideas as to their possible application. On the other hand, it is also a fact that none of them had materialized because of a variety of technical problems. This fact in itself should be sufficient indication of the technological difficulties encountered in the development of rotary engines. As things stand today, the NSU-Wankel is the only rotary engine in successful practical use, and as such is now being studied on a worldwide basis. The author feels that the material presented here on the rotary engine should prove of great interest to the students and general public who are concerned with the engineering of internal combustion engines.

This book is entitled "Rotary Engine", however, its scope is limited to the description of the NSU-Wankel engine developed jointly with NSU, based on Felix Wankel's invention.

I should like to stress again that this engine is still in the development stage, so the data presented here are illustrative of concepts and ideas. It would be the author's pleasure if this book could be of any help to the readers in better understanding the NSU-Wankel engine. The entire contents of this book were written in close and intensive cooperation with the following people working in the engineer-

ing, research, design, testing and material sections of the Rotary Engine Research Division of Toyo Kogyo Co., Ltd. The author would like to express his sincerest appreciation to all of them.

- | | |
|--|------------------------------------|
| 1. The Concept of Rotary Engines | Kazuhiko Moriyama |
| 2. Basic Dimensions | Yasuo Tatsutomi |
| 3. Basic Construction | Yasuto Terazawa
Hiroshi Ohzeki |
| 4. Gas Sealing | Yutaka Hirose |
| 5. Cooling | Kazuo Maekawa |
| 6. Lubrication | Kaneaki Takagi |
| 7. Engine Vibration | Yasuyuki Morita |
| 8. Ignition System | Masao Shibagaki |
| 9. Engine Performance and Combustion | Nagao Takeuchi
Masaharu Shimoji |
| 10. Multi-rotor Engine | Kazuhiko Moriyama |
| 11. Manufacturing Method | Yoshihiko Nakamura |
| 12. Applied Examples of Rotary Engines | Kazuhiko Moriyama |
| 13. Exhaust Emission of Rotary Engine | Takumi Muroki |

October 1971

Kenichi Yamamoto

1. THE CONCEPT OF THE ROTARY ENGINE

1.1 History of the Development of Rotary Piston Engines

Rotary engines, which have attracted great attention since the appearance of the NSU–Wankel engine, have a long history. The original idea is said to have come from the rotary piston type water pump which dates back to the 16th century.

Since that time, it has been generally agreed that the simple function of a rotary piston gives it a definite advantage over the combined mechanism of a reciprocating piston and a crank. Because of the simplicity, various types of rotary engines have been proposed. As a matter of fact, the rotary mechanism has long been in practical use in the field of volumetric type piston machines such as pumps, blowers and compressors, which are in a reverse relationship to the internal combustion engine. However, in internal combustion engines, the only rotary piston mechanism to become practical so far is the NSU–Wankel engine.

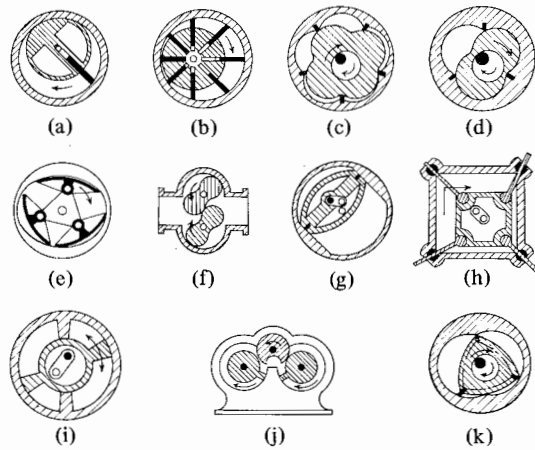


Fig. 1.1 Various concepts of rotary piston mechanism

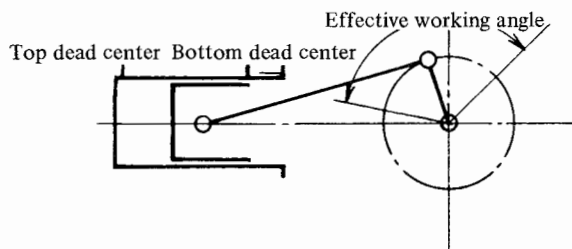


Fig. 1.2 Principle of the reciprocating engine

Among the greatest obstacles encountered in creating the rotary engine, compared to the reciprocating engine, were :

- (i) Difficulty in assuring seal tightness of the working chamber under high pressure.
- (ii) Incomplete establishment of optimum intake and exhaust systems satisfactorily matching the thermodynamic operating cycle of gas.

Felix Wankel had long been interested in rotary engines of all kinds, including those used in compressors and pumps. He began to conduct investigations to sort out the known types, and to lay them out systematically.

He went into technical cooperation with NSU* and in early 1954 he presented his ideas on a rotary engine, which were accepted as having good possibilities. This actually marks the beginning of the joint research program of NSU and Wankel.

This new rotary engine can be classified into the following two types, by the characteristics of the piston (rotor) motion :

- (i) Single rotation machines (Drahtkolbenmaschinen : DKM)
- (ii) Planetary rotation machines (Kreiskolbenmaschinen : KKM)

With both types, the contour of the inner surface of the outer casing is composed of a peritrochoid. Inside this casing is an internal piston, the apex of which always slides along the peritrochoid. The operating principle is that the relative rotation of the internal piston against the casing causes the space between the walls of the two to change continuously.

In the early stage of the NSU-Wankel research effort, the single rotation type was the first studied. Preliminary investigation was conducted on a compressor application and the feasibility of volume change of the working chamber was confirmed, with the type in which the outer casing and the internal piston rotate in the same direction around their respective axes.

* NSU and AUTO UNION were united as AUDI NSU AUTO UNION in Aug., 1968.

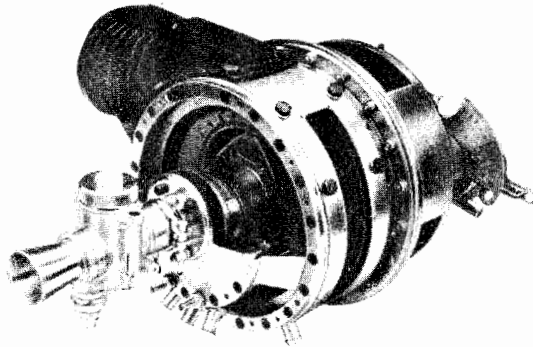


Fig. 1.3 Model DKM engine

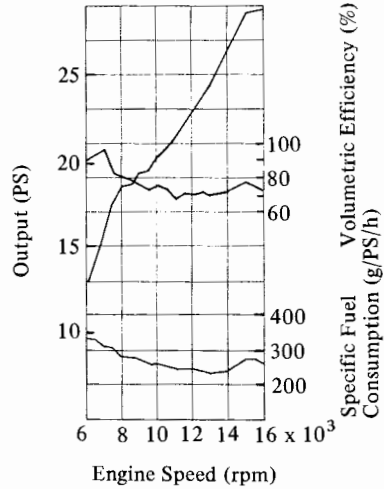


Fig. 1.4 Performance characteristics of the Model DKM 54 engine

In 1957, after further development of this compressor version, a prototype of the rotating piston type engine was successfully tested. This was called the DKM 54 type, and it had a volume of 125cc for each of the three working chambers. Although the test result (Fig. 1.4) was encouraging, this type was so complex in structural design that substantial changes in its construction became inevitable before it got beyond the early experimental stage.

In 1958, the basic engine construction was changed to the planetary rotation type, and a series of prototype manufacturing and testing projects were started on the Model KKM 125 engines with 125cc displacement per working chamber and the Model KKM 250 with 250cc displacement.

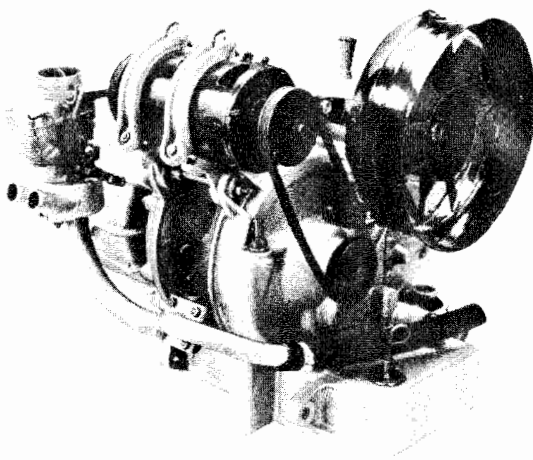


Fig. 1.5 Model KKM 250 engine

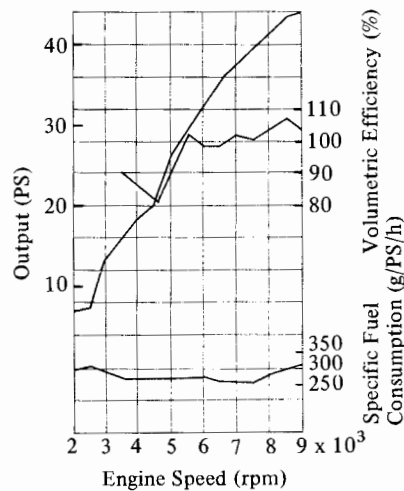


Fig. 1.6 Performance characteristics of the Model KKM 250 engine

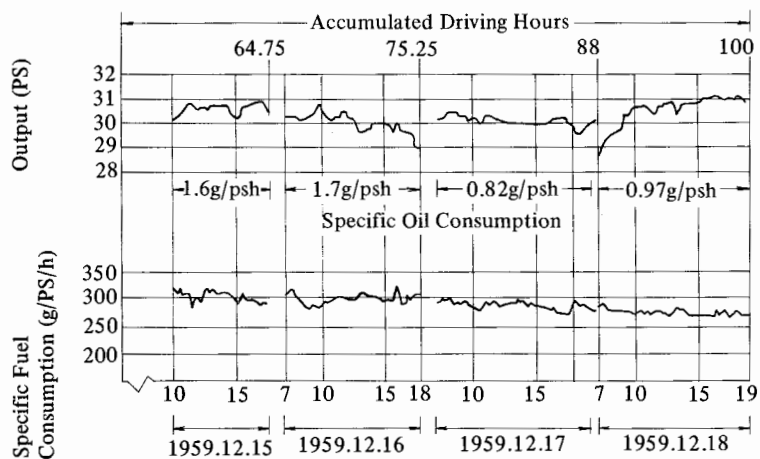


Fig. 1. 7 Model KKM 250 durability test (Full load : 5500 rpm)

The tests confirmed that this planetary rotation type engine had no critical defect as an internal combustion engine.

This planetary rotation type engine is a dynamically reverse version of the single rotation type, in that the center of gravity of the internal piston rotates as it revolves around the center of the output shaft, while the outer casing remains stationary.

Since this change in engine type, further development has resulted in a considerable simplification of the engine construction and improvement in reliability. In fact, it may be said that the basis for the NSU–Wankel engine was established by the decision to change to the planetary rotation type construction.

Since that time, technical agreements have been made one after another for the commercialization of this type of rotary engine, and extensive development projects are now emerging for gasoline, diesel and hybrid engines, according to the plans set by the companies under license.

Table 1. 1 License Agreements on the NSU-Wankel Engine

As of April, 1971

Company	Date	Country	Item
1) Curtiss-Wright Corp.	Oct. 1958	U. S. A.	All types of Engine
2) Fichtel & Sachs AG.	Dec. 1960	West Germany	Gasoline Engine
3) Yanmar Diesel Co., Ltd.	Feb. 1961	Japan	Gasoline Engine Diesel Engine
4) Toyo Kogyo Co., Ltd.	Feb. 1961	Japan	Gasoline Engine
5) Klöckner-Humboldt-Deutz AG.	Oct. 1961	West Germany	Diesel Engine
6) Daimler-Benz AG.	Oct. 1961	West Germany	Gasoline Engine Diesel Engine
7) MAN (Maschinenfabrik Augsburg Nürnberg AG.)	Oct. 1961	West Germany	Diesel Engine
8) Friedrich Krupp GmbH	Nov. 1961	West Germany	Diesel Engine
9) Alfa Romeo S.p.A.	Apr. 1964	Italy	Gasoline Engine
10) Rolls-Royce Limited of Derby	Feb. 1965	England	Multi-fuel Engine Diesel Engine
11) Dr. Ing. h.c.F. Porsche KG.	Mar. 1965	West Germany	Gasoline Engine
12) Outboard Marine Corp.	Mar. 1966	U.S.A.	Gasoline Engine
13) Comotor S.A.	May 1967	Luxembourg	Gasoline Engine Multi-fuel Engine
14) Johannes Graupner	Sep. 1967	West Germany	Gasoline Engine
15) Savkel Ltd.	Aug. 1969	Israel	Gasoline Engine
16) Nissan Motor Co., Ltd.	Oct. 1970	Japan	Gasoline Engine
17) General Motors Corp.	Nov. 1970	U.S.A.	All types of Engine
18) Suzuki Motor Co., Ltd.	Nov. 1970	Japan	Gasoline Engine

Especially notable are the projects for applying these concepts to automotive engines and to small multi-purpose engines. These projects have progressed at a speed that can be considered nothing less than revolutionary in the history of internal combustion engines. This is why the future of the rotary engine has attracted so much interest.

1.2 Trochoid

When using the so-called trochoidal curves for the configuration of the inner surface of the outer casing and for the internal piston, one of the following three curves is used, drawn with the transfer ratio $i=rg/r$ as a rational number. They are the peritrochoid of Fig. 1. 8, the epitrochoid of Fig. 1. 9 and the hypotrochoid of Fig. 1. 10. Note that the transcendental circumferential curves drawn with the transfer ratio of an irrational number, and the intersecting circumferential curves drawn when the choice of the condition $r' \leq r$ is improper. Both of them will produce circumferential curves not suitable for the purpose of the rotary piston machines, consequently they are not applicable.

1. 2. 1 Peritrochoid

When the revolving circle D_r (radius r) rotates around the outer circumference of a fixed base circle D_g (radius rg), the peritrochoid is defined as the locus of the generating point P_1 (the generating radius R) on the extension line of the rolling circle's radius. The essential conditions for this case are :

$$rg < r ; i = rg/r < 1 ; R > r \quad (1. 1)$$

Fig. 1. 8 shows the generation of the two-lobe peritrochoid when $i = 2 : 3$, which is used for the inner surface contour of the outer casing of the NSU-Wankel planetary rotation type engine.

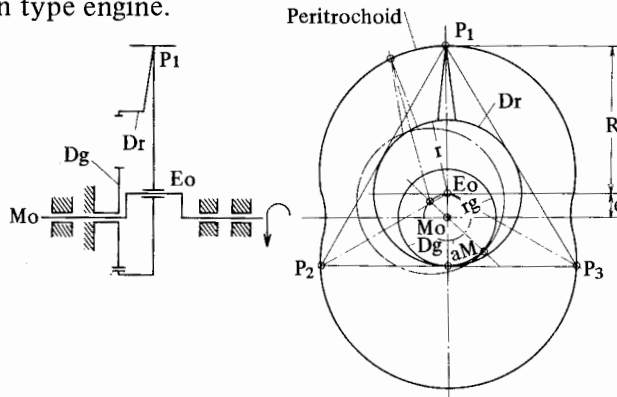


Fig. 1. 8 Generation of the two-lobe peritrochoid

1. 2. 2 Epitrochoid

When the revolving circle D_r (radius r) rotates around the fixed base circle D_g (radius rg), the peripheral curve, drawn by the generating point P on the revolving circle radius, is called the epitrochoid. General conditions are :

$$rg \geq r ; i = rg/r \geq 1 \quad (1. 2)$$

When $rg > r$; $r' < r$; $rg/r = 2 : 1$, the obtained epitrochoid is substantially the same as a two-lobe peritrochoid.

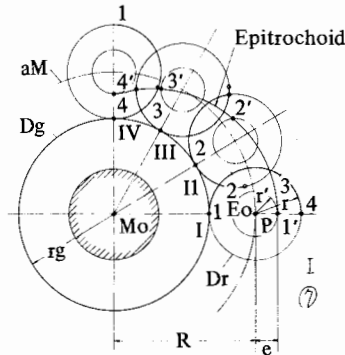


Fig. 1. 9 Generation of the two-lobe epitrochoid

1. 2. 3. Hypotrochoid

Fig. 1. 10 shows an example of a three-flank hypotrochoid when $i = 3 : 2$.

When the revolving circle Dr (radius r) rotates while in contact with the inner surface of a fixed base circle Dg (radius rg), the hypotrochoid is defined as the locus curve of a generating point P (generation radius R). The conditions for this case are :

$$rg > r ; i = rg/r \geq 1 ; R > r \quad (1. 3)$$

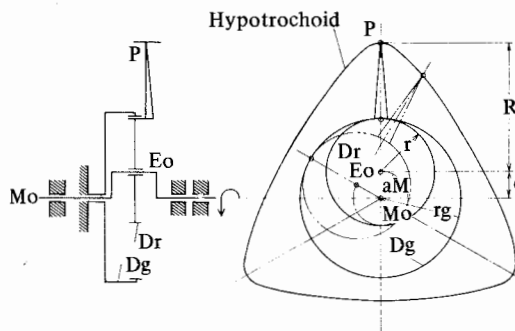


Fig. 1. 10 Generation of the three-flank hypotrochoid

1. 3 Trochoid Envelopes and their Possible Combinations

When using trochoidal curves for the basic contour of rotary piston machines, the following two types may be employed :

- (i) The combination of trochoid and its inner envelope

When the trochoid is used for the inner surface of the outer casing, the internal piston takes the shape of the trochoid inner envelope.

(ii) The combination of trochoid and its outer envelope

When the internal piston forms the trochoid, the trochoid outer envelope is employed for the inner surface of the outer casing.

The NSU-Wankel engine, which makes use of the three-flank inner envelope for the internal piston while using the two-lobe peritrochoid for the inner surface of the casing, is typically representative of the first case.

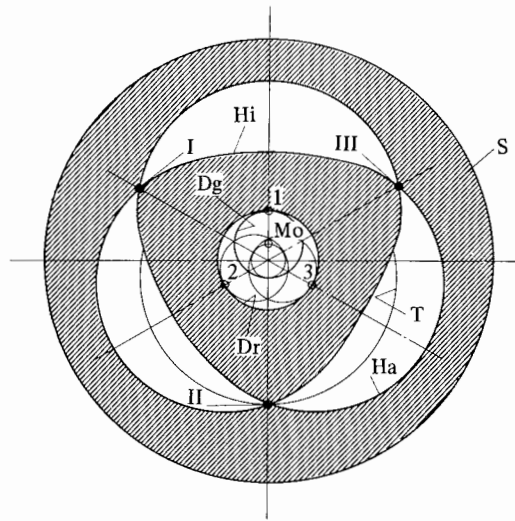


Fig. 1. 11 Inner and outer envelopes of the two-lobe peritrochoid

Fig. 1. 11 shows an example of a two-lobe peritrochoid envelope when $i = Dg/Dr = 2 : 3$. In this case, the peritrochoid T can be considered a locus of thin band form, and at its center Mo the base circle Dg is located.

The base circle Dg rotates around the revolving circle Dr which is fixed on the opposite plane S. Consider plane S cross-sectioned completely. When the peritrochoid T of band form moves around, the plane S is divided into two regions, one with the cross-sectioning completely removed and the other with the cross-sectioning still remaining. The dividing curves of these two regions are envelopes. Curve Ha, the outer border of the peritrochoid T, is the outer envelope, while curve Hi, the inner border of the peritrochoid is the inner envelope. In this case, the corner points I, II and III of these inner and outer envelopes are always in contact with the peritrochoid, so that they do not move radially and therefore can be considered stationary. From these characteristics, it can be presumed that when any of these envelopes (inner or outer) is used as a basis for rotary piston machines, the sealing pieces radially arranged at these corner points can easily follow the movement of the rotor at high revolutions.

Fig. 1. 12 illustrates the possible combinations of the trochoid and its envelope when $i = 1 : 2, 2 : 3, 3 : 4$ and $4 : 5$.

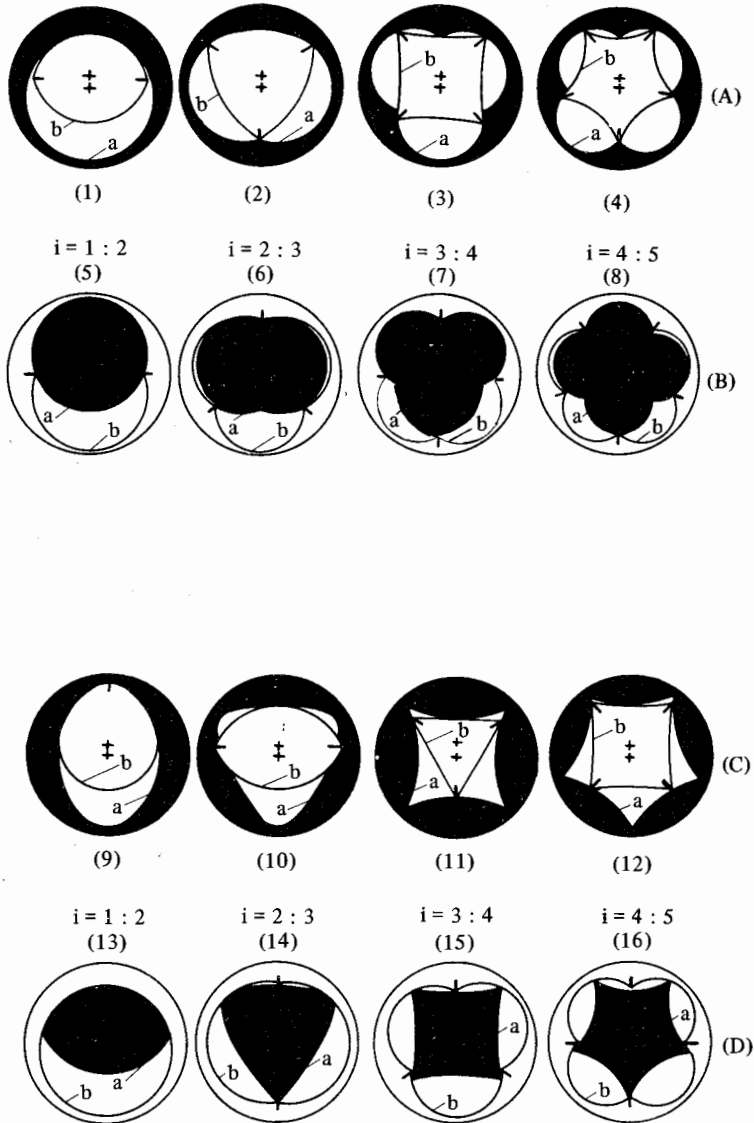


Fig. 1. 12 Possible combinations of the trochoid and its inner and outer envelopes

- (A) In this series there are the combinations of the arcs of the peritrochoid (a) with lobe number (n) for the inner surface of the outer casing and its inner envelopes of the peritrochoid (b) with $n + 1$ apex or flank for the internal piston. In this case, a transfer ratio of $i = n/n + 1$ exists.
- (B) This series shows the combinations of the peritrochoid (a) with $n = 1, 2, 3$ and 4 lobes for the internal piston and its outer envelope (b) for the outer casing.
- (C) In this series there are the combinations of the hypotrochoid (a) with $n = 1, 2, 3$ and 4 flanks and its inner envelope (b). The (D) series is a combination of the hypotrochoid (a) for the internal piston and its outer envelope (b) for the outer casing.

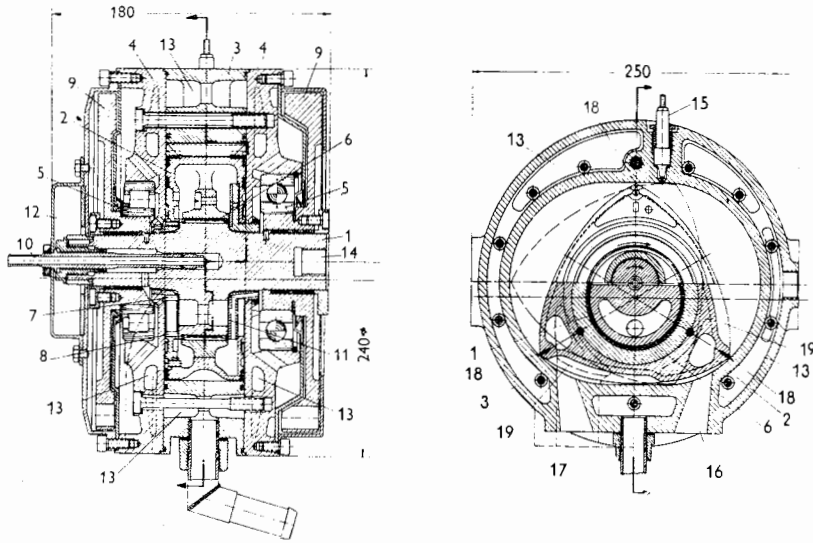
Some of these combinations have been known for some time through patent bulletins. For example, the type using the peritrochoid for the internal piston was patented in Germany under patent No. 156127 by Colley as a steam engine of the rotary piston type. Under English patent No. 583075, B. Maillard employed the hypotrochoid for the internal piston of a compressor.

Another example is the French patent No. 853807 in which De la Vand attempted to apply hypotrochoids to an internal combustion engine. The idea of using the peritrochoid for the outer casing and its inner envelope for the internal piston contour with $i = 1 : 2$ was first tried by Paul Kirchhoff, and was patented under German patent No. 8689, and research was conducted with this type on Oldham blowers. It is known that Planche & Cie of France has also tried a similar type for compressors and blowers in recent years. It was F. Wankel, however, who first proposed the ideal $i = 2 : 3$ and $3 : 4$ type for internal combustion engines and expansion mechanisms.

1.4 The Basic Structure of a Planetary Rotation Engine and its Operation

Fig. 1. 13 shows the longitudinal, and cross-section views of the planetary rotation engine KKM 250 which became the original prototype of the so-called NSU-Wankel engine.

Fig. 1. 14 is the expanded view of the same engine broken down and showing its structure.



- | | |
|----------------------|---|
| 1 : Eccentric shaft | 11 : Oil scavenging vane inside the rotor |
| 2 : Rotor | 12 : Contact breaker |
| 3 : Rotor housing | 13 : Cooling water jacket |
| 4 : Side housing | 14 : Connecting joint for drive shaft |
| 5 : Main bearing | 15 : Spark plug |
| 6 : Rotor bearing | 16 : Exhaust port |
| 7 : Stationary gear | 17 : Intake port |
| 8 : Rotor gear | 18 : Apex seal |
| 9 : Flywheel | 19 : Rotor combustion chamber recess |
| 10 : Lubricant inlet | |

Fig. 1. 13 Sectional view of the model KKM 250 engine

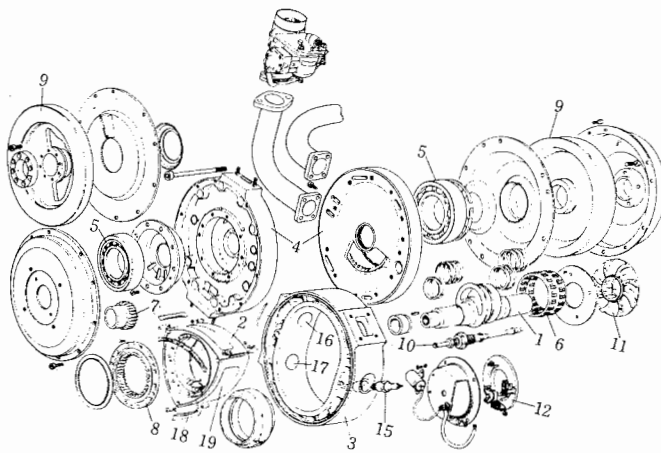


Fig. 1. 14 Expanded view of the model KKM 250 engine

As the major component, the eccentric shaft (1) which is the output shaft, supports the rotor (2) through the rotor bearing (6) at the central eccentric ring portion which corresponds to the rotor journal. The internal gear (8) installed at the end of the rotor, mates with the external gear (7) fixed on the side housing (4), constituting peritrochoidal phase gears with the transfer ratio $i = 2 : 3$.

Therefore, as the eccentric shaft rotates the rotor revolves around the center axis of the eccentric shaft while rotating itself on the eccentric rotor journal. Through this mechanism, the ratio of the output shaft rotation to that of the rotor is set at $3 : 1$ and the locus of the rotor apex always slides according to the same singular peritrochoid curve.

The side housings containing the main bearings (5), and the trochoidal housing with which the rotor apex seals (18) come in contact, are bolt tightened. The cooling water flows through the water jacket (13) inside these housings. The inlet for the cooling water is located at the lower part of the rotor housing. The water divides, and the streams flow upward and in parallel, inside the side housings and the rotor housing.

The rotor is oil cooled by lubricating oil, which is supplied under pressure to the oil passage (10) in the center of the eccentric shaft. Then it flows to the rotor bearing through oil passages located radially in the rotor journal portion, and finally into the hollow chamber inside the rotor. When the oil level inside the rotor is higher than the outer diameter of the stationary draining vane (11), the surplus oil is drained through radial and axial passages which are interconnected. This maintains constant oil level, and thereby eliminates engine vibration due to changes of oil quantity in the rotor.

All of these rotating components, including the eccentric shaft, rotor, bearing and the flywheel (9), are dynamically balanced with the quantity of the cooling oil inside the rotor taken into consideration. Unbalanced weight of the rotor and its journal portion are corrected by holes made near the outer edge of the flywheels on both ends of the eccentric shaft.

The intake and exhaust ports, (16) and (17), and the spark plug (15) with its opening, are located on the trochoid wall. Combustion recesses (19) are provided on the three surfaces of the rotor flank for obtaining proper compression as well as for preventing the division of the operating gas at the two constricted parts of the trochoid at top dead center.

Fig. 1. 15 shows the basic operation mode of the planetary rotation engine. Rotor position shown in Fig. (I) presents working chamber V_1 , at minimum volume, which corresponds to the "top dead center" position of the reciprocating engine. Here, the rotor journal portion (e) of the eccentric shaft (k) in the center of the trochoid (b) faces left and chamber V_1 composed of the trochoid and the

adjacent contour of the rotor (a) is separated from chambers V_2 and V_3 by the top apex seals (1) and (2), which are parallel to the shaft. Note that this chamber V_1 , which is just at the beginning of the intake stroke, is also in the port overlap position, with the intake and exhaust ports (h), (i) opening onto the combustion recess in the rotor.

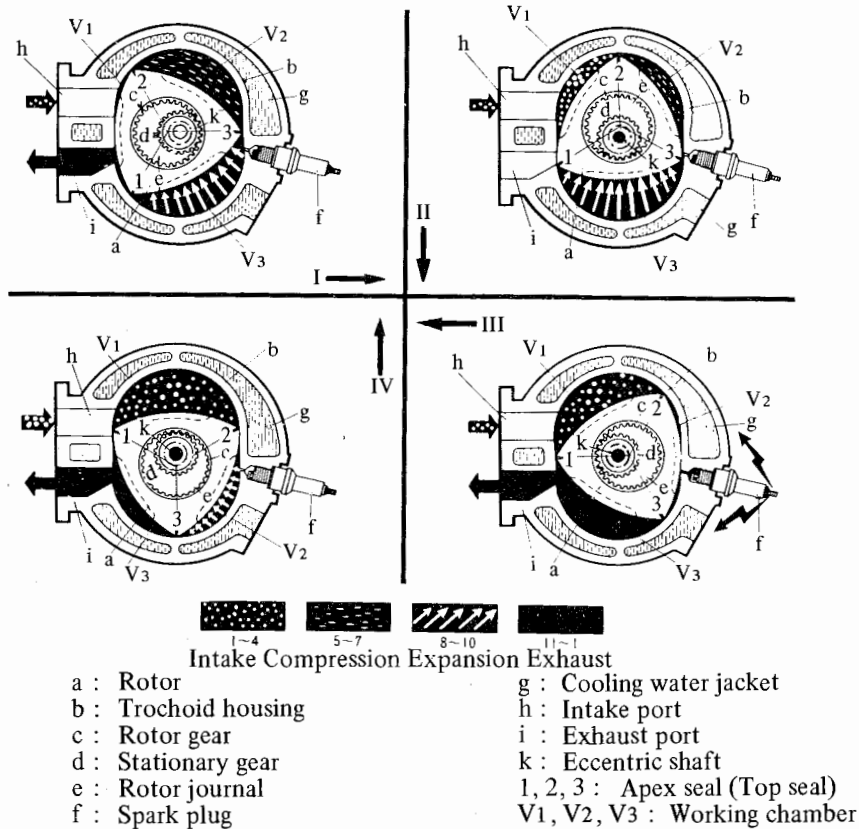


Fig. 1. 15 Working cycles of the planetary rotation engine

Fig. (II) shows the eccentric shaft rotated 90 degrees from the position in Fig. (I) with intake volume of the chamber V_1 gradually increasing.

Chamber V_1 next takes the position shown in Fig. (III), and then the position of maximum intake volume in Fig. (IV), as it passes through "bottom dead center." The intake stroke ends when the tip of apex seal 1 passes the upper end of the intake port (h).

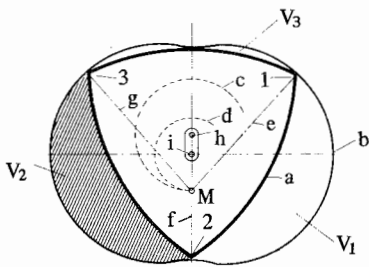
This suction stroke, therefore, continues for 270 degrees in terms of the rotating angle of the eccentric shaft.

To avoid repetitive illustration of the operating mode, chamber V_2 instead of chamber V_1 is considered in returning to Fig. (I) for the explanation of the second rotation of the eccentric shaft. The compression stroke shown by chamber V_2 proceeds in Fig. (II) until it hits top dead center position of Fig. (IV). At the

proper timing just before hitting top dead center, the gas is ignited by the spark plug (f), causing combustion to take place. Fig. (IV) shows the beginning of the expansion stroke of chamber V_2 . The expansion stroke in the succeeding third rotation of the eccentric shaft is shown by following chamber V_3 from Fig. (I).

The expanding of chamber V_3 in Fig. (II) shows the bottom dead center position giving it maximum volume, just after which the exhaust port is opened. Further, as the eccentric shaft rotates, as shown in Figs. (III) and (IV), the exhaust volume of chamber V_3 becomes smaller to complete the exhaust stroke, and then goes back again to the chamber V_1 position of Fig. (I).

Thus, one cycle of the planetary rotation engine is completed by one rotation of the rotor and three rotations (1080°) of the eccentric shaft. Each of the four operating strokes from suction to exhaust takes place in a $1080^\circ/4 = 270^\circ$ rotating angle of the eccentric shaft, which is quite a different pattern of operation from that of a 4-stroke cycle reciprocating engine, where each stroke is in a $720^\circ/4 = 180^\circ$ rotating angle of the crankshaft.



- 1~3 : Rotor apex seals
- $V_1 \sim V_3$: Working chamber (V_1 : Compression, V_2 : Compression, V_3 : Intake and exhaust top dead center)
- a : Rotor
- b : Inner wall of the housing
- c, d : Rotor gear and stationary gear
- e, f, g : Normal to the peritrochoid
- h : Rotor journal center
- i : Eccentric shaft center
- M : Intersecting point of normals to the peritrochoid and the mating point of the phase gear

Fig. 1. 16 Output torque generating mechanism

Movement of the rotor (a) is considered as the rotation of each rotor apex around the intersection point (M) of each normal to the peritrochoid at the point of contact of each rotor apex.

Since the internal gear of the rotor meshes with the fixed external gear at point (M), the rotor can rotate around this point. Therefore, when high pressure from chamber V_1 is applied to chamber V_2 , where combustion is taking place, the gas pressure provides tangential torque to the rotor journal center (h), which is in turn

converted to the output torque of the output eccentric shaft (i), thereby imparting a clockwise rotation to the rotor around the instantaneous rotation center (M). In this case, since chamber V_3 is in a symmetrical position relative to the instantaneous rotation center of the rotor, as well as the rotor journal center, chamber V_3 does not contribute to the torque conversion. It is only the pressure difference in the chambers V_1 and V_2 that produces the torque on the output shaft.

1.5 Structure and Operation of Single Rotation Engines

Fig. 1. 17 shows, for reference, the operating mode of the rotating piston engines which served as the starting point for the development of planetary rotation engines, as mentioned in 1. 1.

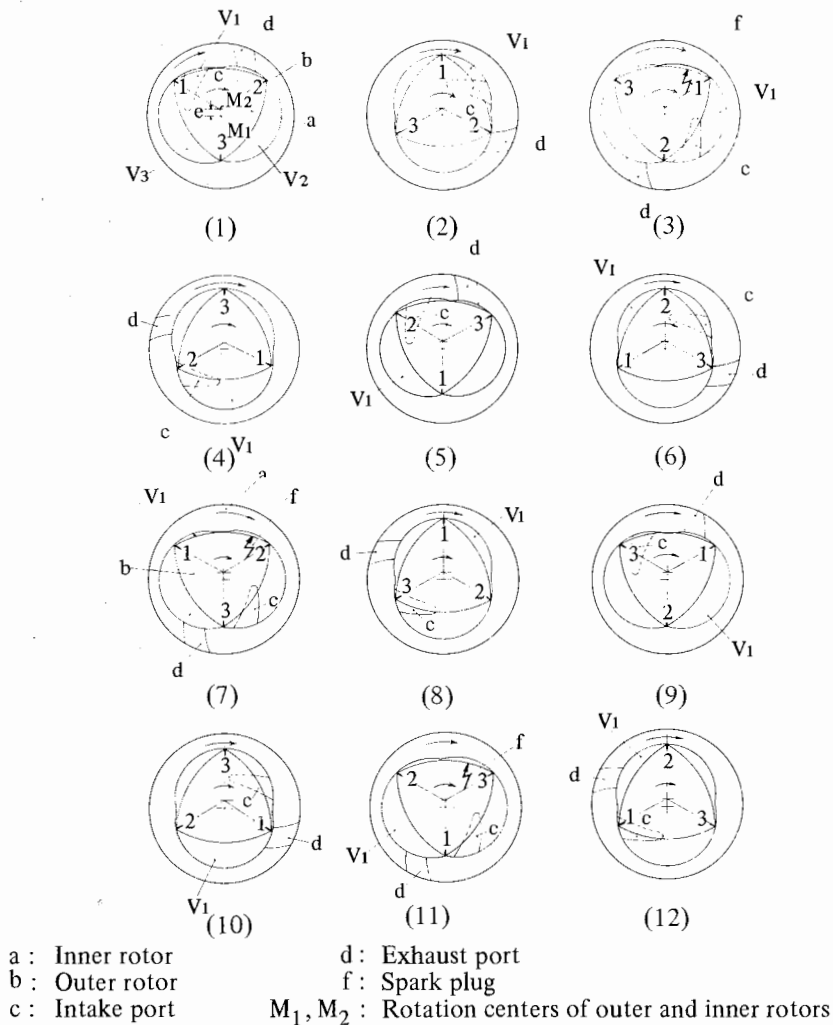
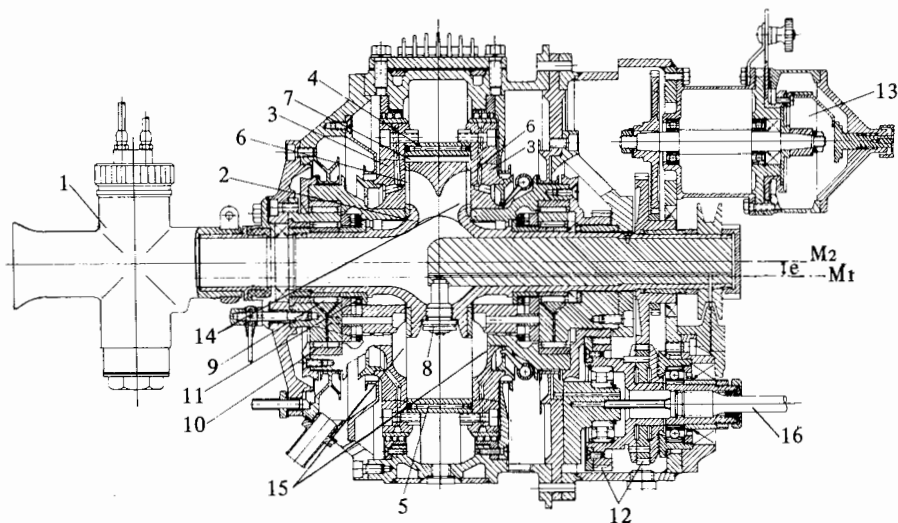


Fig. 1. 17 Basic operation of a single rotation engine



- | | |
|--|--|
| 1. Carburetor | 9. Inner rotor bearing |
| 2. Inner rotor | 10. Outer rotor bearing |
| 3. Side of outer rotor | 11. Ring seal |
| 4. Outer rotor central portion | 12. Phase gears for outer and inner rotors |
| 5. Cooling water jacket in the outer rotor | 13. Contact breaker |
| 6. Inner side seal plate | 14. Inlet hole for intake gas |
| 7. Apex seal | 15. Intake port |
| 8. Spark plug | 16. Output shaft |

Fig. 1. 18 Longitudinal section view of the model DKM 54 engine

Let us look at chamber V_1 of Fig. 1. 17 (1). The chamber V_1 is at minimum volume in the overlap position with the intake and exhaust ports, c and d, both open.

In Fig. 1. 17 (2), the outer rotor b and the inner rotor a have rotated 90° and 60° respectively, in a clockwise direction. Chamber V_1 is increasing its volume with the exhaust port d completely closed and the intake port partially opened.

In Fig. 1. 17 (3), the intake port c is almost fully opened, and passing through the maximum intake volume stage, Fig. 1. 17 (4), the intake stroke is completed, after which the compression stroke takes place as the intake port is gradually closed as shown in Figs. 1. 17 (5) and (6).

In Fig. 1. 17 (7), chamber V_1 is at compression top dead center, and when the gas is ignited by the spark plug, f, installed in the inner rotor, it will go into the expansion stroke, as shown in Figs. 1. 17 (8) and (9), then into the exhaust stroke with the exhaust port opened as shown in Figs. 1. 17 (10), (11) and (12).

Fig. 1. 18 shows the longitudinal sectional view of the single rotation engine-model DKM 54.

The basic conditions are when the central portion (4) of the outer rotor with its two-lobe peritrochoidal inner surface, and the inner rotor (2) of three-flank composed of the peritrochoid inner envelope, are placed in line with each other at a

distance of “e” (eccentricity) and they rotate in the same direction around their own axes M_1 and M_2 at the speed ratio of 2 : 3.

The central portion (4), and the outer rotor which is composed mainly of the side portions (3), are water-cooled. The spark plug (8) installed in the wall of the inner rotor receives high tension voltage from the lead wire running through the hollow shaft. The intake mixture from the carburetor (1) goes into the operating chamber by way of the intake port (14) of the inner rotor and another intake port (15) on the side portion of the outer rotor.

In this mechanism, the speed ratio of both rotors is determined by the gears (12) and the output is taken from the outer rotor through these gears.

In comparing the single rotation engines with the planetary rotation type, we find that while the operating mechanism and the movement of the piston are reversed, the volume change of the working chamber and the sliding speed of the radial seal piece on the inner rotor apex (the apex seal) are, in fact, quite the same in both engines.

1.6 Features of the Planetary Rotation Engine

When the planetary rotation engine, which has now been successfully developed for practical use as the NSU-Wankel engine, is compared with present day reciprocating engines, the following advantageous features can be seen :

- (i) It is possible to make engines lighter and more compact. The ratio of the effective volume (the volume of the working chamber) to the total engine volume, can be increased. These features will be effective in the simplification of the engine mechanism, in the improvement in durability which is attributed to the reduced number of moving parts, and in the reduction of manufacturing cost.

Fig. 1. 19 shows the rough trends of specific output in gasoline engines.

- (ii) It can be expected to attain high speed operation, which is essential for high specific output. Namely, being free from reciprocating inertia force caused by piston, intake and exhaust valve mechanisms, it is possible for it to attain a high allowable

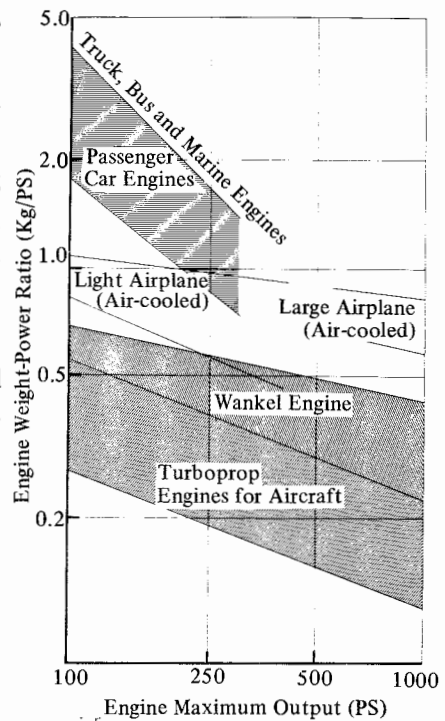


Fig. 1. 19 Comparison of engine weight-power ratio

engine speed. Of course there is another possibility for attaining still higher speed operation, by employing the multi-rotor system based on reduction of rotor size.

- (iii) It is possible to assure more flexible operation because of reduced torque variation. This stems from the fact that the rotor working chamber of 120° phase difference is unique in having the operational and functional features of both 4-stroke and 2-stroke engines, giving a larger degree of design freedom for improving the output performance.
- (iv) It is possible to reduce the noise level of the engine. This is a combined advantage, which comes from the elimination of vibration sources mainly by virtue of minimum torque vibration and perfect balancing of inertia forces, and from the substantially lower level of engine mechanical noise. Rotary engines are therefore considered to possess the essential features required for high quality engines.

Fig. 1. 20 shows the comparison of engine noise levels.

- (v) It has wide application adaptability. To assure the use of internal combustion engines in various fields of application, it is essential to establish the optimum operational mode of engines most effective in each field. For this purpose various research and development projects are now being conducted in the areas of both the mode of operation and construction. Examples are, gasoline engines with carburetors and fuel injection systems, diesel engines, which can use lower quality fuel, hybrid engines including a multi-fuel system, and research into the possibility of multi-stage expansion.

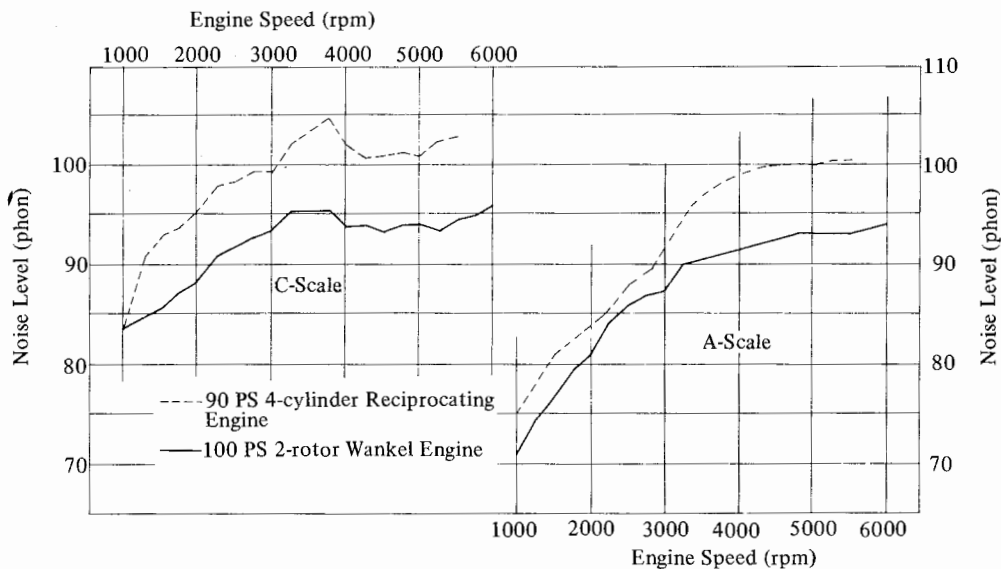


Fig. 1. 20 Comparison of engine noise levels (during full throttle acceleration)

Reference Materials

- 1) Franz Huf : Zur Geschichte der Rotationskolbenmaschinen. Automobil Revue, No. 49 (1961).
- 2) Felix Wankel : Einteilung der Rotations-Kolbenmaschinen. Stuttgart, Deutsche Verlags-Anstalt. Fachverlag (1963).
- 3) W. Froede : Entwicklungsarbeiten an Drehkolben und Kreiskolben-Verbrennungsmotoren. VDI Berichte, Nr. 45 (1960).
- 4) Felix Wankel, W. Froede : Bauart und gegenwärtiger Entwicklungsstand einer Trochoiden-Rotationskolbenmaschine. MTZ, 21/2 (1960).
- 5) Walter Siepmann : Vom Oldham-Ventilator zum Wankelmotor. Kraftfahrzeugtechnik. (2/1962).
- 6) R. F. Ansdale : Rotary Combustion Engine Part 1, 2, 3. Automobile Engineer, December (1963), January (1964), February (1964).
- 7) W. D. Bensinger : Rotationkolbenmotoren für Drauffahrzeuge. ATZ 66/4 (1964).

2. BASIC DIMENSIONS

2.1 Geometric Analysis of Basic Dimensions

The geometric analysis of the NSU–Wankel type rotary engine consists of a combination of the peritrochoid and its inner envelope.

2.1.1 Equation of a peritrochoid

The peritrochoid which gives the inner surface of the rotor housing is shown in Fig. 2. 1. Theoretically, the peritrochoidal curve is defined as a locus of point P on the segment \overline{OBP} fixed on a revolving circle B (radius q), which rolls in an inscribed manner on the outer circumference of a fixed base circle A (radius p).

Thus, the coordinate (x, y) of point P is expressed as

$$\begin{cases} x = e \cos \alpha + R \cos \theta \\ y = e \sin \alpha + R \sin \theta \end{cases} \quad (2.1)$$

θ is related to α by the relationship $\widehat{tg} = \widehat{fg}$ (shown by the bold solid line in Fig. 2. 1), assuming that point t on circle A and point f on circle B are in contact when $\alpha = 0$,

from which, $\theta = (1 - p/q) \alpha$

assuming $(1 - p/q) = 1/m$

the equation of the peritrochoid is generally expressed as

$$\begin{cases} x = e \cos \alpha + R \cos \alpha/m \\ y = e \sin \alpha + R \sin \alpha/m \end{cases} \quad (2.2)$$

From the above conditions, the relationship between p and q is

$$p/q = (m-1)/m \quad (2.3)$$

From the viewpoint of mechanism, the term m in the above formula should always be an integer, assuming that point P returns to its starting position.

For further consideration, assuming $n = m-1$, (n) represents the number of peritrochoidal lobes or nodes (caved point) and (m) the number of apexes or flanks (arc shaped contours) on the inner envelope described later.

For the NSU–Wankel type rotary engine, $n=2$, $m=n+1=3$. In other words, this curve is made up of a combination of a two-lobe peritrochoid and a three-flank inner envelope.

The equation of the peritrochoid, from equation (2.2), becomes

$$\begin{cases} x = e \cos \alpha + R \cos \alpha/3 \\ y = e \sin \alpha + R \sin \alpha/3 \end{cases} \quad (2.4)$$

where the distance (e) between the center of base circle A and that of the revolving circle B, is referred to as “eccentricity”. The arm length R on the revolving circle B is referred to as the “generating radius” of the peritrochoid.

2. 1. 2 Inner envelope of the peritrochoid

From the mechanical standpoint, the contour of a rotor revolving along a peritrochoid can be represented by a two-lobe peritrochoid inner envelope.

As in Fig. 2. 2, the envelope of a group of curves drawn by the peritrochoid represented by fixed point P on circle A, which rolls in a circumscribed manner on the inner circumference of fixed circle B is discussed mathematically below.

From Fig. 2. 2, the coordinate (X,Y) of point P is expressed in the form of

$$\begin{aligned} X &= e \cos \beta + x \cos \beta/2 + y \sin \beta/2 \\ Y &= e \sin \beta - x \sin \beta/2 + y \cos \beta/2 \end{aligned} \quad (2.5)$$

On substitution of equation (2. 4), assuming

$$\begin{cases} \beta = u - 3v \\ \alpha = \beta/2 = u + 3v \end{cases}$$

the equation of the group of curves is as follows :

$$\begin{aligned} X &= 2e \cos 3v \cdot \cos u + R \cos 2v \\ Y &= 2e \cos 3v \cdot \sin u + R \sin 2v \end{aligned} \quad (2.6)$$

The envelope is given by combining the equations of the group of curves with the following conditions :

$$\begin{cases} \frac{dX}{dv} = \frac{\partial X}{\partial v} + \frac{\partial X}{\partial u} \cdot \frac{du}{dv} = 0 \\ \frac{dY}{dv} = \frac{\partial Y}{\partial v} + \frac{\partial Y}{\partial u} \cdot \frac{du}{dv} = 0 \end{cases}$$

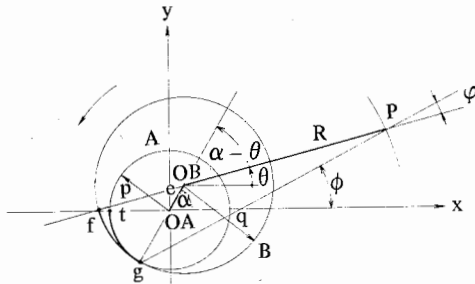


Fig. 2. 1 Coordinate expression of the peritrochoid

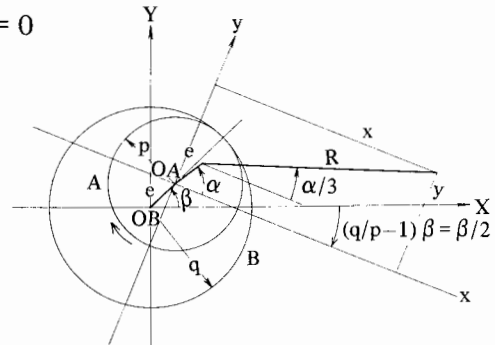


Fig. 2. 2 Coordinate expression of the peritrochoid inner envelope

Then, the equation for the envelope becomes :

$$\begin{cases} X = R \cos 2v + \frac{3}{2} \cdot \frac{e^2}{R} (\cos 8v - \cos 4v) \\ \quad + e \left(1 - \frac{9e^2}{R^2} \sin^2 3v\right)^{1/2} \cdot (\cos 5v + \cos v) \\ Y = R \sin 2v + \frac{3}{2} \cdot \frac{e^2}{R} (\cos 8v + \sin 4v) \\ \quad + e \left(1 - \frac{9e^2}{R^2} \sin^2 3v\right)^{1/2} \cdot (\sin 5v - \sin v) \end{cases} \quad (2.7)$$

where the negative sign values are equivalent to the positive sign values derived

from an increase in v by π .

This function represents a cyclic function with a period of 2π radians. Fig. 2. 3 shows the envelope thus obtained.

In Fig. 2. 3 (b), the bold solid lines show the inner envelopes and the fine solid lines the outer envelopes. It follows, therefore, that the bold solid line represents the rotor contour for an actual mechanism.

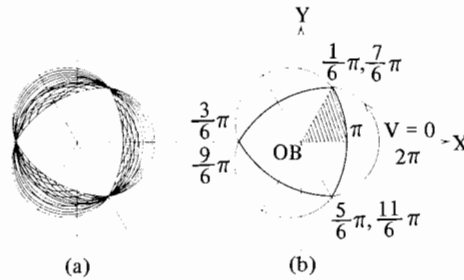


Fig. 2. 3 Inner and outer envelopes of the two-lobe peritrochoid

2. 1. 3 Leaning angle and the trochoid constant

The angle formed by the radial direction at the rotor apex and the normal to the trochoid is called the leaning angle.

In Fig. 2. 1, since an instantaneous rotational center of point P coincides with contact point g of base circle A and revolving circle B. \overline{Pg} represents the normal at point P to the trochoid.

Therefore, letting ϕ be the angle formed between \overline{Pg} and the x axis

$$\tan \phi = -\frac{dx}{dy} = \frac{3e \sin \alpha + R \sin \alpha/3}{3e \cos \alpha + R \cos \alpha/3} \quad (2. 8)$$

Since the leaning angle φ is the angle between $\overline{PO_B}$ and $\overline{P_B}$ from the previous definition,

$$\varphi = \phi - \alpha/3$$

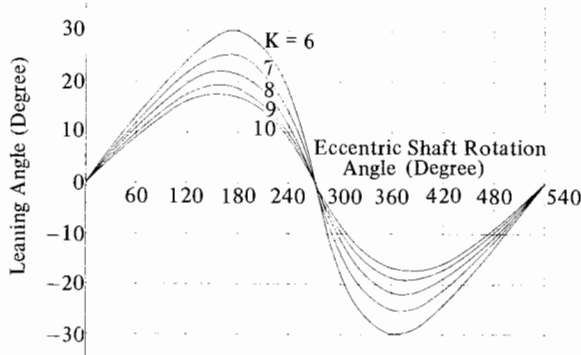


Fig. 2. 4 Variation of leaning angle

Then, upon substitution of $\cos \phi$ and $\sin \phi$, which are obtained from equation (2, 8), the leaning angle can be expressed as follows :

$$\cos \phi = \frac{3 e \cos \frac{2}{3} \alpha + R}{\left(9 e^2 + R^2 + 6 eR \cos \frac{2}{3} \alpha\right)^{1/2}} \quad (2. 9)$$

When $\cos \frac{2}{3} \alpha = -3e/R$, the maximum leaning angle is obtained, for which the expression becomes :

$$\begin{cases} \cos \phi_{\max} = \left\{ 1 - \left(\frac{3 e}{R} \right)^2 \right\}^{1/2} \\ \sin \phi_{\max} = \frac{3 e}{R} \end{cases} \quad (2. 10)$$

It follows from equation (2. 4) that this peritrochoid is a cyclic curve with a period of $\alpha = 6\pi$, in which the four maximum leaning angles exist in one cycle of the peritrochoid. Fig. 2. 4 gives the relationship between the leaning angle ϕ and α .

The magnitude of leaning angle may be taken as one factor for representing the geometric features of the peritrochoid.

From equation (2. 10), for example, assuming

$$K = R/e \quad (2. 11)$$

K is able to represent the trochoidal configuration, which is known as the trochoid constant.

Consider the engines as having the same width ; since working volume is proportional to the product of e and R , as will be dealt with later. Therefore, the size and the configuration of the peritrochoid will vary as shown in Fig. 2. 5, according to the value of the trochoidal constant K mentioned above, assuming that working volume is constant i.e. $e.R = \text{constant value}$.

Where the value of K is small, the peritrochoid will also be small, but the maximum leaning angle ϕ_{\max} will become larger. On the other hand, the greater the value of K the smaller ϕ_{\max} becomes, while the greater the peritrochoid in the reverse manner. The larger the value of K , the larger the theoretical compression ratio ϵ_{th} , which will be discussed later.

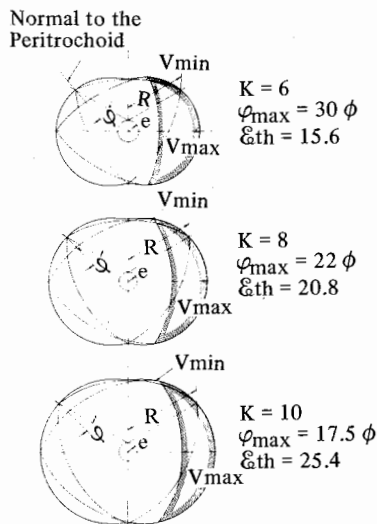


Fig. 2. 5 Effect of the trochoid constant on the peritrochoid configuration

Therefore, the trochoid constant K should be determined according to the required characteristics for the rotary engine in question. For this, in general, a value between 6 and 10 is selected for K.

2. 1. 4 Circumferential velocity of the rotor apex

The circumferential velocity of the rotor apex is one representative value denoting the sliding velocity of the rotating components, which also defines the characteristics of an engine, along with the leaning angle and trochoid constant. Introducing the relation $\sigma = \omega t$ (ω : angular velocity) into equation (2. 4) and substituting with respect to time, the circumferential velocity is given as,

$$v = \left\{ \left(\frac{dx}{dt} \right)^2 + \left(\frac{dy}{dt} \right)^2 \right\}^{1/2} \quad (2. 12)$$

$$= \frac{\omega}{3} \left(9 e^2 + R^2 + 6 eR \cos \frac{2}{3} \alpha \right)^{1/2} \quad v_{\max} = \frac{\omega}{3} (3 e + R) \quad \alpha = 0, \quad 3 \pi$$

(In equation (2. 12),

$$v_{\min} = \frac{\omega}{3} (R - 3 e) \quad \alpha = \frac{3}{2} \pi, \frac{9}{2} \pi$$

Further, in equation (2. 12), when a point at an appropriate distance from the rotor center is substituted for the generating radius and employed for R, the velocity at that point is obtained.

2. 2 Volumetric Change and Working Volume of the Working Chamber

2. 2. 1 Volumetric change of the working chamber

The volume of the working chamber is the product of the area which is surrounded by the inner surface of the rotor housing (the peritrochoid) and one flank of the rotor (the trochoid inner envelope), and the width of the rotor housing.

First, the area change of the working chamber will be determined.

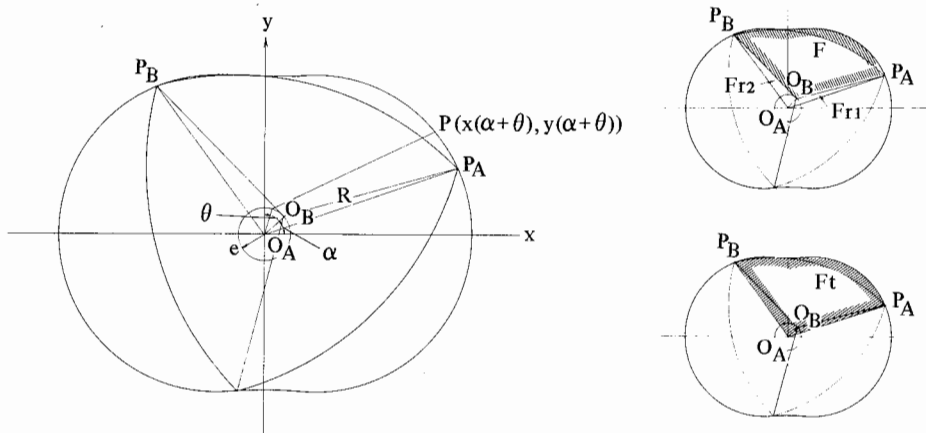


Fig. 2. 6 Volume change of the working chamber

As illustrated in Fig. 2. 6 considering the case when rotor center O_B is located at the distance of α from x axis, area F surrounded by rotor center O_B and peritrochoid $\widehat{P_A P_B}$ is as follows :

$$F = F_t - (F_{r1} + F_{r2})$$

where

$$F_t = \frac{1}{2} \int_0^{2\pi} \left(x \frac{dy}{d\theta} - y \frac{dx}{d\theta} \right) d\theta$$

The coordinate of point P is from equation (2. 4), given as,

$$\begin{cases} x_{(\alpha+\theta)} = e \cos(\alpha + \theta) + R \cos \frac{1}{3}(\alpha + \theta) \\ y_{(\alpha+\theta)} = e \sin(\alpha + \theta) + R \sin \frac{1}{3}(\alpha + \theta) \end{cases}$$

$$\begin{aligned} \text{Therefore, } F_t &= \frac{1}{2} \int_0^{2\pi} \left\{ \left(e^2 + \frac{R^2}{3} \right) + \frac{3}{4} eR \cos \frac{2}{3}(\alpha + \theta) \right\} d\theta \\ &= \left(e^2 + \frac{R^2}{3} \right) \pi - \sqrt{3} eR \sin \left(\frac{2}{3} \alpha + \frac{\pi}{6} \right) \end{aligned} \quad (2. 13)$$

and

$$\begin{aligned} F_{r1} &= \frac{1}{2} eR \sin \frac{2}{3} \alpha \\ F_{r2} &= \frac{1}{2} eR \sin \left(\frac{2}{3} \alpha + \frac{\pi}{3} \right) \end{aligned} \quad (2. 14)$$

On calculation of these equations,

$$F = \pi \left(e^2 + \frac{R^2}{3} \right) - \frac{3\sqrt{3}}{2} eR \sin \left(\frac{2}{3} \alpha + \frac{\pi}{6} \right) \quad (2. 15)$$

In equation (2. 15), subtracting F_{\min} obtained when $\sigma = \pi/2$ from F, and multiplying the quotient by width (b) yields the volumetric change (v) in the working chamber :

$$V = \frac{3\sqrt{3}}{2} eRb \left\{ 1 - \sin \left(\frac{2}{3} \alpha + \frac{\pi}{6} \right) \right\} \quad (2. 16)$$

2. 2. 2 Volume of the Working Chamber

The volume of the working chamber (the displacement volume) V_H is given as the maximum value from equation (2. 16).

$$V_H = 3\sqrt{3} eRb \quad (2. 17)$$

In this working chamber area F_H is given as

$$F_H = 3\sqrt{3} eR \quad (2. 16)$$

In equation (2. 17), assuming the trochoid major axis $A=2(R+e)$ and minor axis $B=2(R-e)$, the volume of the working chamber can also be determined as,

$$V_H = \frac{3\sqrt{3}}{16} (A^2 - B^2) b \quad (2. 19)$$

In Fig. 2. 7, the calculation chart (nomogram) is presented for the determination of the working chamber volume from the basic dimensions of an engine.

The relationship between the effective area F_p of the rotor surface, equivalent to the projected piston top area, and the working chamber dimensions is,

$$F_p = \sqrt{3} Rb$$

Therefore,

$$V_H = 3F_p \cdot e. \quad (2. 20)$$

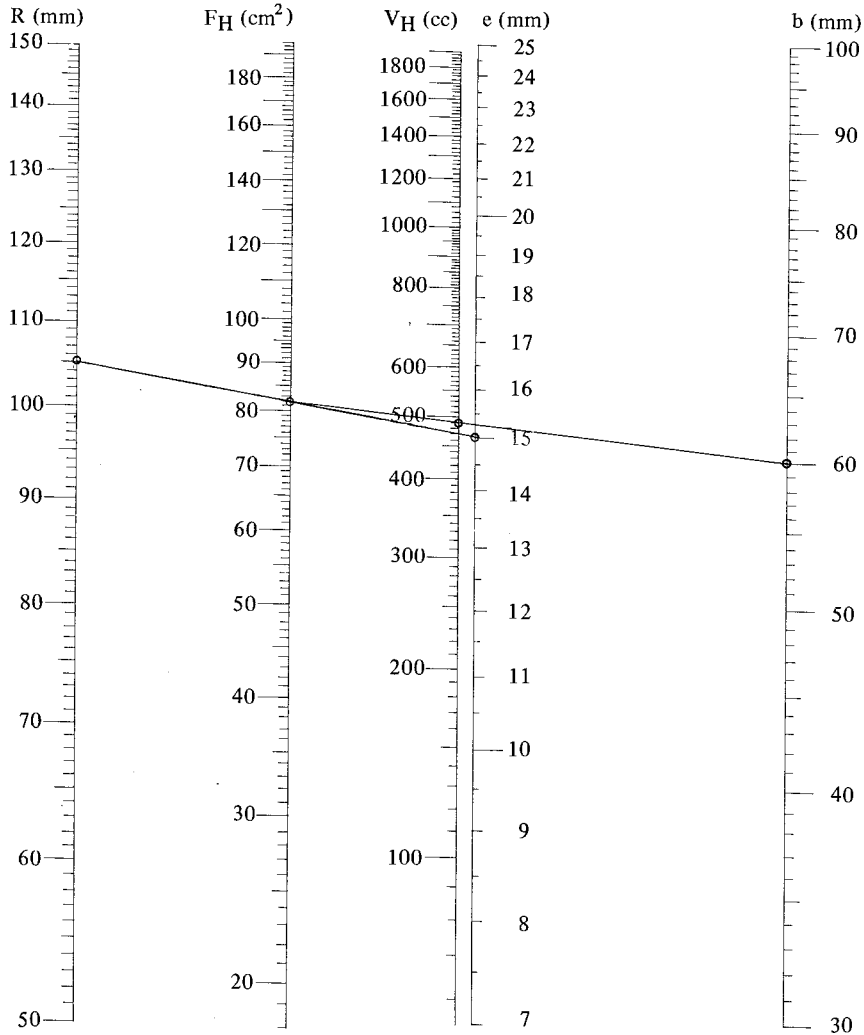


Fig. 2. 7 Nomogram for calculating the working chamber volume

2.3 Basic Dimensions and Theoretical Compression Ratio

First of all, the relationship between the basic dimensions and the compression area F_c is treated below.

From Fig. 2. 8, it follows that

$$F_c = F_t - (F_r + F_{r1} + F_{r2}) \quad (2. 21)$$

Values of F_t and F_{r1}, F_{r2} in the equation (2. 21), are obtained by assuming $\alpha = \pi/2$ in equations (2. 13) and (2. 14).

$$F_{t(\alpha = \pi/2)} = \pi \left(e^2 + \frac{1}{3} R^2 \right) - \sqrt{3} eR$$

$$F_{r1(\alpha = \pi/2)} = F_{r2(\alpha = \pi/2)} = \frac{\sqrt{3}}{4} eR$$

Next, F_r is equivalent to the sectioned area in Fig. 2. 3, thus :

$$\begin{aligned} F_r &= 2 \times \frac{1}{2} \int_{v=\pi}^{v=\frac{7}{6}\pi} \left(X \frac{dY}{dv} - Y \frac{dX}{dv} \right) dv \\ &= (2 R^2 + 4 e^2) \frac{\pi}{6} - 2 eR \left\{ 1 - \left(\frac{3e}{R} \right)^2 \right\}^{1/2} \\ &\quad - \left(\frac{2}{9} R^2 + 4 e^2 \right) \sin^{-1} \frac{3e}{R} \end{aligned} \quad (2. 22)$$

Substitution of equation (2. 10) and rearranging gives :

$$F_r = \frac{\pi}{3} (R^2 + 2 e^2) - 2 eR \cos \varphi_{\max} - \left(\frac{2}{9} R^2 + 4 e^2 \right) \varphi_{\max} \quad (2. 23)$$

Then substituting the last three values into equation (2. 21) gives the theoretical compression ratio expressed as :

$$F_c = 2 eR \cos \varphi_{\max} + \left(\frac{2}{9} R^2 + 4 e^2 \right) \varphi_{\max} + \frac{\pi}{3} e^2 - \frac{3\sqrt{3}}{2} eR \quad (2. 24)$$

Theoretical compression ratio \mathcal{E}_{th} is expressed as follows :

$$\begin{aligned} \mathcal{E}_{th} &= \frac{V_H + V_c}{V_c} = \frac{F_H + F_c}{F_c} \\ &= \frac{2 eR \cos \varphi_{\max} + \left(\frac{2}{9} R^2 + 4 e^2 \right) \varphi_{\max} + \frac{\pi}{3} e^2 + \frac{3\sqrt{3}}{2} eR}{2 eR \cos \varphi_{\max} + \left(\frac{2}{9} R^2 + 4 e^2 \right) \varphi_{\max} + \frac{\pi}{3} e^2 - \frac{3\sqrt{3}}{2} eR} \end{aligned} \quad (2. 25)$$

Fig. 2. 9 shows the relationship between the theoretical compression ratio and leaning angle φ and the trochoid constant k .

In an actual engine, the combustion chamber is built by providing a cavity on its arc-shaped rotor outer surface configuration and in addition, a gap is provided

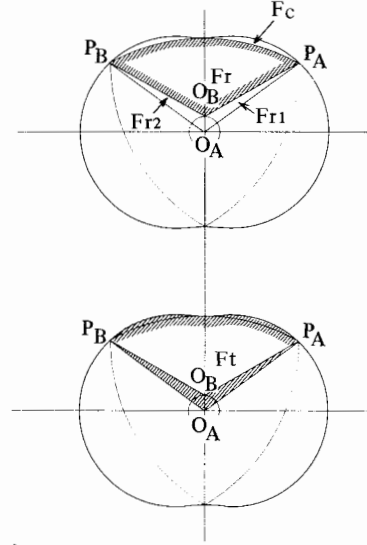


Fig. 2. 8 Theoretical compression ratio

between its peritrochoidal inner surface and the arc-shaped rotor contour. Furthermore, the spark passage bore for the spark plug, of course, affects its compression ratio.

From this, we can gather that if the total volume of these is expressed as V_r , actual compression ratio can be determined by

$$\epsilon_c = \frac{V_H + V_c + V_r}{V_c + V_r} \quad (2.26)$$

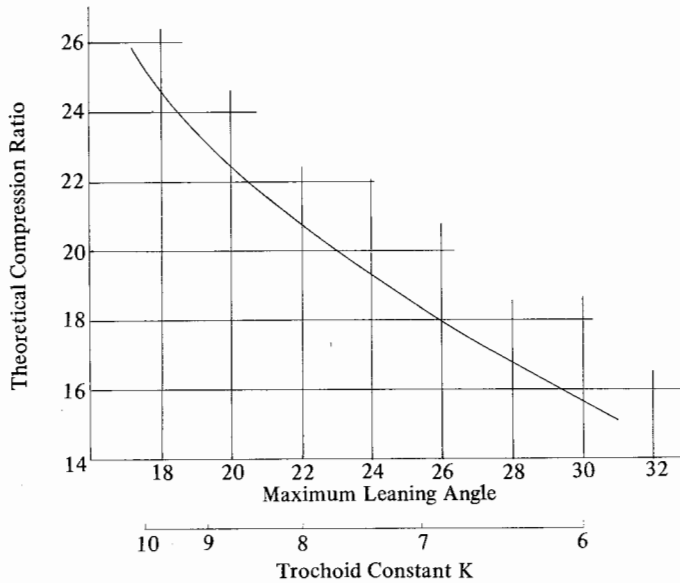


Fig. 2.9 Effect of the maximum leaning angle on the theoretical compression ratio

2.4 Basic Dimensions and Fundamental Construction of the Rotary Engine

In designing a rotary engine, when the volume of the working chamber has been determined, the basic geometric dimensions such as the eccentricity (e), the generating radius R and the width of the rotor housing (b) are decided upon. For this, various factors in connection with these basic geometrical dimensions should be taken into consideration.

In this section, the relationship between the basic geometrical dimensions and the basic structure of an engine are described.

2.4.1 Basic dimensions and intake and exhaust ports

The area of the intake and exhaust port is one of the most important factors influencing the engine performance characteristics. Especially, in the case of rotary engines, these two are further significant in that the choice of the basic geometric

dimensions determines the maximum possible areas of the intake and exhaust ports.

In Fig. 2. 10, the comparison of the location of the intake and exhaust ports, and the configuration of the opening, with various values of the trochoid constant, in case of the working chamber volume being constant, with the width of the rotor housing and the value of $e.R$ being constant, was made under a constant port timing. It is clearly observed that the larger trochoid constant K provides the larger peri-trochoid configuration, which enables the selection of a larger port area. In actual design, however, these port areas are also limited by the port configuration, etc., in consideration of port overlap and gas seal tightness.

2. 4. 2 Basic dimensions and the construction of the engine output shaft system

The basic geometric dimensions of an engine affect the determination of the dimensions of the output shaft including the rotor, in other words, the eccentric shaft system.

From Fig. 2. 1 and expression (2. 3), it follows that :

$$q - p = e$$

$$\frac{p}{q} = \frac{(m-1)}{m} = \frac{2}{3}$$

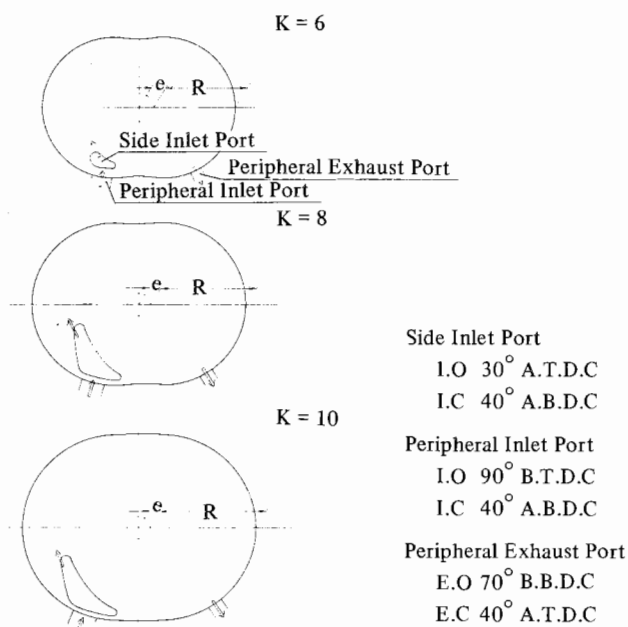


Fig. 2. 10 Effect of the trochoid constant on the trochoid contour and intake and exhaust port configurations

Therefore,

$$P = 2e, \quad q = 3e \quad (2.27)$$

where $2p = 4e$ and $2q = 6e$ express the diameters of the pitch circles of the external gear fixed to the side housing and of the internal gear of the rotor, respectively.

From Fig. 2. 11, we get :

$$a_m = 2e - \frac{d_m}{2} \geq 3e - \frac{d_r}{2} \quad (d_r \geq d_m + 2e) \quad (2.28)$$

where the value of a_m is properly selected according to the tooth number of the fixed external gear and its module.

Therefore, the eccentricity (e), once determined, will inevitably determine the minimum values of the diameter d_m of the main bearing journal and of the diameter d_r of the rotor bearing journal.

These two values of d_m and d_r should be designed in consideration of the stress and deflection of the output shaft, the surface pressure and life-time of the bearing, etc.

Since a_r is the distance between the pitch circle diameter of the rotor internal gear and the arc-shaped rotor contour, the proper value should be determined in accordance with the number, size and location of the sealing pieces installed to the rotor side face, such as side seals and oil seal rings to be discussed later.

The values of (e) and (R) should also be designed by taking earlier account of the value of a_r , because, as seen from the equation (2. 28), a_r is necessarily determined by those two values.

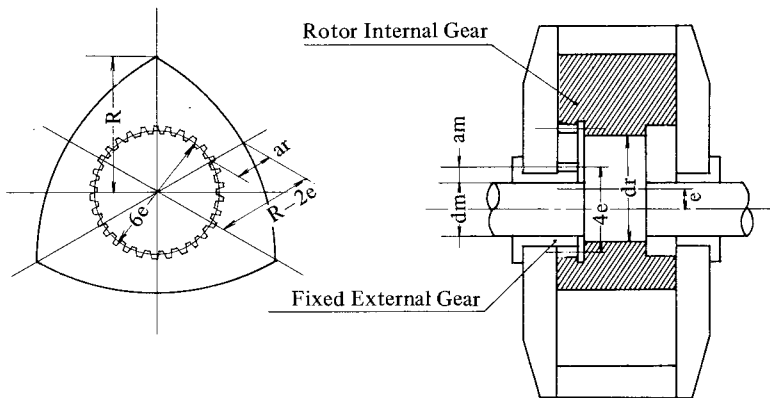


Fig. 2. 11 Relationship between eccentricity and output shaft system

2.5 Practical Examples of Basic Dimensions

Some actual examples of the geometric representation of the basic dimensions are shown in Table 2. 1, where (a) represents the amount of equidistance. The curve obtained by performing the parallel translation of the peritrochoid by an amount (a) is now in practical use on actual engines, as will be discussed in Section 4. 2.

V_H in this Table is calculated by its substitution for the generating radius R and the introduction of the relationship $R' = r + a$

Table 2. 1. Example of basic dimensions

V_H (cc)	e (mm)	R (mm)	a (mm)	b (mm)	K	φ_{\max}
60	7.6	47	0.5	32	6.18	29
125	9.5	65	0.5	40	6.85	26
150	10.5	66	1	41	6.28	28.5
250	11.0	84	1	52	7.63	23.2
400	14.0	89	1	59	6.36	28.2
500	14.0	100	2	67	7.14	24.8
500	15.0	101	4	60	6.73	26.5

Reference Materials

- 1) Othmar Baier : Die Kinematik der Drehkolben und Kreiskolbenmaschinen und ihre Fertigungsmöglichkeiten. VDI Berichte, Nr. 45 (1960).
- 2) W. Meyer zur Capellen : Kinematik der Umlaufrädertriebe und ihre Anwendung auf Wankelmotor. Industrie-Anzeiger, Juli (1961).
- 3) H. Kuhner : Das theoretisch mögliche Verdichtungsverhältnis von Trochoidenmaschinen MTZ, 26/9 (1965).
- 4) R. F. Ansdale : The Wankel RC Engine, London Iliffe Books Ltd. (1968).

3. BASIC STRUCTURE

3.1 Intake and Exhaust Systems

3.1.1 Intake and exhaust port layout

Four-stroke reciprocating engines carry out gas exchange by their pistons, while rotary engines do so by means of direct opening and closing of the intake and exhaust ports by the rotor. This intake and exhaust port system has, in a word, the advantages of simple structure and accurate port timing over the whole range of engine speeds.

(1) Port layout systems

There are three basic intake and exhaust port layout systems used in rotary engines :

- (i) Peripheral port
- (ii) Side port
- (iii) Combination port

The peripheral port (Fig. 3. 1a) provides an intake port on the inner surface of the rotor housing trochoid. Port timing is controlled by the apex seal of the rotor top when it passes the port opening. The side port system (Fig. 3. 1b) has the intake port on either one side or both sides of the side housing. Fig. 3. 1c shows an intake port layout using both the peripheral and side ports. The exhaust port is on the trochoidal inner surface.

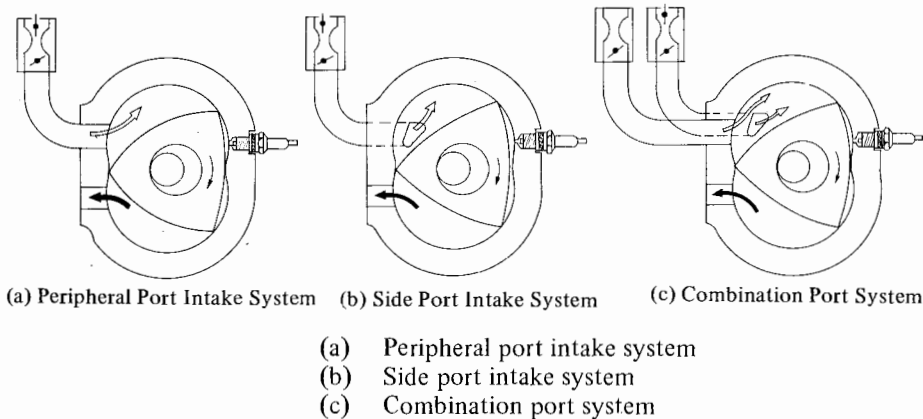


Fig. 3. 1 Basic arrangement of intake ports

(2) Side port configuration

Fig. 3. 2 illustrates an example of the intake port configuration of the side port system which controls the port timing by the arc-shaped contour of the rotor. The port outer edge line (A) is more or less determined by the contours of the side seal and the corner seal. The port inner edge line (B) is determined by its relation with the sliding line of the oil seal ring inserted in the rotor side face, so that this

line is closely related with oil seal construction. The edge line (C) governing the full closure of the port is subjected to no structural restriction and so is shaped to obtain maximum engine performance. Some examples of the opening areas currently used are shown in Table 12. 2.

Among examples using the peripheral intake port system are NSU's automobile engines and Fichtel & Sachs' small general-purpose engine, and as examples of the side intake port system there are Toyo Kogyo's automobile engines.

(3) Intake system of the two-rotor engine

Fig. 3. 3 shows the concept of the intake system for two-rotor engines. This system utilizes a two-stage carburetor having a primary system (P) for low speed operation and a secondary system (S) which works in cooperation with the primary system for high speed and heavy load operation. There are separate intake passages for both the primary and secondary systems from the carburetor to the intake ports.

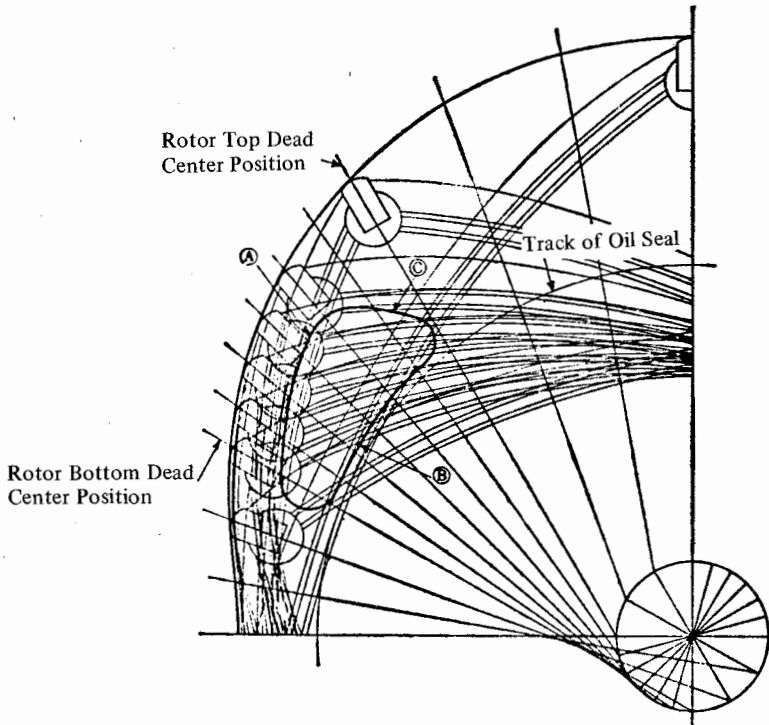


Fig. 3. 2 Side port configuration, showing tracks of gas and oil seals

- (a) is a side port intake system combined with a two-barrel carburetor.
- (b) also shows an example of the side port intake system using a four-barrel carburetor, now in use for automotive engines.
- (c) is an example of the peripheral port system combined with a two-carburetor system. This system is also now in use.

(d) depicts an example of a combination port system using a three-barrel carburetor in which the primary is connected to the side port and the secondary to the peripheral port. This system furnishes an attractive construction in terms of engine performance.

Both (c) and (d) intake port systems generally provide a port valve close to the trochoidal inner surface in the secondary system air intake passage. This port valve is mechanically linked to the primary valve of the carburetor to open after the primary valve opens to a certain point.

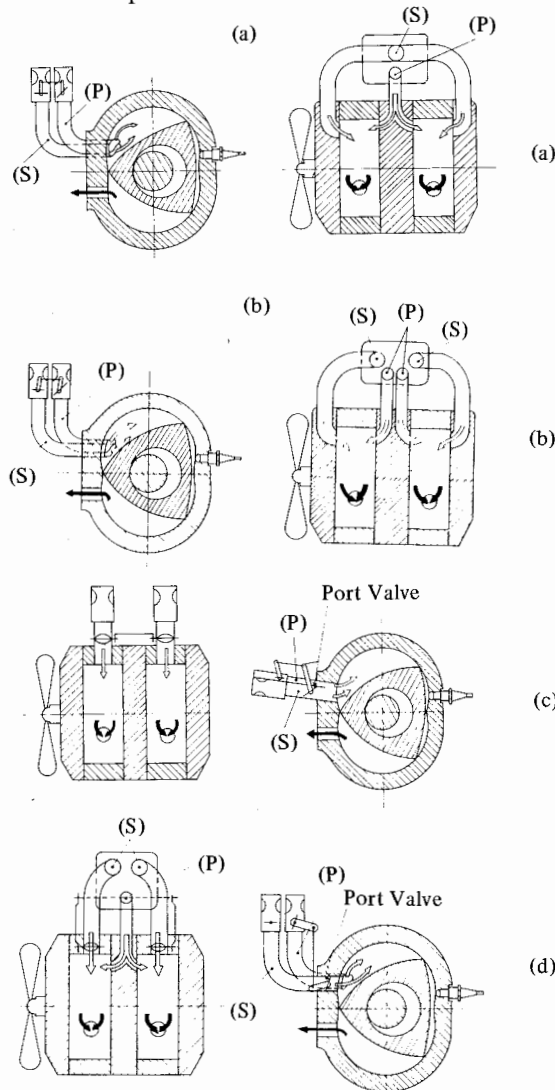


Fig. 3.3 Intake and exhaust flow for two-rotor engine

(4) Features of the independent flow passage system

Intake systems combining the two-stage carburetor and the independent intake air passage have three advantageous characteristics.

- (i) Large intake air port area is attainable, which contributes to higher volumetric efficiency resulting in higher output.
- (ii) Optimum sectional area of the intake port can be gained to match driving conditions. Especially, the higher intake air velocity in the primary system of the carburetor makes possible the promotion of fuel vaporization in the range of usual running speeds, giving promise to enhanced combustion efficiency.
- (iii) Homogeneous distribution of the intake mixture is made possible. It is always difficult for a multi-cylinder reciprocating engine to provide homogeneous manifold distribution, because of the difference in intake pipe length to each cylinder and the pressure interference between adjacent cylinders in reciprocating engine. With the independent intake passage system, the effect of pressure interference is eliminated by the structure shown in (b) and (c) in Fig. 3. 3.

3. 1. 2 Port timing

Two important factors in choosing intake and exhaust systems are port timing and configuration of the port opening leading into the combustion chamber. Careful consideration should be given to these two factors in view of their effects on engine performance and driveability.

(1) Opening timing and area of port

Fig. 3. 4 shows the port opening time/area and the opening process of each system in comparison with that of a 4-stroke reciprocating engine.

In reciprocating engines, it is difficult to employ a large opening time/area, owing to restrictions imposed by valve lift and valve diameter, while in rotary engines a relatively wide range of areas can be chosen.

In addition, each of the intake and exhaust processes occupies 270 degrees of the output shaft rotation compared with 180 degrees of the crank shaft in reciprocating engines, so that the opening time/area of rotary engines is far greater than that of reciprocating engines. This feature is considered to be one of the factors permitting better intake and exhaust efficiencies.

(2) General features of peripheral and side port systems

Comparing the peripheral and side port systems, we find advantages and disadvantages in both :

- (i) In the peripheral port system, where a large diameter port is provided on the trochoidal inner surface, the intake port opens far ahead of top dead center of the intake stroke. This gives an increase in effective compression ratio and a high volumetric efficiency. On the other hand, there is a design restriction on the intake and exhaust port timing. This restriction is imposed by the conditions that $O_E + C_E > 90^\circ$ and $O_I + C_I > 90^\circ$ as shown in Fig. 3. 4. This makes it necessary to determine optimum port configuration and port timing within the limitation. Generally, the overlap periods of the intake

and exhaust port layout become long when the peripheral port layout is employed for both intake and exhaust systems. This results in roughness when idling and operating under light load conditions. This is caused by the dilution of the intake gas by the exhaust gas partially inducted into the intake chamber because of high negative pressure in the intake pipe.

- (ii) In the side port intake system, port timing is controlled by the arc-shaped contour of the rotor. This system, because of its structure, opens the intake and exhaust ports after the rotor has passed top dead center beginning each stroke. Therefore the port overlap period is far shorter than that of the peripheral port system, and combustion stability during idling or over the range of ordinary operation is greatly improved.

We can say, then, that the peripheral port intake system is more suitable for the requirements of high performance at high speed than for low speed or partial load operation. The side port intake system, on the other hand, is suitable for engines requiring stable performance over a wide operating range from partial load at low speed to heavy load at high speed, although it is considered to be inferior to the peripheral port system in high speed output.

(3) Effect of port system type on torque characteristics

Fig. 3. 5 illustrates an example of the effect of these intake and exhaust port systems on engine performance at full load by plotting the shaft torque characteristics against engine speed.

Special attention should be paid to the combination with the side port exhaust system. This type holds great promise of future development because of the larger degree of freedom in its construction.

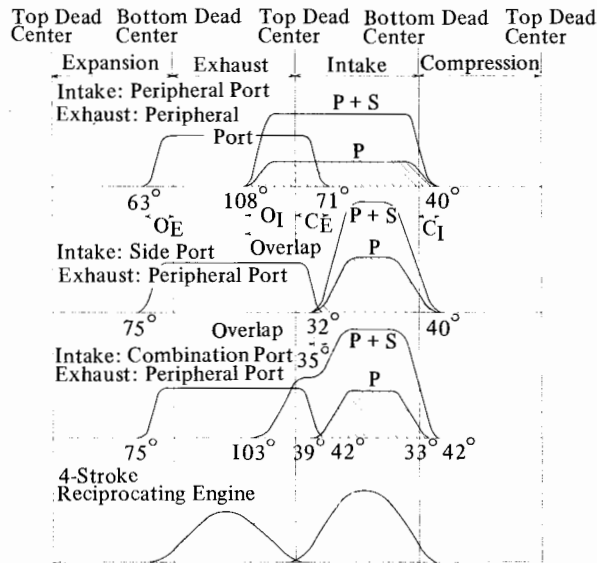


Fig. 3. 4 Intake/exhaust port open/closed periods and opening time/area

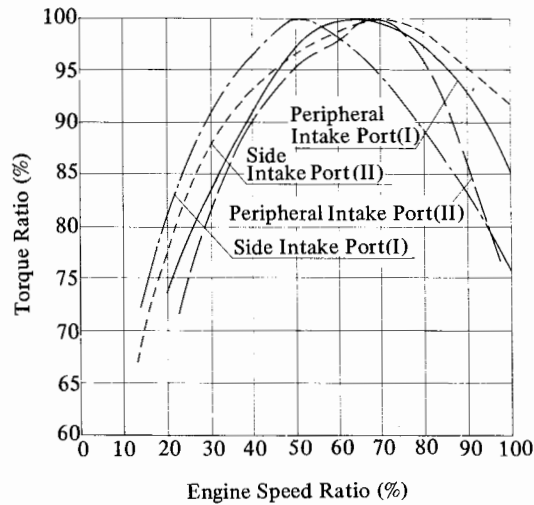


Fig. 3. 5 Engine/shaft torque characteristics

3. 1. 3 Examples of intake and exhaust port construction

(1) Peripheral port intake system

Fig. 3. 6 illustrates the intake system structure of the Model NSU-KKM 612 two-rotor engine. The short intake pipe contains independent primary and secondary passages connected to a two-stage carburetor. This prevents flow resistance for intake air, the effect of port overlap and the pressure interference of intake air between front and rear rotor chambers. Use of a port valve makes the intake pipe volume as small as possible.

The primary and secondary intake air passages join together inside the rotor housing to ensure proper intake air velocities matched to various operating conditions.

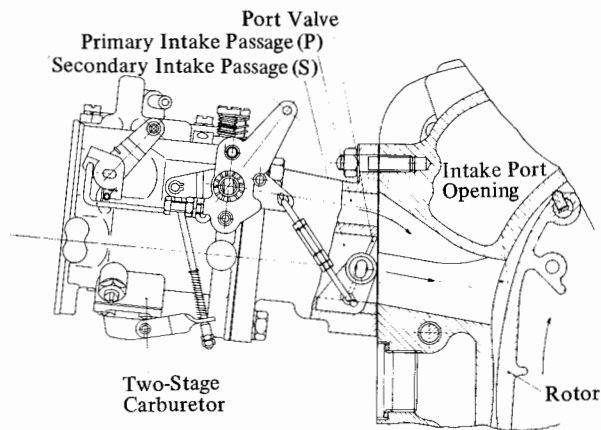


Fig. 3. 6 Peripheral port system sectional view

(2) Side port intake system

Fig. 3. 7 shows in outline the intake/exhaust operation of Toyo Kogyo's Model 0820 two-rotor engine, a combination of two-stage, four-barrel carburetor and dual exhaust manifold system. Fig. 3. 7 (b) shows a sectional view of the Model 0820. Preheating of the riser by exhaust gas is performed on only the primary intake passage. This promotes vaporization of the intake mixture during light load operation, and minimizes the reduction in charging efficiency during heavy load operation, when secondary intake is activated.

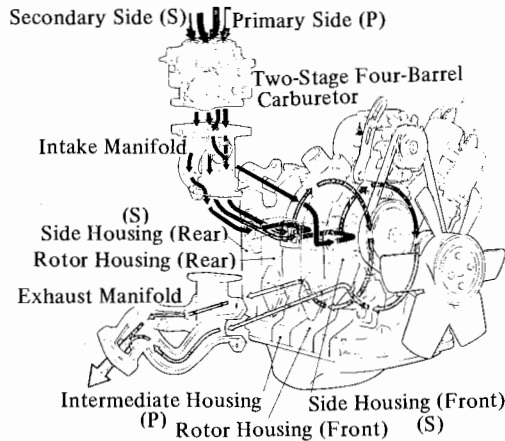


Fig. 3. 7 (a) Side port intake system structure

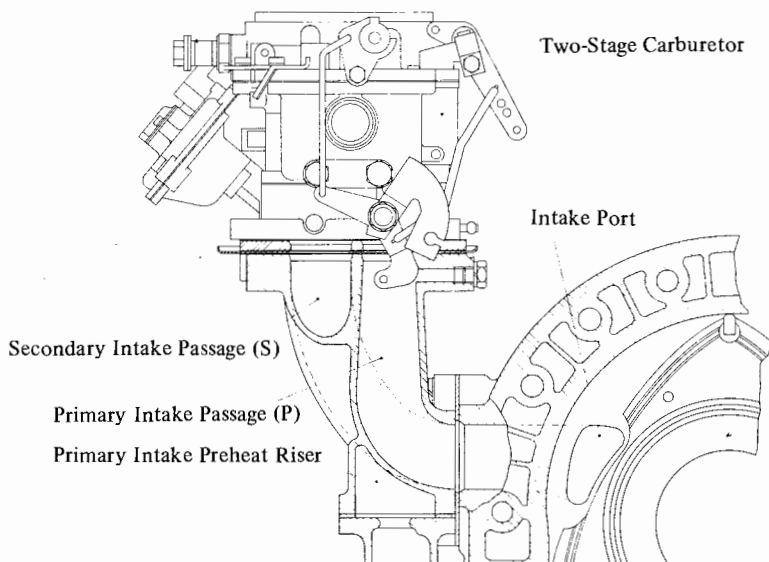


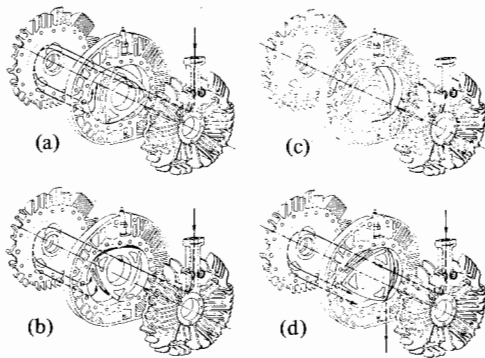
Fig. 3. 7 (b) Side port intake system sectional view

Fig. 3. 8 shows the intake passage of the Fichtel & Sachs' Model KM 37 single-rotor air-cooled engine employing the side port intake system. The intake mixture of fuel and lubricating oil is inducted into the combustion chamber through the

intake port, passing through the passage inside the side wall, the flow starting from the inlet port in one side housing, through the passage inside the rotor and around the rotor bearing, to the outlet port in the other side housing. Intake efficiency and high power performance are limited in this system owing to its comparatively long intake passage, and to the temperature rise of the intake mixture accompanied by rotor cooling. However, this system is noteworthy for its light weight, compactness, and low manufacturing cost.

(3) Exhaust port

As for the exhaust port a peripheral one is used generally. Depending on desired output, driveability, etc., a variety of port configuration including circular, rectangular and multiple ports are conceivable. Fig. 3. 9 shows an example of multiple ports adopted by Toyo Kogyo. In this instance where the port is divided into three openings on the trochoid surface, the abrupt expansion of combusted gas at the instant the apex seal opens the exhaust port is alleviated, and the exhaust noise level is much lowered as compared with the conventional port with a single opening.



- (a) Chamber 1-2 intake ends
- (b) Chamber 1-2 compression, top dead center, ignition
- (c) Chamber 1-2 expansion ends, exhaust begins
- (d) Chamber, 1-2 exhaust ends, intake begins

Fig. 3. 8 Side port intake system of single-rotor air-cooled engine

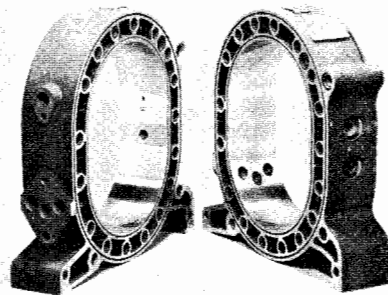


Fig. 3. 9 Multiple port

3.2 Housings

In designing the rotor housing and the side housing, which structurally correspond to the cylinder block and cylinder head in reciprocating engines, mechanical stresses as well as the thermal stress effects of the combustion gas must be taken into consideration. Especially careful design of these housings is of the utmost

importance, because deformation of the trochoid on which the gas seals slide or of the side wall of the side housing, would directly affect sealing effectiveness and hence engine performance.

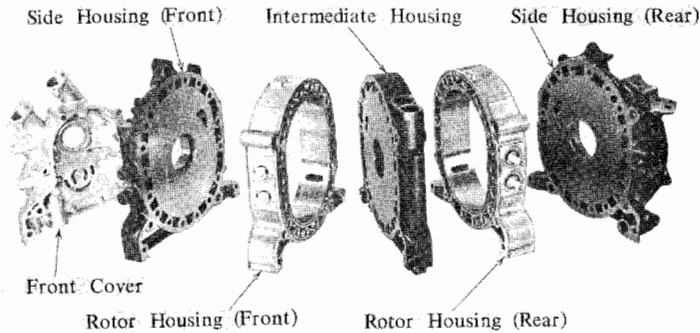


Fig. 3. 10 Two-rotor engine housing construction

3. 2. 1 Essentials of rotor housing design

Housings are considered subject to at least these four stresses :

- (1) Mechanical stress, which has a close relationship to the strength and the rigidity of the housing. This stress, which is cyclic, is mainly caused by repetition of pressure variations. The amplitude and the absolute magnitude of the stress are proportional to the mean effective pressure and combustion pressure.
- (2) Thermal stress due to nonuniform temperature distribution in the housing. In rotary engines, components exposed to the combustion process are separated from those exposed to the intake process. This causes thermal stress around and between these different working areas. This temperature gradient in the housing increases in proportion to engine output. As the engine output or operating conditions are varied, this temperature difference changes, causing an additional increase in thermal stress. Careful attention should be paid to this phenomenon because of the frequent load changes that are required of automotive engines.
- (3) Thermal shock stress appearing on the surface of the combustion chamber, which is exposed to the high temperature of the combustion gas. This is a factor which seriously affects the fatigue life of the housing surface.
- (4) Stress due to the tightening of the bolts to attach the housings in assembling the engine. This stress also varies according to thermal effect.

The actual stress imposed on the housing is the complex resultant of these stresses interacting with each other, and frequently the result is quite a severe stress.

The combustion region, for example, is subject to much more severe thermal conditions than in the reciprocating engine, since each rotation of the output shaft

is accompanied by combustion. This makes a heavy thermal-load concentration in the combustion region of the housing, which all but eliminates the cooling effect of the fresh intake charge.

Also, the permissible maximum temperature is limited by the two factors of performance and durability. These in turn are dependent upon combustion, lubrication, and temperature limits of the materials. The low temperature range during the intake and compression cycles also affects engine output performance, and has an effect on charging efficiency and atomization of the intake mixture. Therefore, care should be taken in design of the housing so that the maximum temperature in the high temperature region surrounding the combustion chamber is lowered and the differences in temperature over the whole trochoid are reduced to a minimum.

There are two types of available systems for cooling the housing, water cooling and air cooling. Up to now, the former has most often been used for higher output engines and the latter mainly for smaller engines or for special purpose engines.

3. 2. 2 Rotor housing materials

Fig. 3. 11 shows external views of a typical water-cooled and an air-cooled rotor housing.

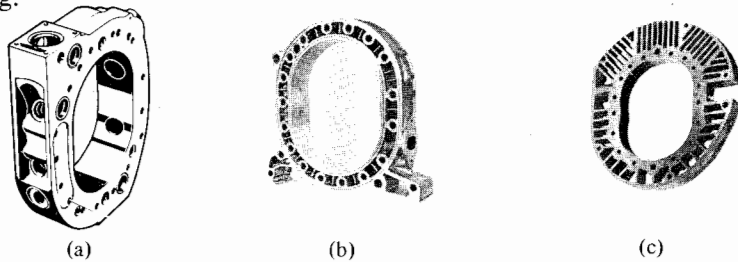


Fig. 3. 11 Rotor housing

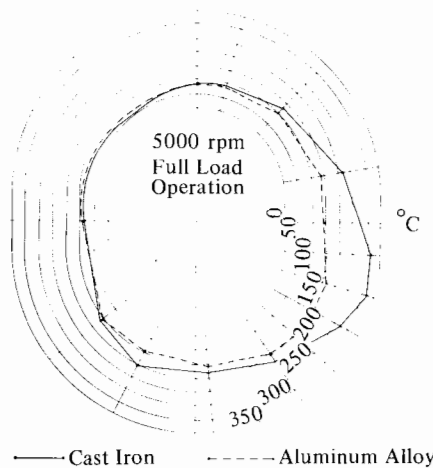


Fig. 3. 12 Comparison of trochoid surface temperature (water cooling)

(a) shows a circumferential-flow type housing in which cooling water flows along the trochoid. This type has a completely closed sectional structure. (b) shows the axial flow type cooling system in which the cooling water flows axially outside the trochoid. (c) shows the axial flow type air-cooled housing.

Fig. 3. 12 shows the results of temperature distribution measurements taken on the trochoid surface at rotor housings made of cast iron and of aluminum alloy. The temperature is about 140° higher for the cast iron housing than for the aluminum alloy housing, and far exceeds the permissible temperature for maintaining the lubricant oil film.

Thus, the application of cast iron to engine housings encounters difficulties under heavy load operating conditions. From the above consideration, it follows that materials such as Aluminum Alloy AC4A (SAE 309) and AC4D (SAE 322), which have high strength under high temperature conditions, excellent durability and elongation should be used. Table 3. 1 gives the chemical composition of Gamma Silmin Aluminum Alloy.

Table 3. 1 Chemical composition of rotor housing material

Chemical composition (%)								
	Cu	Si	Mg	Zn	Fe	Mn	Ti	Al
AC4A	up to 0.2	8.0~ 10.0	0.3~ 0.8	up to 0.7	up to 0.7	0.3~ 0.8	up to 0.2	balance
AC4D	1.0~ 1.5	4.5~ 5.5	0.4~ 0.6	up to 0.3	up to 0.6	up to 0.5	up to 0.2	balance

3. 2. 3 Wear resistant treatment of the trochoid surface

The surface of the trochoid requires a hardening treatment to improve resistance to wear from contact with the apex seals.

For this purpose, the application of chromium electroplate on the trochoid surface has proved effective when combined with metalized carbon for the apex seals. This chromium electroplate on aluminum alloy is shown in Fig. 3. 13.

The chromium layer is about 0.15 mm thick and has a Vicker's hardness in the range of 800 to 900 which is far higher than that of heat-treated cast iron or steel.

Chromium reveals strong resistance to corrosion from such combustion products as H₂SO₄, H₂S, HNO₃ and NH₄OH.

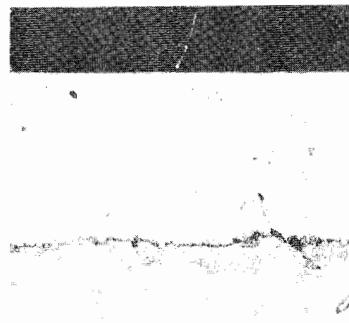


Fig. 3. 13 Section of hard chromium electroplate before honing

In addition, the chromium has a remarkably small coefficient of friction compared with that of other materials. These properties are quite effective in reducing wear of the trochoid surface.

Direct chromium plating on aluminum is not always easy technically. Thin chromium plating in particular has a problem in stability. In 1967 Toyo Kogyo concluded an agreement with National Lead Company in the U. S. on T. C. P. (Transplant Coating Process), and as a result of research and development has completed a T. C. P. rotor housing having an 80 C sprayed layer as the base for a further reliable chromium plating on the trochoid surface.

When special cast iron is used for the apex seals, a trochoid surface electroplated with nickel containing silicon carbide powders has proved effective in some practical uses. Various interesting attempts will no doubt be made in the treatment of the trochoid surface as advances in the development of rotary engines are made.

3. 2. 4 Wear resistant treatment of the side housing

(1) Metal spraying

Aluminum alloys are employed in high-power engines for the side housing, for considerations of weight reduction and cooling efficiency. As is the case with the rotor housing, Gamma Silmin Alloy (AC4A) is often the alloy used, after T-6 treatment (solution heat treatment, precipitation hardening). In this case, the surface of the side wall on which the seal pieces slide is metal sprayed to form a strong wear-resistant layer.

An effective treatment is one in which the aluminum alloy is bonding-coated by an inner layer of molybdenum as the sprayed metal, on which 0.8% carbon steel wire is sprayed so that the resultant layer is about 0.2mm in thickness.

Table 3. 2 Chemical composition of metal-spray wire material

Chemical composition (%)						
Molybdenum wire	Fe 0.016	Cu 0.0078	Ni 0.030	Unevaporated scale 0.006	Balance Mo	—
0.8% carbon steel wire	C 0.80	Si 0.28	Mn 0.53	P 0.021	S 0.017	Balance Fe

Table 3. 2 gives examples of the constituents contained in the metal spray wire. The reason why molybdenum is used as an under-coating material lies in the increased adhesiveness of a 0.8% carbon steel to aluminum alloy. As is well known, even molybdenum has a high melting point and a resiliency at 900°C 30% higher than that of steel at normal temperature.

In addition, it has a high specific gravity, which enables the molten grains of sprayed metal to strongly adhere to the aluminum alloy. Another favorable feature of molybdenum is the exposure of its fresh metal surface due to the rapid evaporation of the oxidized film on the old surface, when it is heated over 800°C in air.

Therefore, molybdenum adheres to the aluminum alloy of the base metal as its diffusion progresses and the molybdenum grains also adhere well to each other. Thus, a strong bonding layer is formed between the aluminum alloy and the molybdenum, and this improves the adhesive characteristics of the applied sprayed layer of 0.8% carbon steel. The special properties of the sprayed 0.8% carbon steel are derived from the rapid cooling of the molten grains, which results in the formation of a hard surface layer by the complete transformation of the carbon steel to martensite. In this martensite matrix, FeO and a porous structure effective in retaining a lubricating film are formed, and an ideal wear-resistant sliding surface is obtained.

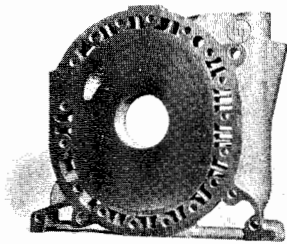


Fig. 3. 14 Metal-sprayed side housing

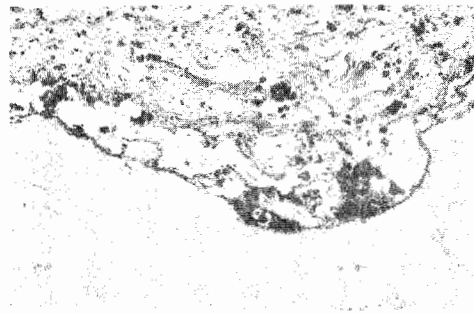


Fig. 3. 15 Section of metal-sprayed layer

Fig. 3. 14 shows an example of the metal-sprayed side housing. Fig. 3. 15 shows the microscopic structure of the metal-sprayed surface magnified 120 times. On the aluminum alloy can be observed the molybdenum layer, on which the sprayed layer of 0.8% carbon steel was converted into martensite, in the form of stripes. Measurements on the amount of wear distributed on the sliding surface of the side housing are shown in Fig. 3. 16.

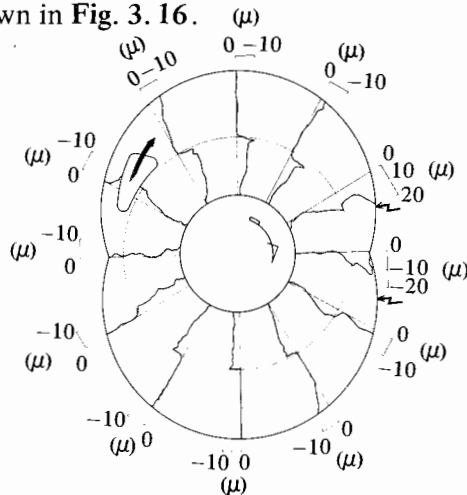


Fig. 3. 16 Wear on side housing sliding surface

The engine was run on a bench simulating the running conditions for a 100,000 km trip. A maximum wear of about 15μ was developed where the side seal travelled around the minor axis of the trochoid in the high temperature region. A relatively high amount of wear along the sliding trace of the oil seal ring is observed in the vicinity of the major axis of the trochoid in the cool region of the intake side. The absolute value of the wear depth, however, remains small. It can be said that the wear resistant properties of the metal-sprayed 0.8% carbon steel layer pose no problem in actual use.

(2) Induction hardening

The use of cylinder-cast-iron for the side housing, with induction-hardened side wall sliding surfaces, is an effective means of reducing the number of manufacturing processes and improving the rigidity of the housing. This method has already been applied successfully.

Fig. 3. 17 shows an example of the side housing to which induction hardening was applied. In this method, the radially striped hardened layer is deposited so that an increase in grinding stock due to the accumulation of hardening strains is held to the minimum possible level.

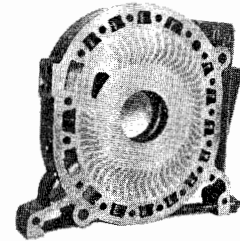


Fig. 3. 17 Induction hardened side housing

3.3 Rotor

3.3.1 Function and structure

The rotor is provided, as in the case of piston, with gas seal pieces (the apex seals, side seals and corner seals) to keep the working chamber gas-tight. Also, oil seal rings are provided to prevent lubricating oil from leaking up into the combustion chamber. The outer arc-shaped surface of the rotor is provided with a recess to attain effective combustion.

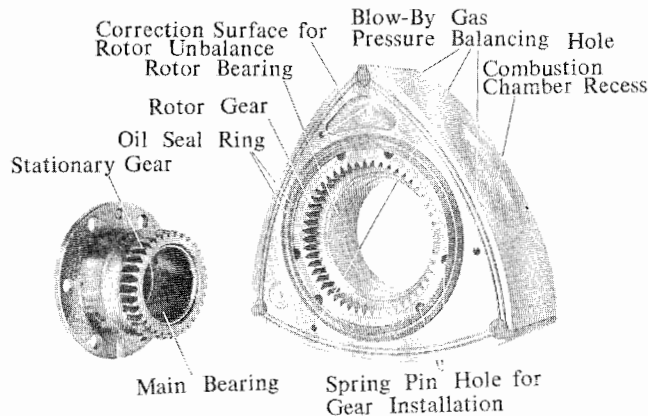


Fig. 3. 18 Rotor and stationary gears

The rotor also performs the function of the connecting rod in a reciprocating engine. It is fitted at one side with a rotor gear and mated with an stationary gear fixed on the side housing so that the rotor apex always rotates while tracing the trochoidal curve.

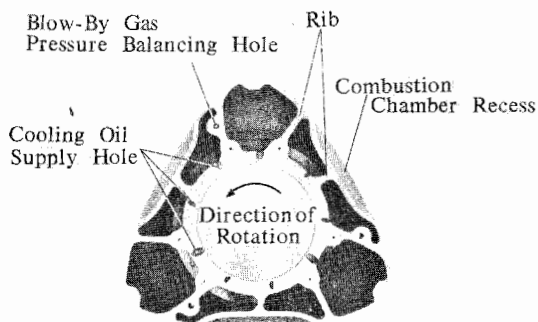


Fig. 3. 19 Rotor cross section

Fig. 3. 19 shows a cross-sectional view perpendicular to the rotor axis. The combustion chamber recess offers a very large freedom of designing, and an optimum configuration as required by the engine can be obtained by changing its depth and width, by largely varying the recess configuration and by shifting its position back and forth in the circumferential rotating direction.

The arrangement of ribs forming the hollow chamber inside the rotor should be made with due consideration of the internal cooling effect as well as the strength of the structure.

For this purpose, in the example shown in Fig. 3. 19, the ribs are slanted to trail the direction of rotation so as to improve the flow efficiency of the cooling oil, instead of arranging the ribs in simple radial form. Three holes passing through both sides of the rotor are provided for balancing the blow-by gas pressure between the oil seal and the side seal on both sides of the rotor. In the case of the peripheral port engine especially, pressure difference between the rotor sides can occur abruptly. Those holes balance such pressure difference, thus stabilizing the rotor position and preventing a rotor side from suddenly contacting the rubbed surface of the side housing.

In theory, the arc-shaped contour of the rotor is based on the inner envelope of the peritrochoid. However, it is not always necessary to apply this in practice. In fact, an approximate circular arc is often used in consideration of clearance for thermal expansion.

One of the major functions of the rotor configuration is to control the port timing. For example, when the peripheral layout is adopted for the intake and exhaust ports, the port timing is controlled by means of the apex seals provided at the three apexes of the rotor, while in the side port layout with the intake and exhaust ports provided in the side housing, both sides and the arc-shaped configuration of the rotor function as the intake and exhaust valves.

3.3.2 Rotor materials

The requirements for the materials of the rotor are summarized as :

- (i) High strength at high temperature and high fatigue resistance
- (ii) Low specific gravity
- (iii) High coefficient of thermal conductivity
- (iv) Low coefficient of thermal expansion
- (v) Good wear resistance
- (vi) Good casting and machining properties.

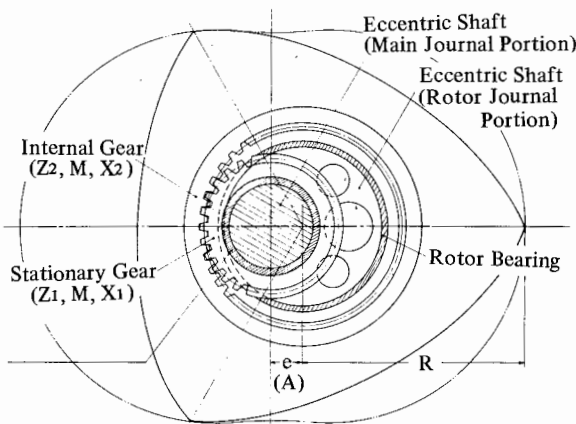
Up to the present time, special cast irons such as ductile cast iron have been widely used to satisfy items (i), (iv) and (v). The high specific gravity and small coefficient of thermal conductivity of the ductile cast irons are compensated for by reducing rotor weight through improved rotor construction and by forced cooling inside the rotor.

In order to attain higher speeds and higher specific output, reduction of rotor weight is a major problem, and in this sense a rotor of aluminum series alloy can be said to be one of the directions future research will take.

3.4 Design of the Phasing Gear

The phasing gears, consisting of the stationary external gear fixed on the side housing (which also functions as the housing for the main bearing), and the internal gear installed inside on one side of the rotor, are automatically determined by the basic dimensions of the engine, especially as to trochoid eccentricity (e) and trochoid generating radius (R) as mentioned in Section 2.4.2.

Therefore, these phasing gears are generally designed as shifted spur gears, in which case the mating equations for the shifted internal gear are expressed as



$$\text{inv } \alpha = 2 \tan \alpha_h \frac{X_2 - X_1}{Z_2 - Z_1} + \text{inv } \alpha_h \quad (3.1)$$

$$A = A_o + yM + a_s \quad (3.2)$$

$$A_o = \frac{Z_2 - Z_1}{2} M \quad (3.2a)$$

$$y = \frac{Z_2 - Z_1}{2} \left(\frac{\cos \alpha_h}{\cos \alpha} - 1 \right) \quad (3.2b)$$

$$a_s = \frac{S_n}{2 \sin \alpha} \quad (3.2c)$$

Fig. 3.20 Construction of the trochoid phase gears

where :

α : Operating pressure angle	y : Coefficient of increase in center distance
α_h : Cutter pressure angle	a_s : Center distance increase to provide backlash to gear
x_1 : Addendum modification coefficient of the external gear	S_n : Normal backlash
x_2 : Addendum modification coefficient of the internal gear	A : Center distance between shifted gears
z_1 : Number of teeth of the external gear	A_0 : Center distance between standard gears
z_2 : Number of teeth of the internal gear	M : Module

When using equations (3. 1) and (3. 2), letting the center distance (A) between the mating gears equal the eccentricity of the rotor journal, that is, $A=e$, and the ratio of the tooth number of the stationary gear to that of the rotor gear $z_1 : z_2=2 : 3$. The normal backlash (S_n) is determined by taking into account the clearance of the rotor bearing and that of the main bearing.

Normalized structural steels such as S450 are used as the material for the gears.

The following gear dimensions of an engine with a single working chamber volume of 491cc are presented as an example :

Center distance of mating gears	A	: 15
Module	M	: 1.75
Cutter pressure angle	α_h	: 20°
Number of teeth of external gear	z_1	: 34
Addendum modification coefficient of external gear	x_1	: 0.301
Number of teeth of internal gear	z_2	: 51
Addendum modification coefficient of internal gear	x_2	: 0.40

3.5 Tooth Load

It is considered that tangential loads act on the tooth faces of the phasing gears, when variations in the rotor rotating speed are caused by non-uniform gas pressure distribution or by rapid pressure rise during the expansion process, while the exhaust port is closed. The tooth load is affected by both operating conditions and the structural conditions of the phase gears.

- (i) The effects of the operating conditions on the tooth load are as follows :
- (1) The tooth load tends to increase with increasing engine speed.
 - (2) The tooth load increases as the engine load increases.
 - (3) The tooth load increases with advancing spark timing.
 - (4) The tooth load increases significantly when abnormal combustion such as knocking or pre-ignition occurs.

- (ii) The effects of the structural conditions of the phase gears on the tooth load are generally smaller than those mentioned above, and include such factors as :
- (1) The torsional rigidity of the gear train
 - (2) Normal backlash, the pitch error and the tooth shape error of the gears
 - (3) Bearing clearance
 - (4) Moment of inertia of the flywheel

Fig. 3. 21 shows the measured tangential loads working on the teeth of the stationary gear for a typical case.

The fundamental means to reduce the tooth load of the phase gears lie in the possible elimination of the non-uniform gas pressure distribution exerted on the arc-shaped configuration of the rotor. It is also effective to absorb the tooth load through changing the effective elasticity of the phase gears. For this purpose, such means as shown in Fig. 3. 22 (b) by which the rotor and the rotor gear are connected by spring pins in place of bolts as in Fig. 3. 22 (a), have been found to be effective.

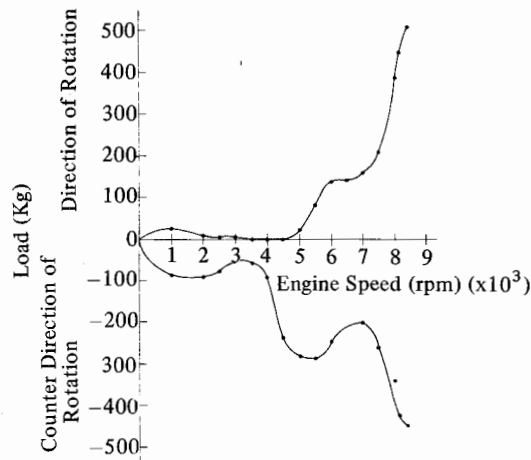


Fig. 3. 21 Tooth load of the stationary external gear

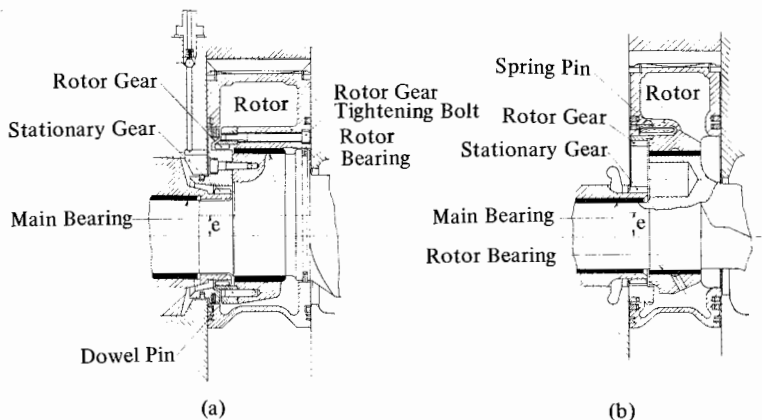


Fig. 3. 22 Structure of rotor installation

3.6 Eccentric Shaft and Bearing

Such materials as chromium steel and chromium molybdenum steel have been used for the eccentric shaft, which corresponds to the crankshaft in reciprocating engines. Each journal part of the shaft is hardened either by cementation or induction hardening.

Both Figs. 3. 23 and 3. 24 illustrate examples of the eccentric shaft construction of a two-rotor engine which employs a forced lubrication system.

A key-groove is machined in the front part of the shaft so that an arc-shaped balancing weight as well as a gear or a V-pulley for driving auxiliary equipment can be attached to the front end. The tapered rear end is designed so that a flywheel, which functions as a balancing weight, can be fastened to it. The rotor journal is eccentrically formed (with eccentricity e) relative to the main journal axis, like the crank-pin journal in reciprocating engines.

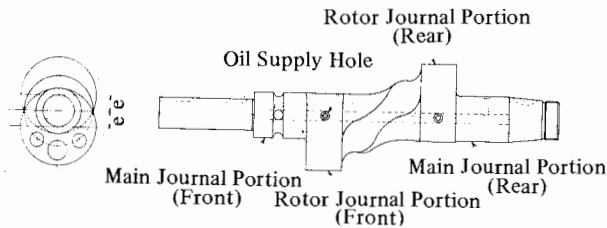


Fig. 3. 23 Two-rotor engine eccentric shaft

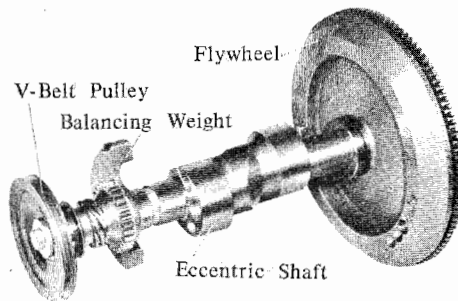
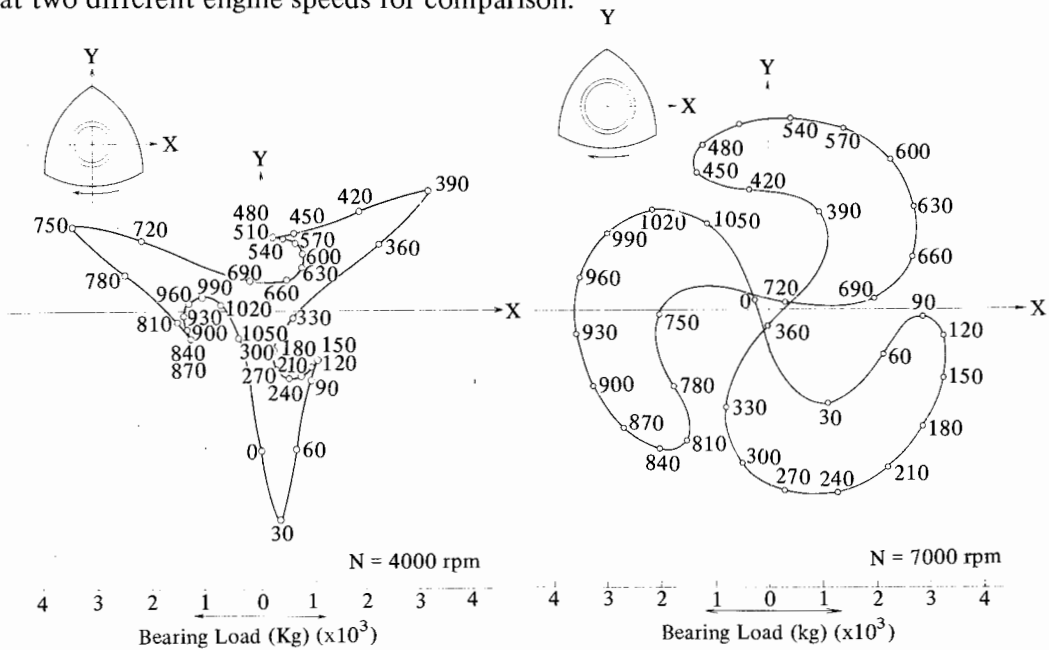


Fig. 3. 24 Construction of two-rotor engine output shaft system

The rotor journal receives the force of combustion working on the arc-shaped configuration of the rotor through the rotor bearing, and the force is converted into output torque. An oil passage is provided through the shaft center for the lubrication of both main and rotor bearings and for the cooling of the rotor.

Roller bearings are used in smaller sized engines for the output shaft bearings such as the rotor and main bearings, whereas copper lead alloys or aluminum alloys are often used for engines operating over a wide range of speeds and under severe load conditions. When using these high speed bearings, various means should be employed to prevent bearing seizure, such as the prevention of any roughness on the

bearing surface, maintenance of oil cleanliness, and assurance of a moderate oil temperature in the equilibrium state. Special attention should be paid to the rotor bearing, since the load distribution at high speed differs greatly from that at low speed, as shown in the polar diagram. Therefore, the oil supply paths for these parts should be carefully designed. Fig. 3. 25 shows the polar diagram of the rotor bearing load for an engine with a single working chamber volume of 491cc measured at two different engine speeds for comparison.



The number shows the rotation angle of the eccentric shaft with combustion top dead center as 0°.

Fig. 3. 25 Rotor bearing load polar diagram

Reference Materials

- 1) Japan Metal-Spray Society : Yosha-benran (Metal-Spray Handbook). Nikkan-Kogyo Press (1964)
- 2) A. K. Wood : A New Method of Making Cylinder Bore Wearproof. SAE Paper 784 A, January (1954)
- 3) Kei Matsui and Takaro Sasame : Application of Metal-Spray to Rotary Engine. Nihon Yosha Kyokai-shi (Japan Metal-Spray Journal, Vol. 5, No. 2 (1968)

4. GAS SEAL

4.1 Principal Construction

The gas seal pieces in a rotary engine correspond to the piston rings in a reciprocating engine. They must serve not only to prevent compressed gas leak and blow-by of combustion gas, but also to release a part of the heat captured by the rotor onto the wall of the housings. The gas seal of a rotary engine, therefore, should satisfy the following principal conditions :

- (i) The gas seal for the working chamber should form a complete, continuous sealing line.
- (ii) The seal should maintain enough pressure to keep the sealing line intact even when the gas pressure or inertia working on the seal changes during operation.
- (iii) It should be able to allow the clearance requirements for thermal expansion and manufacturing tolerance.
- (iv) It should maintain proper oil film over the surface where the gas seal comes into contact.

The gas seal of the NSU-Wankel engine is designed to meet fully these basic conditions, and due to a great amount of effort directed toward improvements in construction and materials, the seal has become completely practicable both in sealing effect and durability.

In the NSU-Wankel engine, the working chamber is composed of the stationary parts (rotor housing and side housing), and the rotor, which moves in relation to the stationary parts. The gas tightness of the working chamber is maintained by preventing gas leakage through the gap between the rotor apex and the trochoid surface of the rotor housing, and the gap between the side of the rotor and the surface of the side housing.

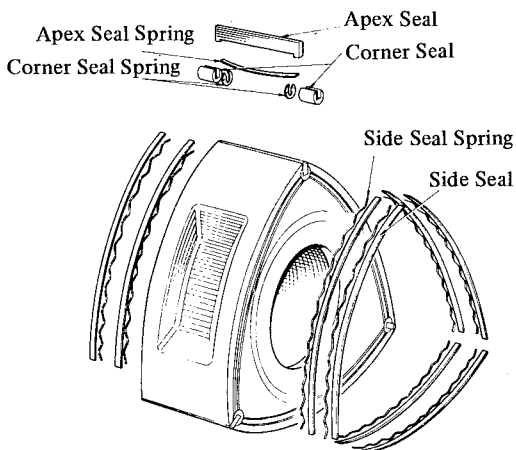


Fig. 4. 1 Basic layout of gas seals

The basic layout of the gas seal pieces for the sealing effect is illustrated in Fig. 4. 1. The apex seal is installed on each apex of the rotor. The arc-shaped side seal is used on both sides of the rotor. At each of the joints of these seals, a cylindrical corner seal is installed. All of these seals are backed by springs.

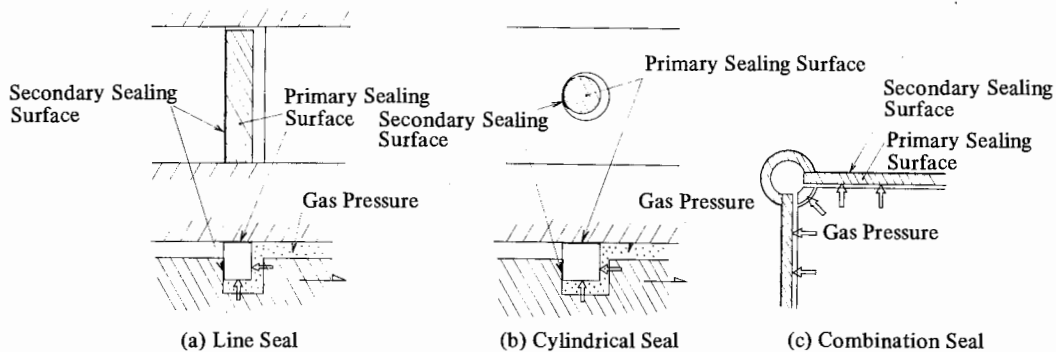


Fig. 4. 2 Function of gas seals

The working principle of these gas seals is illustrated in Fig. 4. 2. Shown in (a) is a line seal, the type used as side seals and apex seals in the grooves of the rotor. (b) is a cylindrical seal, the type used as corner seals. Each of these seals is pushed two ways by gas pressure, first to one side of the groove, and then onto the sliding surface. The former is referred to as the "Secondary sealing surface" and the latter, the "Primary sealing surface". The basic requirement of a gas seal is to maintain sealing effect on these two surfaces.

The line seal naturally has two ends, and some clearance has to be provided at each end for heat expansion. Therefore, gas leakage at the ends is inevitable, and it is impossible to provide complete sealing by only combining line seals. In order to fill the gap at the end and provide complete sealing, a cylindrical seal is adopted at the joint as illustrated in (c). Shown in Fig. 4. 3 is a magnified sketch of the sectional view of the seal joint. The part where the side seal and corner seal join is designed so that, while a continued sealing line is maintained with necessary clearance held, each seal piece can operate independently of the others. As a result, the seals are allowed to have thermal expansion, and the seal can move up closer to the sliding surface to take up wear on the seal piece, so as not to hamper the sealing effect.

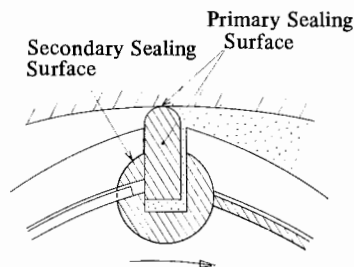


Fig. 4. 3 Gas seal joint

As was explained in the previous chapter, which deals with the basic principles, the pressure for pushing the gas seal, while the engine is in operation, is obtained from the gas pressure and the pressure difference between two adjoining working chambers. Therefore, the spring installed beneath each seal piece serves primarily to provide the necessary push on the seal at the time of engine start. Therefore the initial spring load can be made light.

However, if the sealing edge were in direct contact with the metal surface, the microscopic roughness of the surface would cause gaps, and result in a poor sealing effect. It would also lead to increased wear and friction losses resulting

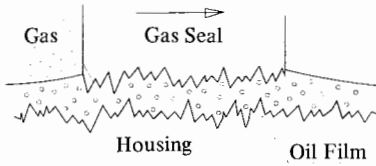


Fig. 4. 4 Function of the oil film

from seizure of the metal-to-metal sliding surfaces. Therefore, it is necessary to maintain a proper oil film on the sliding surface to permit the seal to ride on the film surface as shown in Fig. 4. 4. Various positive lubricating methods are employed in order to attain this.

4.2 Apex Seal

As previously mentioned in connection with the geometrical construction of the trochoid, the apex of the rotor leans. This leaning motion, which should be held to less than 30 degrees, is helpful in reducing wear on the apex seal. For, if the apex is made to slide on the inside surface of the trochoid making the same line contact all the time, it will heat very rapidly and result in extreme wear of the apex.

In an actual example, curve "L_a" is parallel to the peritrochoid "L₂", and the top surface of the apex seal is finished round to a radius of "a", equivalent to the distance between "L_t" and "L_a". As a result, the contact line between the top surface of the apex seal and the inside wall of the rotor housing moves around the rounded top surface of the apex seal within the leaning angle of $\pm \varphi_{max}$ thus assuring superior anti-wear characteristics. The center of the leaning is on "L_a".

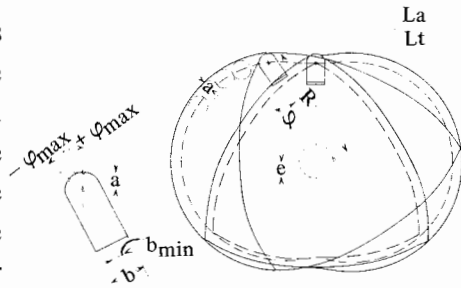


Fig. 4. 5 Parallel peritrochoid curve and leaning motion of apex seal

The minimum width (b) of the apex seal should be determined, giving consideration to the extent of leaning, according to the following :

where : $b \geq 2 a \sin \varphi_{max} ; b \geq \frac{6ea}{R}$

- a : Equidistance of peritrochoid
- φ_{max} : Maximum leaning angle of rotor apex
- e : Eccentricity of eccentric shaft
- R : Generating radius of peritrochoid

Fig. 4. 6 compares the sliding speed of the top surface of the apex seal with that of the piston ring of a reciprocating engine of comparable size. As seen from the drawing, the maximum sliding speed of the apex seal is about 16% faster than that of

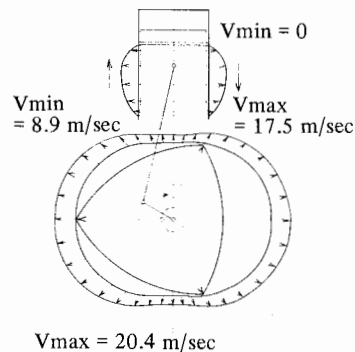
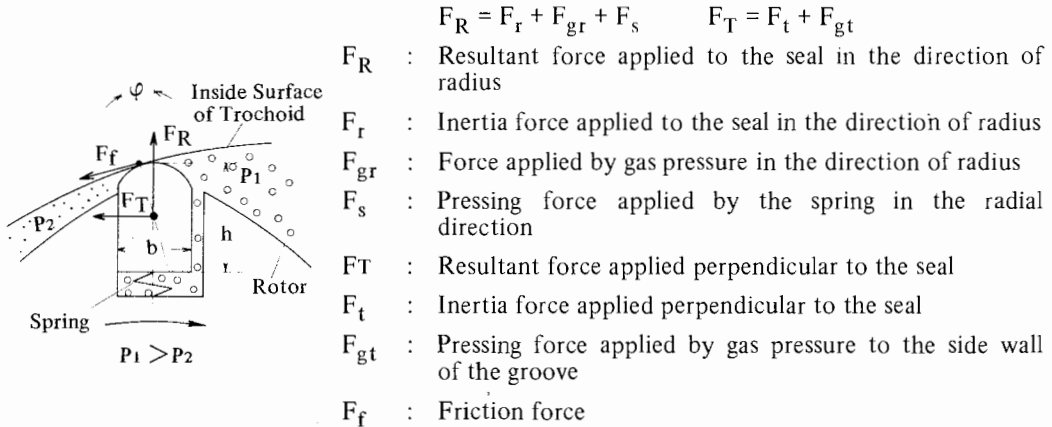


Fig. 4. 6 Sliding speed of the apex seal and sliding speed of a piston ring.

the reciprocating engine. However, with a reciprocating engine, at both top and bottom dead center, the direction of slide reverses and the sliding speed becomes zero momentarily. This tends to break the oil film and causes substantial wear of the cylinder at those spots. In the rotary engine, the seal continues moving in the same direction, so the difference between the maximum and minimum seal speeds is relatively little. This is quite helpful in preserving the oil film.



- $F_R = F_r + F_{gr} + F_s \quad F_T = F_t + F_{gt}$
- F_R : Resultant force applied to the seal in the direction of radius
 - F_r : Inertia force applied to the seal in the direction of radius
 - F_{gr} : Force applied by gas pressure in the direction of radius
 - F_s : Pressing force applied by the spring in the radial direction
 - F_T : Resultant force applied perpendicular to the seal
 - F_t : Inertia force applied perpendicular to the seal
 - F_{gt} : Pressing force applied by gas pressure to the side wall of the groove
 - F_f : Friction force

Fig. 4. 7 Forces working on apex seal

Fig. 4. 7 illustrates the various forces exerted on the apex seal. The most important is the force applied by gas pressure. Others are inertia, friction, and spring force. All of these forces, with the exception of spring force, change in strength and direction continuously as the rotor rotates.

The pressing force applied by gas pressure in the direction of the radius is expressed by the following equation when $P_1 > P_2$.

$$F_{gr} = P_1 l \left\{ b - \left(\frac{b}{2} - a \sin \varphi \right) \right\} - P_2 l \left(\frac{b}{2} + a \sin \varphi \right)$$

$$= l \left(\frac{b}{2} + a \sin \varphi \right) (P_1 - P_2)$$

where :

- P_1 : Gas pressure inside high pressure side working chamber
- P_2 : Gas pressure inside low pressure side working chamber
- a : Radius of round top surface of apex seal
- b : Width of apex seal
- l : Axial length of apex seal
- φ : Leaning angle

The strength of pressing force is affected by the degree of lean of the apex edge and the pressure differential between two adjoining chambers.

The pressing force " F_{gt} ", which is applied by gas pressure to the apex seal to push it to one side of the groove, is expressed by the following equation :

$$F_{gt} = P_1 \cdot l \cdot h$$

where :

P_1 : Gas pressure inside high pressure side working chamber

h : Height of apex seal

l : Axial length of apex seal

In practice, there is a time lag between the change of gas pressure of the working chamber and that of the sealing groove because of the resistance in gas passage and the capacity of the open space in the groove. As a result, the pressing force resulting from the gas pressure will be slightly lower than that obtained by the above equation.

As seen from Fig. 4. 8, the inertia force is exerted onto the center of gravity of the apex seal. The resultant force is expressed by :

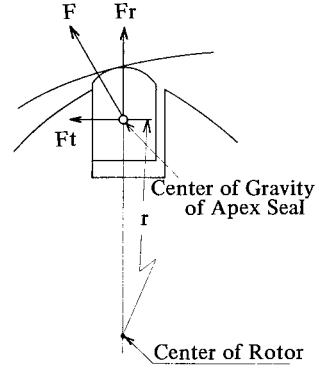


Fig. 4. 8 Inertia force working on the apex seal

$$F = \frac{W\omega^2}{g} \sqrt{e^2 + \frac{r^2}{81} + \frac{2}{9} er \cos \left(\frac{2}{3} \alpha \right)}$$

where :

r : Distance between the center of the rotor and the center of gravity of the apex seal

W : Weight of the apex seal

The resultant force can be divided into two components, one applied radially toward the center of the rotor, and the other perpendicular to the first.

These components are expressed, respectively, by :

$$F_r = \frac{W}{g} \omega^2 \left(\frac{r}{9} + e \cos \frac{2}{3} \alpha \right)$$

$$F_t = \frac{W}{g} \omega^2 e \sin \frac{2}{3} \alpha$$

where :

r : Distance between the center of the rotor and the center of gravity of the apex seal

W : Weight of the apex seal

e : Eccentricity of the eccentric shaft

α : Angle of rotation of the eccentric shaft

ω : Angular velocity of the eccentric shaft

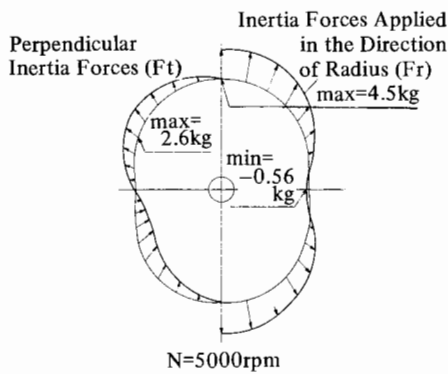


Fig. 4.9 Distribution of inertia forces exerted on the apex seal

The distribution of inertia force working on the apex seal is shown in Fig. 4.9. Shown in the left half of the diagram are perpendicular inertia forces, and the direction is reversed at the minor axis point of the trochoid. Forces applied in the radial direction are shown in the right half, and the value becomes negative near the minor axis point of the trochoid, where as a result the apex seal will receive a force applied in a direction to pull it away from the trochoid wall. This negative force however is easily absorbable by the spring force and gas pressure.

The perpendicular component " F_T " and the radial component " F_R " both of which are applied to the apex seal are expressed by :

$$F_R = F_{gr} + F_r + F_S$$

$$F_r = F_{gt} + F_t$$

where : F_S : Pressing force by spring

The frictional force " F_f " between the apex seal and the trochoid is expressed by :

$$F_f = \mu \cdot F_R / \cos \varphi$$

where : μ : Friction coefficient of the apex seal against the trochoid.

4.3 Side Seal, Corner Seal

The arc-shaped side seals and the cylindrical corner seals are installed on both sides of the rotor, and they serve to maintain gas tightness between the wall of the side housing and the side of the rotor. At points where these two seals join, a clearance of ΔE is provided as illustrated in Fig. 4.10 to allow for thermal expansion and manufacturing tolerance.

These seals, unlike the apex seal, contact the sliding surface with their full surfaces. As a result, there are hardly any problems of wear and effectiveness in sealing.

The pressing force for the sliding surface is exerted by the gas pressure and the spring.

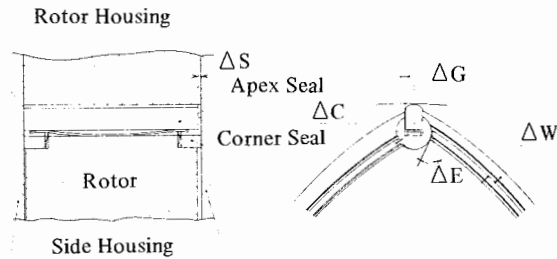


Fig. 4. 10 Clearance for gas seal installation

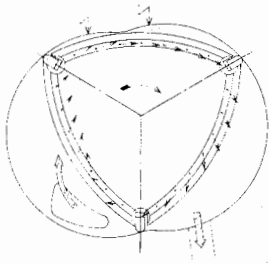


Fig. 4. 11 Directions of side seal sliding

Shown in Fig. 4. 11 is the direction of the side seal movement at a given instant. Since each side seal piece is long and installed away from the center of the rotor, the direction of movement and the strength and direction of the inertia force vary for different points on the seal piece. Therefore, thorough consideration should be given in the design to maintain the oil film and the smooth following up on sliding surface.

4. 4 Notes on Designing Gas Seals

The factors that will affect the sealing are total length of sealing, clearance between individual sealing pieces, and gas tightness around the primary and secondary sealing surfaces.

The sealing line length is of concern primarily with the side seals. Here it is necessary to take special steps to increase the sealing effect by, for example, double sealing. The length of the sealing line is also closely related to the number of rotors used and the specifications of the trochoid design. Therefore, when determining these specifications, it is desirable to give due consideration in the layout of the seals.

As for the clearance of the seal pieces, in addition to ΔE (shown in Fig. 4. 10), consideration must be given to ΔS . It is necessary to take positive measures to reduce ΔS , and one possibility is to adopt the split apex seal shown in Fig. 4. 12. This split type apex seal is referred to as the "Link Type." The trapezoidal center piece and the two triangular end pieces work together to automatically adjust the clearance.

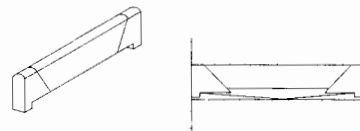


Fig. 4. 12 Split apex seal (Link type)

As for the primary and secondary sealing surfaces, whether or not their sealing is maintained during operation will greatly affect the overall sealing effect. The factors relating to these are the pressing force applied to the seal, oil film, and the following up of the seal on the surface of the housing.

The pressing force applied to the seal must depend on the gas pressure, except when starting. Therefore, the clearances in the seal grooves, which are shown in Fig. 4. 10 as ΔG , ΔW , and ΔC , which form the gas passage to the seal grooves, should be determined carefully. Furthermore, the clearances should be tested out to determine the optimum setting by experimenting with an actual engine.

When determining the clearances, the decision should be based on the gas pressure during operation, the effect of inertia force on the gas seal, thermal expansion, the sticking of the gas seal caused by combustion deposite, and the creep of the seal spring caused by high temperature gas.

Shown in Fig. 4. 13 is the time lag between the change of gas pressure in the combustion chamber and the rise of gas pressure at the bottom of the apex seal. This time lag is related to the absolute pressure of gas in the combustion chamber, the rate of pressure change (dP/dT), and the size of the side clearance ΔG .

Because of this phenomenon, under operating conditions that will cause a sudden rise in pressure (this may be the case when the ignition timing is advanced to the point where knocking almost starts with a full load), lack of pressure under the seal can result, and as a consequence, a part of the combustion gas will sometimes spit back to the intake portion of the engine over the VSP of the apex seal.

To prevent this, a cavity on the side of the apex seal (see Fig. 4. 14) is helpful. This cavity provides a passage for burned gas to reach the bottom of the seal to maintain the sealing effect, even when the top of the seal is pushed to one side by the frictional force at the top or by sudden increase of pressure.

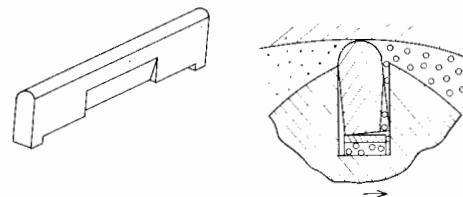


Fig. 4. 14 Function of the apex seal cavity

There are problems involving the fit between the seals and the surfaces over which they slide, since microscopic changes on the surfaces are unavoidable because of uneven temperature distribution and changes in the pressing force. Therefore it is necessary both to attempt to improve the sealing effect by maintaining an oil film on the sliding surface, and to improve the following up of the seal itself by, for instance, using flexible seals. Flexibility is especially a must for the side seal,

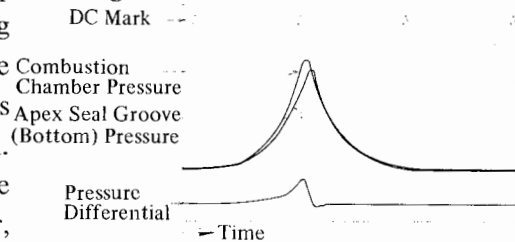


Fig. 4. 13 Time lag in pressure build-up at the bottom of the apex seal groove

because it is long and its movement is quite complex. This flexibility factor should be taken into consideration when determining width and thickness of the side seal.

One of the peculiar features of the rotary engine is the spark plug hole in the trochoid surface. This adds to the gas leakage every time the top of the apex seal passes over the hole, the amount depending on its location. Therefore, it should be located at a spot where the pressure difference between the two adjoining working chambers is relatively small, and the size of the hole should be kept as small as possible. Therefore, the spark plug electrode should be brought as close to the trochoid surface as possible.

4.5 Gas Seal and Sliding Surface Materials

When a minimum clearance high pressure seal is used to improve gas-tightness, it presents a problem of wear on the sliding surface and the seal piece due to friction between the two.

In general, this wear is caused by direct metal-to-metal contact between the two surfaces, foreign particles between the two, and chemical erosion, but metal-to-metal contact is by far the most important cause of the problem in connection with lubricating conditions.

In a rotary engine, the processes of explosion, expansion and exhaust take place each at a specific spot in the housing all the time. As a result, the seal pieces and the sliding surfaces are continuously exposed to high temperature and high pressure combustion gas at these particular spots. Therefore, the lubricating oil in those spots will lose viscosity or even burn out, making it difficult to maintain the oil film. This plus high speed and high power operating tend to lead to critical lubrication conditions.

In order to cope with these, attention should naturally be paid to the means of supplying lubricating oil, cooling the sliding surface, and even distribution of seal-push-up forces. Attention should also be directed to the selection of materials, for both the sliding surface and seal, so as to arrive at a combination that minimizes seizing or wearing even upon direct contact with each other.

The materials for both should of course have strong wear-resistance. Especially the housing material, on which the seal slides, should be of high melting point, and should maintain hardness and strength at high temperature. Also, it should not easily seize with other metals, and it must maintain oil film well.

In view of these conditions, it was an especially difficult task to find the right combination of materials for the trochoid surface and the apex seal, because of the thin line contact between seal and trochoid. The combination of hard chrome plated trochoid surface and cast iron seal, which was adopted at an early stage of development, resulted in wave-like "chatter marks" on the trochoid surface, as shown in Fig. 4. 15. This was caused by a sort of frictional vibration and was

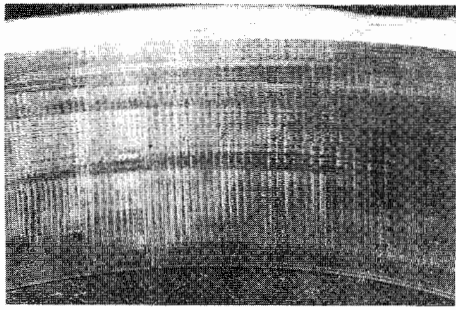


Fig. 4. 15 Chatter marks on trochoid surface

also affected by the conditions of trochoid lubrication, the natural frequency of the seal, and the coefficient of static and kinetic friction. It resulted in separation of the chrome plate from the trochoid, and it presented a big problem, since it severely limited engine life.

Of the many combinations tried since then, the combinations shown in **Table 4. 1** have proved the most satisfactory, and the chatter mark problem has been completely solved. One of the combinations uses an apex seal of special cast iron against a trochoid which is either sprayed with molten tungsten carbide or plated with chrome. The other uses a self-lubricating carbon apex seal, treated by a metal-impregnation process to improve impact resistance, against a hard chrome plated trochoid.

Table 4. 1 Rotor housing surface materials/apex seal materials

Surface materials of the rotor housing trochoid	Apex seal materials
Hard chrome plating	Special carbon
Mix plating of Ni and SiC	Special cast iron
Spraying of molten tungsten carbide	Special cast iron

Shown in **Fig. 4. 16** is a microscopic view of the structure of the carbon apex seal currently in use. The white specks spread throughout the formation are impregnated metal, and the black part is the carbon matrix. Various measures must be taken in controlling the shape, distribution, and quantity of carbon pores to obtain optimum results.

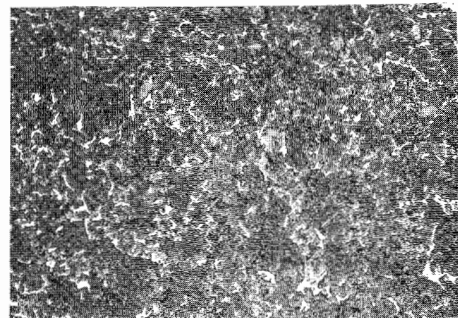


Fig. 4. 16 Microscopic view of carbon seal composition

No particular problems of wear are encountered in the corner and side seals, because of the larger contact areas, and the lubrication conditions which are better than for the apex seal.

For the side and corner seals, the cast iron material normally used for piston rings is used. The chemical analysis of the cast iron material is shown in **Table 4. 2**.

Table 4. 2 Standard composition of side seal materials

Chemical composition (%)								
C	Si	Mn	P	Cr	Ni	Mo	Cu	V
3.50	2.30	0.40	0.20	0.50	1.50	1.50	1.50	0.20

The sliding surface of the side housing is treated by a surface hardening process or by spraying with a metal highly resistant to wear. Representative combinations of these materials are shown in **Table 4. 3**.

Table 4. 3 Side housing surface materials/side, corner seal materials

Side housing surface materials	Side seal and corner seal materials
Molten sprayed Mo	Special cast iron
Molten sprayed 80C steel	Special cast iron
Induction hardened cast iron	Special cast iron

These cast iron seals are surface treated in the same way as piston rings and have a Ferox (oxidized ferrous) coating or a lubrite (phosphate) coating to facilitate the breaking-in process.

In order to provide necessary push-up force for the seal piece when starting, the seal spring is made of beryllium-copper, stainless steel, or some other heat resistant metal which is not subject to high temperature creep. The standard composition of 17-7PH stainless steel is shown in **Table 4. 4**. This 17-7PH stainless steel is of reduced hardening type and can be used safely under bending stress of 136 to 159 kg/mm² at temperatures up to about 370°C.

Table 4. 4 Standard composition of 17-7PH stainless steel

Chemical composition (%)					
C	Si	Mn	Cr	Ni	Al
0.07	0.40	0.60	17	7	1.15

Reference Materials

- 1) Kazuo Takada : Durability of Mazda Rotary Engine, Journal of The Society of Automotive Engineers of Japan Volume 21 No. 9 (1966)
- 2) F. Clar : Reibungs und Verschleißversuche bei hohen Gleitgeschwindigkeiten. VDI-Z, 109, Nr. 16 (1967).
- 3) w. G. Froede : NSU's Double Bank Production Rotary Engine. SAE Paper 680461 (1968).
- 4) W. D. Bensinger : Rotationskolbenmotoren für kraftfahrzeuge. ATZ 66/4.

5. COOLING

5.1 Cooling of Housings

5.1.1 Methods of cooling housings

Each phase of the working cycle of the rotary engine, from intake through exhaust, is performed at a fixed location on the trochoid curve, resulting in uneven heat distribution over the housings. Therefore for efficient cooling of the housings, whether it be by air or water, it is necessary to design the coolant passages and select housing materials with emphasis on minimizing temperature differentials over the entire trochoid, and lowering the maximum housing temperatures, which tend to become higher with the increase of both output and speed of the engine. At the present, one of the following two methods is used, depending on the size of engine and its application.

(1) Circumferential flow cooling

This is a method in which cooling water or air is circulated around the trochoid. The cooling water passages are shown in Fig. 5.1, and Fig. 5.2 shows a typical arrangement of cooling fins for a rotor housing designed for air cooling.

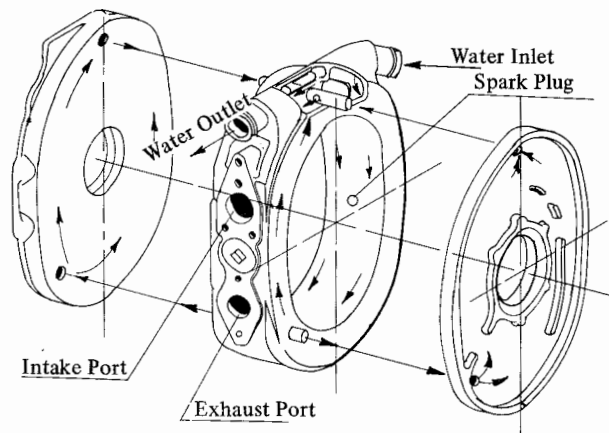


Fig. 5.1 Circular flow cooling

(2) Axial flow cooling

The axial flow air cooling method is one in which cooling air is directed around the exterior of the trochoid in the direction of its axis to remove heat from the housing. Illustrated in Fig. 5.3 is the arrangement of cooling fins on the side housing of an axial flow air-cooled engine. In the case of a water-cooled engine, cooling water flowing through the water jacket of the trochoid in the direction of the axis is turned around at the front and rear housings and flows back and forth between them.

Shown in Fig. 5. 4 is an example of cooling water passage arrangement for an axial-flow water-cooled engine.

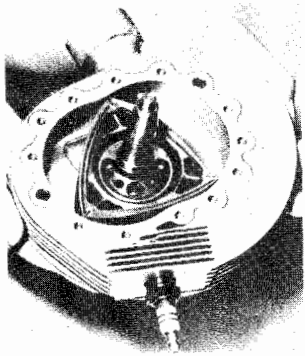


Fig. 5. 2 Air-cooled rotor housing fin arrangement

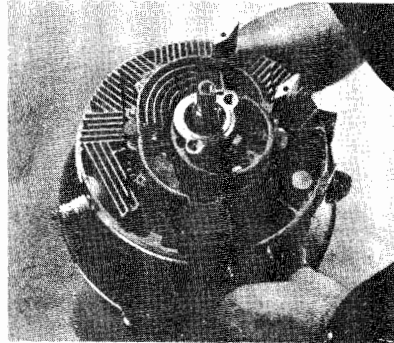


Fig. 5. 3 Air-cooled side housing fin arrangement

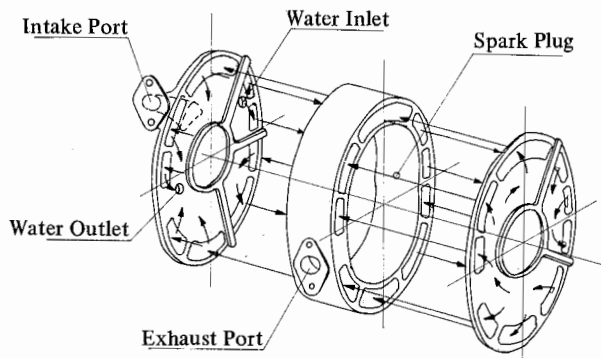


Fig. 5. 4 Axial flow cooling

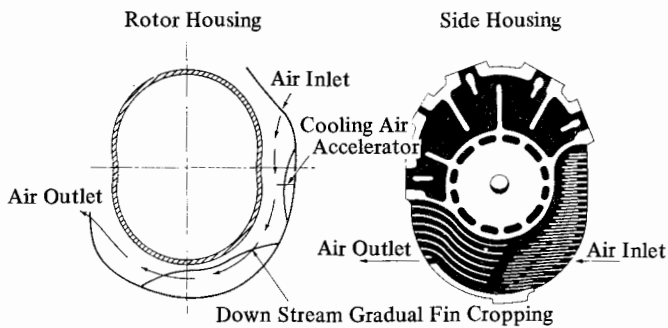


Fig. 5. 5 Cooling air passage for circular flow air cooling

Shown in Fig. 5. 5 is a sectional sketch of the cooling air passage for circumferential-flow air-cooling. As seen from the sketch, the following points are taken into consideration in the design to achieve better cooling effect.

- (i) Arrange cooling fins in such a manner that there are an increasing number of fins in high temperature areas by reducing the thickness of each fin to increase radiating surface.
- (ii) Increase the speed of cooling air passing through high temperature areas.
- (iii) In addition to considerations of volumetric distribution of cooling air, consideration also is given to providing wider passages for low temperature areas to slow down the speed of cooling air flow.
- (iv) Arrange fins located behind high temperature areas in such a manner that high and low fins are located alternately, so as to help reduce pressure loss.
- (v) Divert the cooling air that has passed through the low temperature area to where temperature rise and pressure loss are relatively small, to cool the area around the exhaust port.

Furthermore, to help even out the heat distribution over the water jacket wall around the trochoid of a water-cooled engine, sometimes a design is incorporated to lead a part of the exhaust gas over to the side of the water jacket to heat the area where the intake stroke of the engine operating cycle takes place, and where the temperature is lower because of the cooling effect of evaporation of the fresh intake mixture. An example of this design is illustrated in Fig. 5. 6.

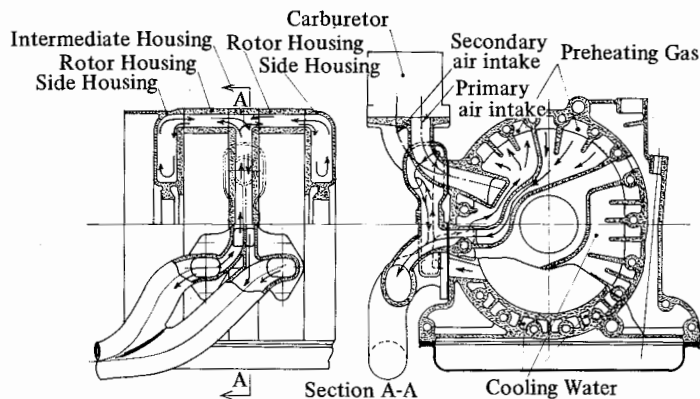


Fig. 5. 6 Preheating by exhaust gas

5. 1. 2 Housing temperature

(1) Water-cooled engine

Fig. 5. 7 shows the effect of partial heating of the housing wall by exhaust gas to compensate for uneven temperature distribution over the wall of the rotor housing, compared with the case of cooling water flowing through all sections of the housing. This method of utilizing exhaust gas for heating appears to be favorable,

because it not only helps reduce temperature differentials all around the wall of the housing, but also provides beneficial secondary effects such as improved vaporization of fuel by preheating of intake at the intake area.

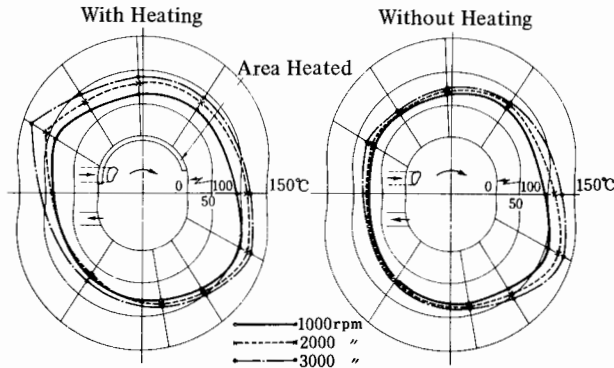


Fig. 5.7 Effect of exhaust gas heat on temperatures along the wall of the rotor housing

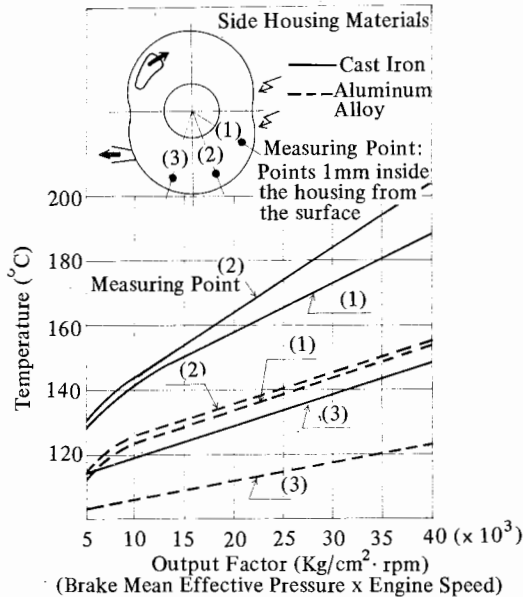


Fig. 5.8 Comparison of side housing temperatures (Cast iron body vs. aluminum alloy)

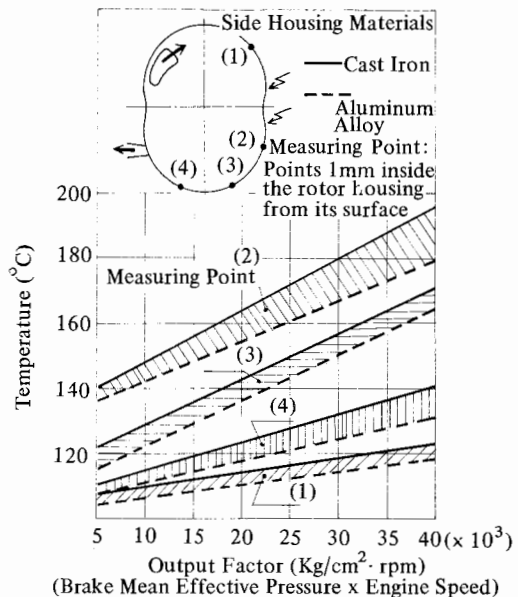


Fig. 5.9 Effect of side housing material on rotor housing temperature

The effect of the housing material is not negligible in keeping down the maximum temperature of the housing wall. As seen from Fig. 5.8 even when the same cooling water passage design is used, the cast iron side housing shows temperatures 20° to 50° higher than those of the aluminum alloy side housing. Furthermore, as shown in Fig. 5.9, the cast iron side housing passes heat onto the rotor

housing, causing its temperature to rise somewhat. In view of this, when a cast iron side housing is to be used, the cooling water passage will have to be designed with extra care.

Fig. 5. 10 shows temperatures around the spark plug hole on a rotor housing. They are about the same as those of the combustion chamber of a conventional reciprocating engine.

(2) Air-cooled engine

Shown in Fig. 5. 11 are temperatures measured along the wall of the housing of a small air-cooled engine where axial flow cooling is used. The maximum temperature is maintained below 200°C, and it is worth noting that there is a low rate of temperature rise with increase in engine speed. The characteristics of the cooling fan for this engine are shown in Fig. 5. 12. They are about the same as those of a comparable size reciprocating engine.

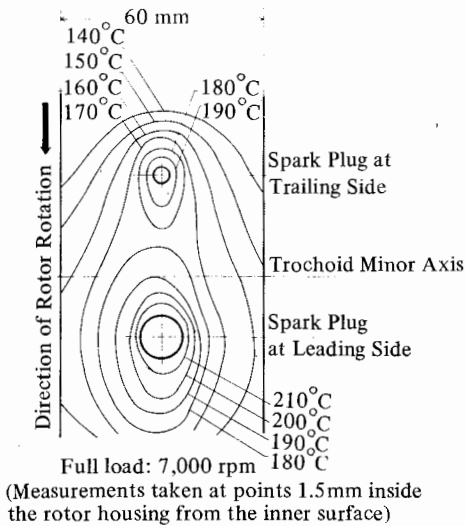


Fig. 5. 10 Temperature distribution on trochoid near spark plug

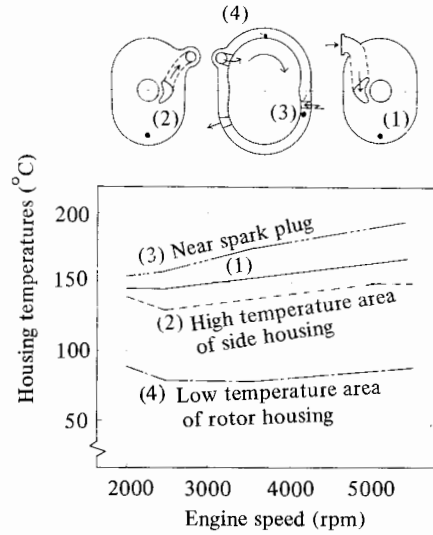


Fig. 5. 11 Temperatures of air-cooled engine housing

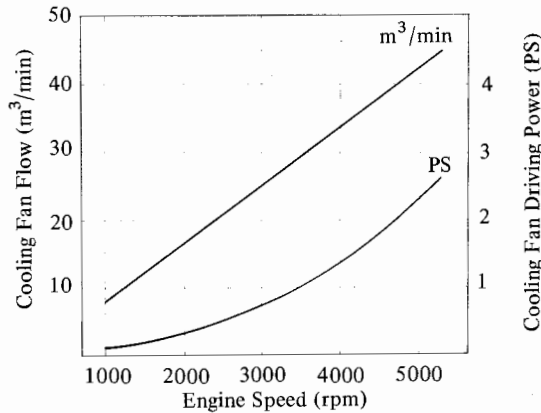


Fig. 5. 12 Characteristics of cooling fan for air-cooled engine

5.2 Rotor Cooling

There are two methods available for cooling the rotor. One of them is to circulate a part of the bearing lubricating oil inside the rotor, and the other is to run intake fuel mixture through the rotor (see Figs. 3. 8 and 6. 1). Both of the methods utilize the unique planetary rotation of the rotor, which applies changing inertia force to the coolant.

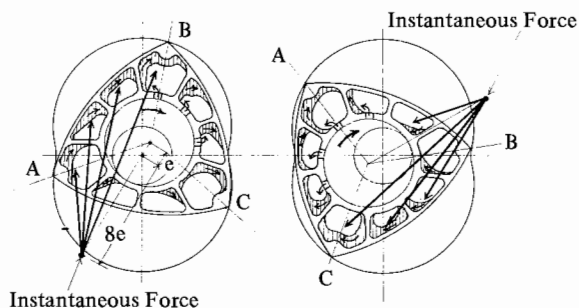


Fig. 5. 13 Cooling oil circulation inside rotor

The circulation of oil inside the rotor for cooling is illustrated in Fig. 5. 13. The cooling oil sprayed into the void of the rotor from the bearing or oil control jet of eccentric shaft is turned around by the changing inertia force applied to it and as it flows along the inside wall of the rotor, it will take heat from the wall. It will then be discharged automatically by centripetal force through the center of the rotor to the engine oil sump. For each revolution of the rotor, centrifugal force and centripetal force each is applied twice to the cooling oil inside the rotor and therefore the cooling oil is discharged from the rotor twice for each revolution of the rotor. Arrows in Fig. 5. 13 show the instantaneous vector of the inertia force applied to the cooling oil. The instantaneous center of inertia force is located at a distance of $8e$ (e : eccentricity of the output shaft) from the center of the output shaft, on the extension of the straight line between the output shaft center and rotor center, in 180° opposite direction from the rotor center. The strength of inertia applied to the cooling oil is in proportion to the distance from the instantaneous center of inertia force.

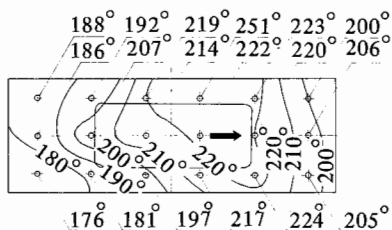


Fig. 5. 14 Rotor surface temperature (Full load : 5,000 rpm)

Fig. 5. 14 shows surface temperatures of a cast iron rotor measured under full load operation.

The amount of cooling oil should of course be limited to a bare minimum to prevent its repetitious circulation within the rotor.

6. LUBRICATION

6.1 Lubrication Methods

Lubrication in rotary engines is concerned primarily with the parts related to the output shaft, such as the bearings of the eccentric shaft and trochoid phase gears, and the sliding surfaces of the gas seal. Lubrication of parts related to the output shaft in a rotary engine is basically the same as in a reciprocating engine. The principally used methods are :

- (i) Lubrication by pressure-forced circulation of oil
- (ii) Lubrication by mist and splash of oil in the intake mixture

Method (i) is a pressurized lubrication system, in which the oil pressure is maintained at 3 to 5 kg/cm² like the crank shaft lubricating system of a 4-stroke reciprocating engine. Therefore, it can ensure thorough lubrication even on flat bearings and other sliding surfaces where the clearance is very small. Method (ii) is similar to the crank shaft lubricating system of a 2-stroke reciprocating engine. It utilizes a fuel-oil mixture and is applicable to places such as the bearings of the eccentric shaft and other places where ball bearings or roller bearings are used and where there is relatively less requirement for lubrication.

As for the lubrication of the gas seal and its sliding surface, due to the peculiarity of their design, the fuel-oil mixture lubrication is normally adopted, and the following two methods are available :

- (i) a premixed fuel-oil mixture in which oil is mixed at a predetermined ratio
- (ii) separate lubrication in which oil is pumped by a metering pump to supply variable ratio fuel-oil mixture

The method most used at present for automobile engines and engines of similar applications, whose speed changes over a wide range and whose load conditions vary greatly, is a combination of the forced circulation and variable fuel-oil ratio systems. The former is used for the parts relating to the output shaft, and the latter for the gas seal and its sliding surface. For the small, multi-purpose engine, whose construction must be simple, the most commonly used method is to run a premixed fuel-oil mixture of 50 to 1 ratio through the engine with the intake gas and apply mist or splash lubrication to both the parts relating to the output shaft and the gas seal sliding surfaces.

Shown in Fig. 6. 1 is the lubrication path in a small engine using the fuel-oil mixture lubricating system. The requirements of lubricating oil for the rotary engine are the same as those for the reciprocating engine, and most important are the following three :

- (i) Low viscosity, so that it can infiltrate well into sliding parts when starting at cold temperatures.

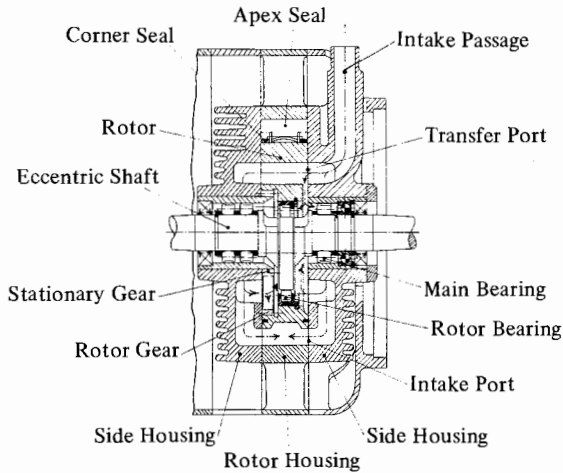


Fig. 6.1 Path of fuel-oil mixture lubrication

- (ii) Good stability against heat and oxidation under high temperature to minimize scale deposit in the combustion chamber.
- (iii) Provision of a strong oil film under critical lubricating conditions.

6.2 Lubrication System for Automobile Engine

Shown in Fig. 6.2 is a typical 2-rotor engine lubrication system, consisting of a full-flow-circulation lubricating system (all the oil flows through the oil filter) and a separate lubricating system (variable fuel-oil mixture ratio).

The system has 7 components, oil pan, oil pump, oil pressure regulator,

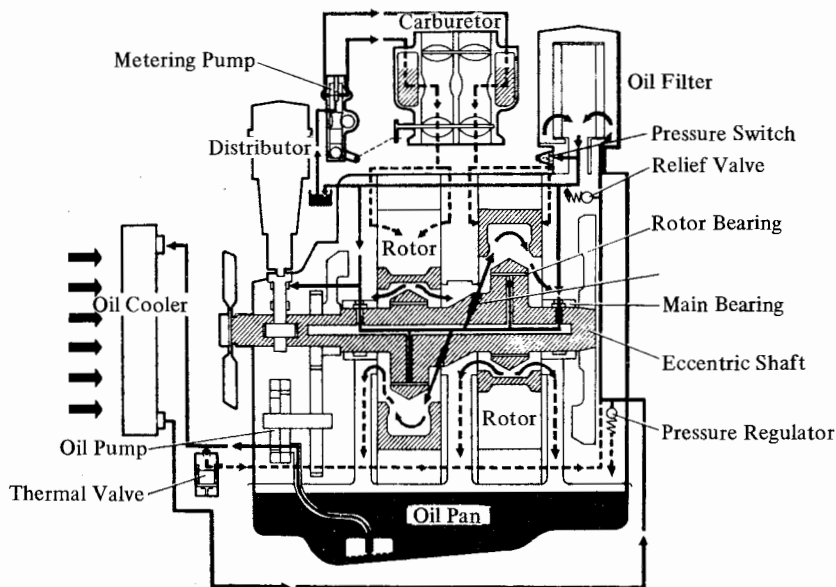


Fig. 6.2 Path of forced circulation lubrication system

oil filter, oil passage, oil cooler, and metering pump, which pumps oil into the intake gas to produce fuel-oil mixture of various ratios.

(1) Lubricating route

The lubricating route shown in figure 6. 2 works in the following manner :

- (i) The lubricating oil in the oil pan is sucked up by the oil pump and sent to the oil cooler or directly to the main oil passage of the housing through the thermal valve, which serves to control the oil temperature.
- (ii) The oil that passes through the oil cooler is sent to the main oil passage of the housing, and after having its pressure regulated, it is cleaned by the oil filter. It then continues to front and rear parts of the main bearing to lubricate all the main journal surfaces of the eccentric shaft, and to the center oil passage of the eccentric shaft.
- (iii) The oil sent through the center passage of the eccentric shaft reaches the rotor journal to lubricate all of the rotor bearings and then it flows into the inside of the rotor to cool it. From there, it returns to the oil pan through the side housings.
- (iv) A part of the oil passed through the oil filter is diverted to lubricate the bearing of the distributor shaft, and part of it flows into the metering pump for lubrication of the gas seal sliding surface. The amount of oil metered by the pump is in proportion to the load condition and engine speed, and it is pumped out to upstream of the throttle valve of the carburetor primary side (P). The oil then diffuses into the intake gas, flows through the intake tube, and is carried to the combustion chamber to lubricate the gas seals and the sliding surfaces.

(2) Amount of lubricating oil

The lubricating oil is sucked up by the oil pump and forced by pressure to flow through the engine to lubricate various parts of the engine in a continuous circulation from the oil pan through the engine. In general, the flow should be maintained at a level which is sufficient to absorb heat of 20 to 80 K cal/PS.h, enough to remove friction heat from the sliding parts and heat from inside of the rotor. Also sufficient oil should be kept in reserve for a sudden increase in the amount of oil circulating through the engine resulting from an increase in engine speed. When the lubricating oil in the oil pan is diverted for lubricating the gas seal sliding surfaces, the amount of oil in the pan should include an amount sufficient to compensate for the amount of oil burned. At present, it is calculated in most cases at a rate of 4 to 5 liters to one liter of engine displacement.

(3) Oil cooler

The temperature of the oil in the oil pan is affected by the engine speed, load condition, and cooling water temperature. A rise in oil temperature affects the retention of oil film over lubricating surface and accelerates the deterioration of

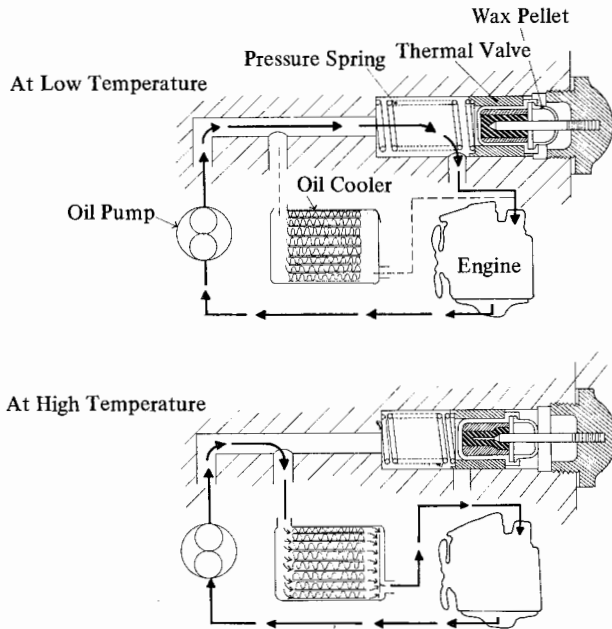


Fig. 6.3 Function of thermal valve

lubricating properties. The cooling of lubricating oil is especially important when the inside of the rotor is cooled by circulating oil. In general, in order to maintain the lubricating oil temperature at 70 to 90°C level, it is necessary to have an oil cooler in the lubricating system for positive cooling.

Shown in Fig. 6. 3 is the function of the thermal valve, which serves to control the oil flow through the oil cooler to shorten the warm-up time when starting the engine. In this system, a wax-type pellet is used as the thermal pellet, the same as that used for cooling water temperature control.

(4) Lubrication of gas seal sliding surface

Lubrication of the gas seal and its sliding surface serves an important role for both reduction of friction and gas sealing. With the apex seal, it is especially hard to form oil film because of its mechanism, and as it has been explained earlier, when a metal apex seal was tried on a chrome plated surface, it resulted in abnormal wear on the trochoid surface. However, no abnormal wear was noticed with the use of a carbon apex seal, which is self-lubricating and superior in reducing friction. Therefore, in such a case, lubrication applied to the sliding surface serves to provide gas sealing rather than to reduce friction. The mechanism of lubricating the side seal is similar to that of lubricating piston rings of a reciprocating engine. The oil film that is left unscrapped on the surface of the side housing by the oil seal serves to lubricate the side seal.

Shown in Fig. 6. 4 is a chart of fuel-lubricating oil ratios for the lubricating system, using a metering pump to diffuse lubricating oil with intake mixture.

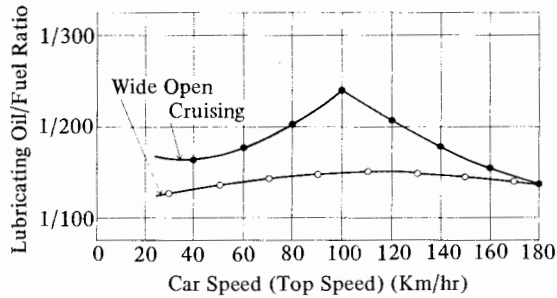


Fig. 6.4 Lubrication by metering pump

The adhesion of lubricant in the sealing grooves, clogging of exhaust port, and smoke from tail pipe, all of which are liable to cause problems when fuel-oil mixture lubrication is adopted, are down to practically negligible levels because the mixing ratios are somewhere between 150 : 1 and 250 : 1.

(5) Oil metering pump

The oil metering pump serves to keep pumping the proper amount of lubricating oil into the intake mixture, which is flowing through the carburetor and intake manifold, so as to diffuse the oil into the gas and lubricate the gas seal and its sliding surface. A plunger pump, which is driven by the output shaft via gears, is commonly used as the metering pump.

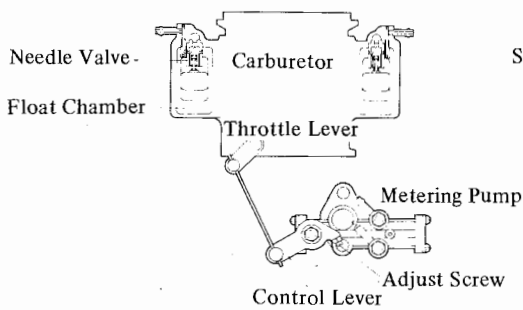


Fig. 6.5 Oil metering system

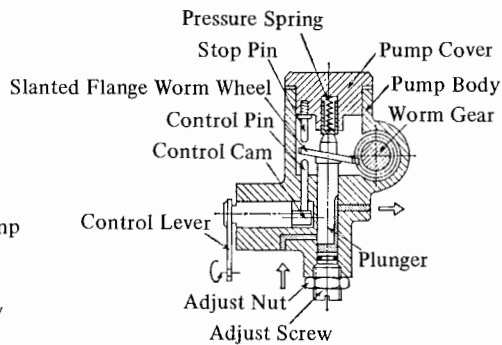


Fig. 6.6 Construction of oil metering pump

Table 6.1 Specifications of oil metering pump

Construction	Worm gear drive variable stroke plunger type
Worm gear ratio	28 : 1
Diameter of plunger	6 Φ
Diameter of inlet	6 Φ
Diameter of output	3 Φ
Capacity	200 cc/hr – 6000 rpm

Shown in Fig. 6.6 are the principal construction features of a variable stroke plunger type metering pump, driven by worm gear. The general specifications of a typical metering pump are shown in Table 6. 1.

As illustrated in Fig. 6. 7, the plunger operates in the following sequence :

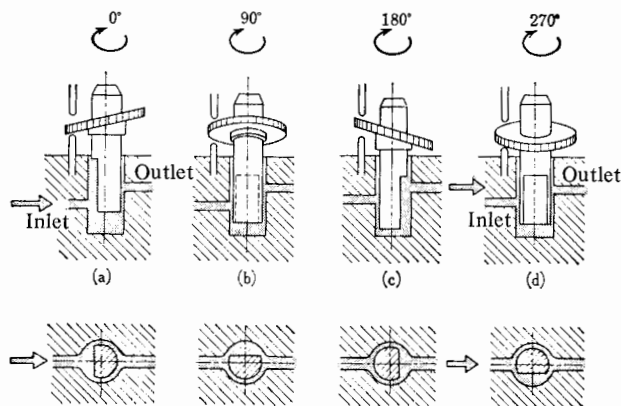


Fig. 6. 7 Pump plunger operation

- When the plunger is in its topmost position, the pump barrel takes oil into its bottom portion.
- As the slanted flange worm wheel turns, the plunger moves down to press on sucked-in oil.
- The cutaway groove of the plunger faces the outlet in the body and pump pushes oil out.
- Both the inlet and outlet are sealed off by the plunger, which moves up to start again with 'suction stroke' (a).

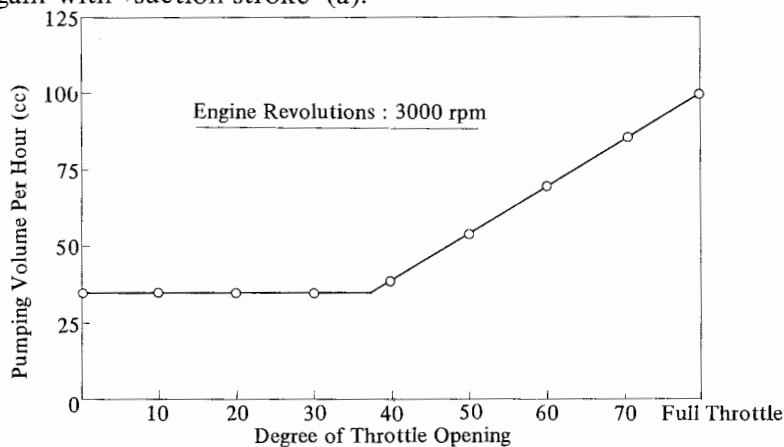


Fig. 6. 8 Pumping characteristics of oil metering pump

Shown in Fig. 6. 8 is the pumping characteristics of a oil metering pump. The pumping volume is controlled not only by controlling the revolution of the plunger in proportion to the revolution of the output shaft but also automatically in proportion to the engine load. For this automatic control, the height of the control pin is adjusted by interlocking the control cam with the throttle valve (so that the lift of the control cam changes in proportion to the throttle valve opening), changing the plunger stroke accordingly.

6.3 Oil Seal

(1) Construction of oil seal

For engines using lubricating oil for cooling the rotor, the rotor must be equipped with an oil seal (oil sealing ring) to prevent oil from leaking through the side of the rotor into the combustion chamber where it will be consumed.

The oil seal must provide the following three functions :

- (i) To lubricate the side seal, it should be able to provide an appropriate oil film over the sliding surface of the side housing.
 - (ii) It should be of such a construction that it is not easily affected by minute changes in the flatness of the side housing surface resulting from thermal and mechanical load on the housing during running.
 - (iii) It should also be of such construction that it does not permit the oil in the rotor to leak into the combustion chamber while the engine is standing still. Oil seals that are presently in common use are classified into the following two types :
- (a) A type which seals between the side housings and the sides of the rotor.

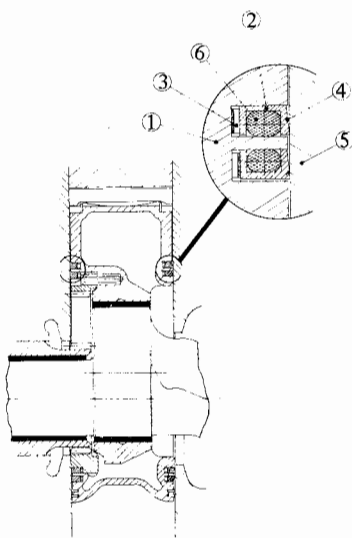


Fig. 6.9 Construction of oil seal (a)

As seen in Fig. 6. 9, an oil ring (2) is installed in each of the concentric grooves located near the center of rotor (1) on both sides of it. Wave form spring (3) installed beneath the oil ring pushes up the oil scraping lip (4) against the side housing (5) to maintain the oil sealing effect.

Each ring has a rubber "O" ring (6) inside to prevent oil leak from the back of the ring.

(b) This is a type which maintains sealing effect primarily between the eccentric portion of the output shaft and the internal surface of the rotor.

The construction of a typical example is shown in Fig. 6. 10. A piston ring (2) is installed on one side of the eccentric portion (1) of the output shaft to provide seals against the internal surface of the rotor (3). On the other side of the eccentric portion, a disc (4) which is concentric with the rotor is installed, and piston rings (5) and (6) are installed in the grooves located in the outer edge of the disc so as to provide a sealing effect between the internal surface of the rotor and the internal surface of the side housing (7). The tension of the ring is assisted by constant-pressure gas leaking through the side seal. In order to maintain the oil sealing effect while the engine is standing still, the oil scraping ring (10), which consists of a rubber "O" ring (9) and a wave form spring (8), is installed on each side of the rotor.

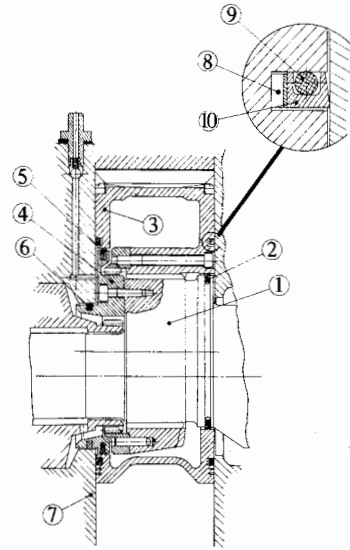


Fig. 6. 10 Construction of oil seal (b)

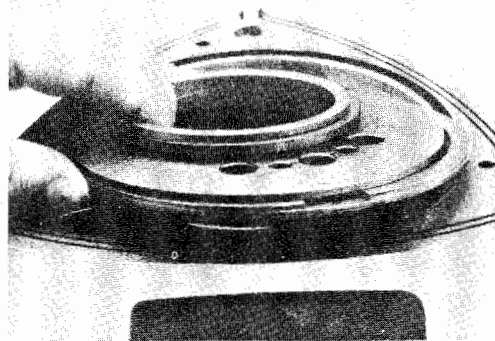


Fig. 6. 11 Oil sealing ring and disc.

Fig. 6. 11 shows a disc and oil sealing rings used in type (b) oil seal.

(2) Function of oil seal

The oil seal equipped with an oil scraping ring on the side of the rotor rotates with the rotor in planetary motion, and therefore, as seen from Fig. 6. 12, a half circle of the oil scraping lip scrapes oil from the surface of the side housing, providing a proper oil film for the side seal sliding surface, while the other half slides on the oil film. In addition to having this intrinsically desirable function, it is also of

simple construction.

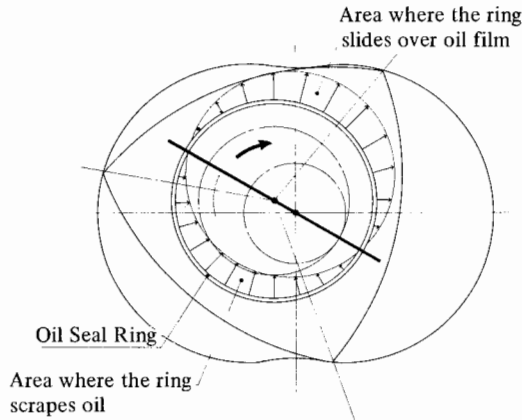


Fig. 6. 12 Function of oil seal

However, requirements in oil seal functions are rigorous, because of the fact that the rotor rotates while maintaining a set axial clearance against the side housing, and because there is the effect of the flatness of the housing surface, which was explained in the preceding section. Factors of the oil seal ring that directly affect sealing are :

- (i) Pressing force of the oil scraping ring
- (ii) Angle and width of lip of the oil scraping ring

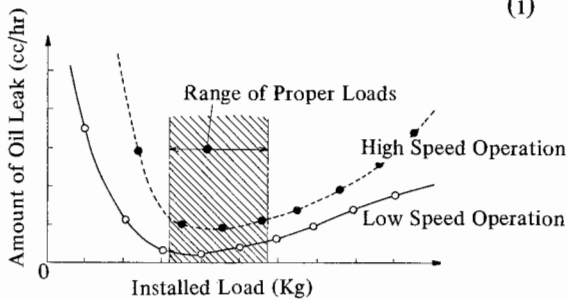


Fig. 6. 13 Effect of back-up spring-load on the oil sealing effect

highly loaded spring, the sealing effect deteriorates. The reason seems to be that too much pressure on the lip causes the ring to break up oil film sticking on the side housing, hampering the seal lip's sliding over the oil film. As a result, most of the oil film on the side housing will be scraped off into the combustion chamber.

- (ii) Angle and width of lip of oil scraping ring

- (i) Pressing force of oil scraping ring

As Fig. 6. 13 shows, there is an appropriate range of spring load for the spring pushing the oil scraping ring against the side housing. The spring load is directly related to the oil scraping lip surface pressure and affects the oil sealing effect. With a

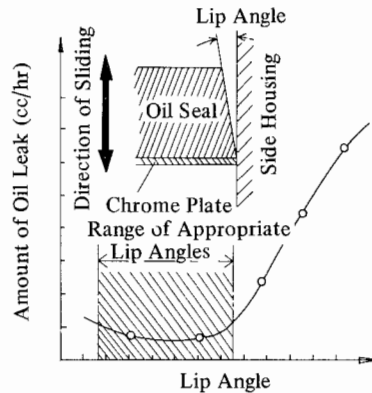


Fig. 6. 14 Effect of oil seal lip angle

Shown in Fig. 6. 14 is the effect of the angle of the lip on the oil sealing effect. This angle should be determined with emphasis on its wedge effect as well as the pressure applied to it, to ensure good oil sealing function. The angle normally adopted is somewhere around 2 to 3 degrees.

To maintain good sealing effect over an extended period of time, increase of the lip width should be avoided as much as possible. Rather, attention should be paid to the selection of proper materials for the ring. In this connection, a chrome plating applied to the internal surface of the ring to form a wear-resisting layer has proved effective in some cases.

6. 4 Blow-by Gas Recirculating System

Shown in Fig. 6. 15 is a system for recirculating blow-by gas which has passed by the side seal on the side of the rotor. Also shown is the ventilation path for prevention of oil deterioration.

With the side port type engine, in which the intake port opens to the side housing, blow-by gas reaching the space enclosed by the side seal and oil seal can always be sucked through the intake port into the combustion chamber to burn again. Therefore, the rotary engine with side inlet ports has an advantage over reciprocating engines in that much less blow-by gas reaches the oil pan. Although this is really a problem which should be solved by improving the sealing, this structural feature of the rotary engine is worth noting, especially when concern over prevention of air pollution is becoming increasingly acute.

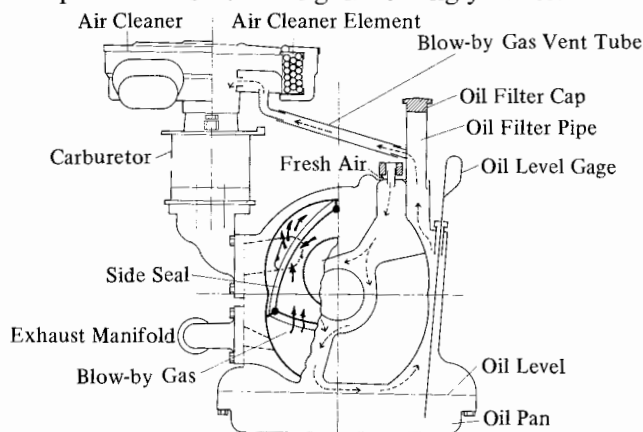


Fig. 6. 15 Ventilation of housing

Reference Materials

- 1) Kazuo Takada : Method of Measuring Internal Phenomena of Rotary Engine and Results of the Measurement, Internal Combustion Engine Volume 6 No. 64 (1967)
- 2) G. Jungbluth : Aus der Entwicklung des Zweifach-Kreiskolbenmotors KKM 612 für den NSU-Wagen Ro 80. MTZ, 28/9 (1967).

7. ENGINE VIBRATION

In order to control engine vibration and achieve high-speed revolution, consideration should be given primarily to the following :

- (i) Effect of inertia force and inertia moment resulting from unbalanced moving parts
- (ii) Fluctuation of torque
- (iii) Torsional vibration of output shaft

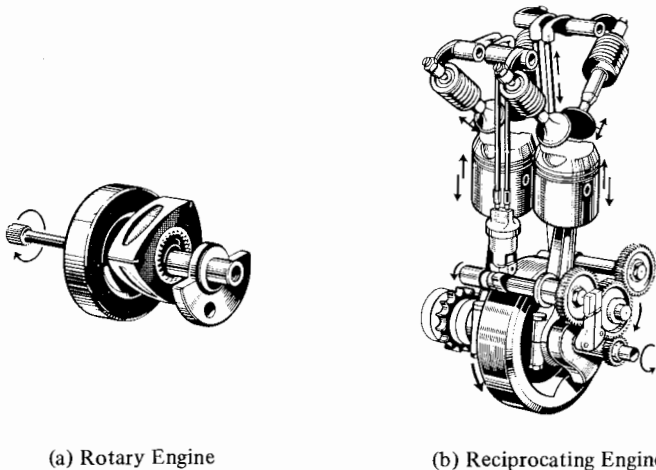
Torsional vibration of the output shaft (crank shaft or eccentric shaft) is a representative example of the vibrations caused by bent or deformed components of the engine. (i) and (ii) have a direct influence over the vibration level of the whole engine.

7.1 Engine Balance

(1) Balancing inertia force

In the case of a reciprocating engine, both the unbalanced rotating masses (crank shaft, connecting rods, etc.) and reciprocating masses (piston, connecting rods, etc.) should be looked at in order to balance the inertia forces generated from the various moving parts.

Unbalanced rotating masses can be corrected relatively easily by applying balancing weights. However, the balancing weight approach does not work for reciprocating masses. Therefore, unbalanced inertia force and inertia moment remain uncorrected, causing a resultant vibration which increases in proportion to the square of engine speed, and acting as limiting factors to the allowable engine speed.



(a) Rotary Engine

(b) Reciprocating Engine

Fig. 7.1 Basic structure of the engine

Table 7. 1 shows the balancing of a reciprocating engine for the typical arrangement of cylinders.

The rotary engine has no reciprocating mass, and therefore only the balancing of the rotating masses is required for off-setting unbalanced inertias resulting from moving parts. The problem of balancing could be solved essentially with the use of counter weight for the mass of the rotor and eccentric mass of the rotor journal, the counter weight being supported by and rotating around the rotor journal corresponding to the crank pin, both of which make planetary motion around the output shaft.

(2) Conditions for balancing rotating masses

Let us take the single rotor engine shown in Fig. 7. 2, and calculate the necessary counter-balance weight :

The statical-balance condition ΣF where the sum of centrifugal force becomes zero is :

$$\Sigma F = Me\omega^2 - (m_F r_F + m_R r_R) \omega^2 = 0 \quad (7. 1)$$

$$Me = m_F r_F + m_R r_R$$

where :

M : Rotor mass plus eccentric mass of rotor journal

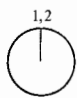

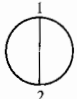
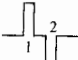

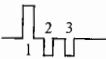
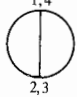



e : Eccentricity of rotor journal

ω : Angular velocity of output shaft

$m_F r_F$ and $m_R r_R$: Balance weights for front and rear of the output shaft

Table 7. 1 Unbalanced reciprocating masses of a reciprocating engine

"X" indicate unbalance

Arrangement of cylinders No. of cylinders	Arrangement of crank (clockwise rotation)	Side view of crank arrangement	Kind of engine 2-stroke, 4-stroke	Unbalanced inertia force				Unbalanced inertia of moment			
				1st	2nd	4th	6th	1st	2nd	4th	6th
Straight 2			4	x	x	x	x				
Straight 2			2		x	x	x	x			
Straight 3			2				x	x	x	x	
Straight 4			4		x	x	x				
Straight 6			4				x				

The dynamic balance condition ΣM_p where the total sum of moment relating to a given spot P on the output shaft is zero is expressed as :

$$\Sigma M_p = m_R r_R \cdot b - m_F r_F \cdot a = 0 \quad (7.2)$$

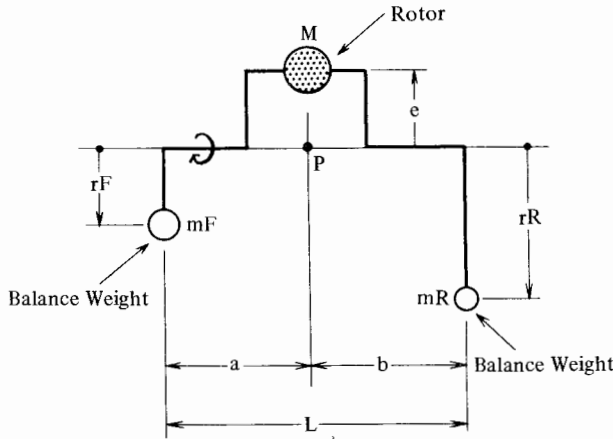


Fig. 7.2 Rotary engine balance

By substituting Equation (7.1) and (7.2), we can express the counter-balance weight for each case as :

$$\left. \begin{aligned} m_F r_F &= -\frac{b}{L} M e \\ m_R r_R &= \frac{a}{L} M e \end{aligned} \right\} \quad (7.3)$$

In the case of a single-rotor engine, balance weights that satisfy Equation (7.3) are placed in the opposite direction to the eccentric deviation of the rotor journal on the shaft on both sides of the rotor. They balance out the moment of inertia also at the same time.

Shown in Table 7.2 are typical balancing conditions for rotary engines of up to 4 rotors, and locations of balancing weights.

Fig. 7.3 shows a 2-rotor engine, in which the rear balancing weight is built into the flywheel so as to reduce engine length.

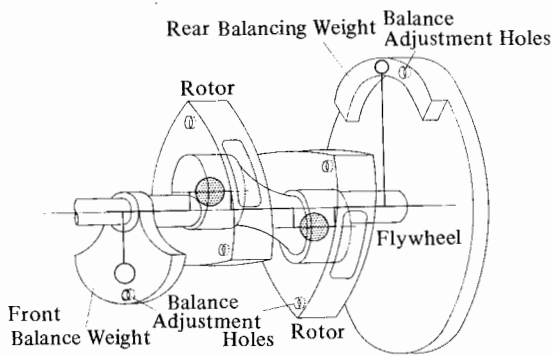


Fig. 7.3 Arrangement of balance weights for a 2-rotor engine

Table 7.2 Conditions of balance of the rotary engine

M : mass of rotor

e : Amount of eccentricity

$m_F r_F \cdot m_R r_R$: Balancing weights required

Number of rotors	Arrangement of balance weight on the rotor (clockwise rotation)	Sketch of eccentric shaft	Conditions of balancing
Single Rotor			$m_F r_F = \frac{b}{L} M e$ $m_R r_R = \frac{a}{L} M e$
2-Rotor			$m_F r_F = m_R r_R = \frac{a}{L} M e$
3-Rotor			$m_F r_F = m_R r_R = \sqrt{3} \frac{a}{L} M e$ $(\theta = 30^\circ)$
4-Rotor			$m_F r_F = m_R r_R = \sqrt{2} \frac{a}{L} M e$ $(\theta = 45^\circ)$

7.2 Fluctuation of Torque

(1) Torque

Shown in Fig. 7. 4 are the processes of torque generation by a rotary engine and a reciprocating engine.

The pressure of gas applied to the rotor flank (P_g) is divided into two component vectors, F_t - pointing in the direction tangent to the locus of the rotor journal, which is eccentric to the output shaft, and P_B - pointing in the direction perpendicular to the main journal.

Therefore, the torque of the output shaft, M_d , is expressed by the following equation :

$$M_d = F_t \cdot e \quad \text{where "e" is eccentricity of rotor journal.}$$

The rotor journal and its eccentricity are equivalent to the crank pin and its cranking radius of a reciprocating engine.

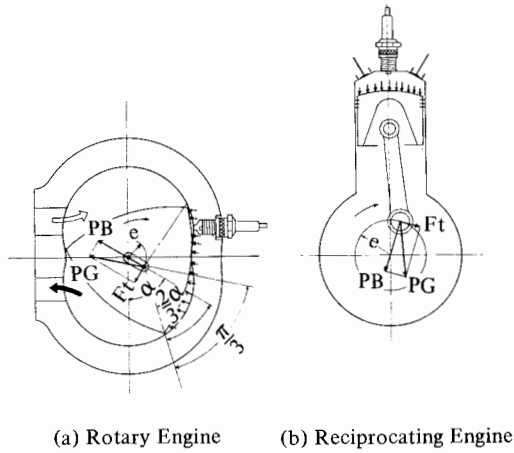


Fig. 7.4 Mechanisms for generating torque

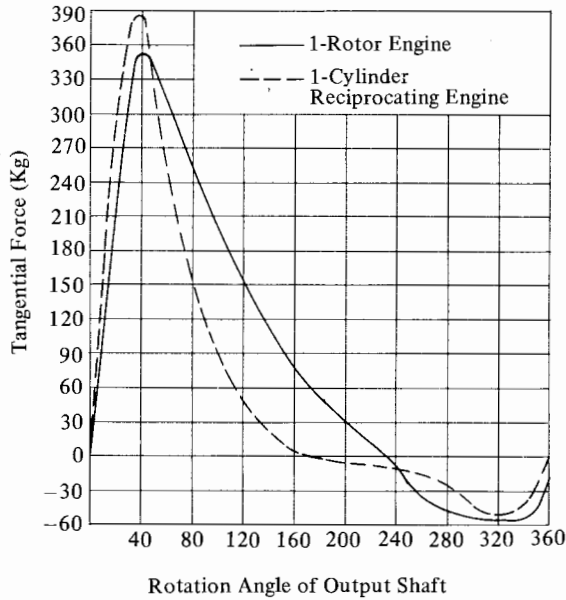


Fig. 7.5 Tangential force curve

The tangential force (F_t) applied to the rotor journal varies with the gas pressure and the rotation angle of the output shaft, as noted in Fig. 7.5.

Therefore, the torque for any rotation angle (α) of the output shaft is expressed by the following equation :

$$Md = Pg \cdot e \cdot \sin \frac{2}{3} \left(\frac{\pi}{2} - \alpha \right) \quad (7.4)$$

The gas pressure curve and torque curve of a single rotor engine are illustrated in Fig. 7.6.

Furthermore, in general, by assuming that the angular velocity of the output

shaft remains constant due to the effect of the flywheel, the mean torque generated in the output shaft is expressed by :

$$M_d (e) = \frac{75 \cdot H \cdot 60}{2 \pi N} = 716.2 \frac{H}{N} \quad (7.5)$$

where :

- Md (e) : Mean torque (kg-m)
- H : Output of engine (PS)
- N : Revolution of output shaft (rpm)

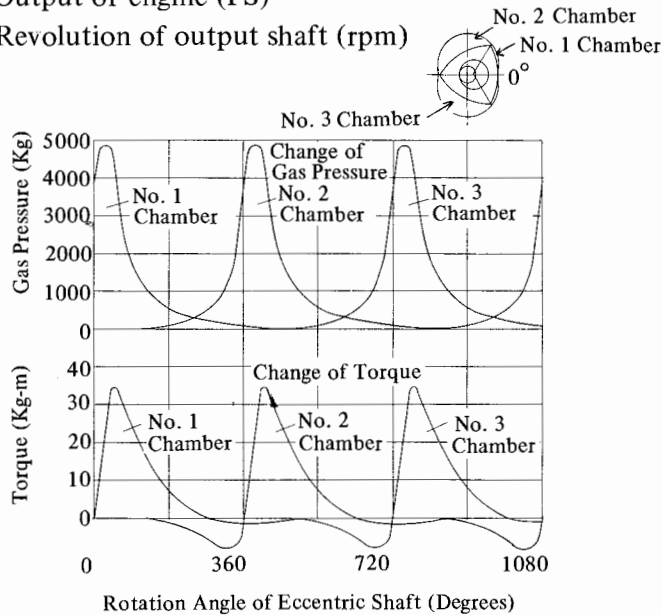


Fig. 7. 6 The gas pressure and torque curves for each chamber of a single rotor engine

(2) Fluctuation of torque

Illustrated in Fig. 7. 7 is a comparison between a 2-rotor engine, a 4-cylinder reciprocating engine and a 6-cylinder reciprocating engine concerning the fluctuation of torque. With the 2-rotor engine, there are two explosions per output shaft rotation, the same number of explosions per rotation as in the 4-cylinder reciprocating engine.

However, in the case of a reciprocating engine, the four strokes from intake through exhaust take place over 720 degrees rotation of the crank shaft, while in the rotary engine, they take place over 1,080 degrees rotation of the eccentric shaft, and the torques generated on each rotor flank overlap each other. As a result, the composite torque curve contains less fluctuation than that of a 4-cylinder reciprocating engine. It is closer to the curve for a 6-cylinder reciprocating engine in terms of torque fluctuation characteristics. The flywheel for a rotary engine, therefore, can be much smaller than one for a reciprocating engine with comparable output. Shown in Fig. 7. 8 is a comparison of the coefficient of speed fluctuation among various engines equipped with a flywheel, which has the same inertia moment.

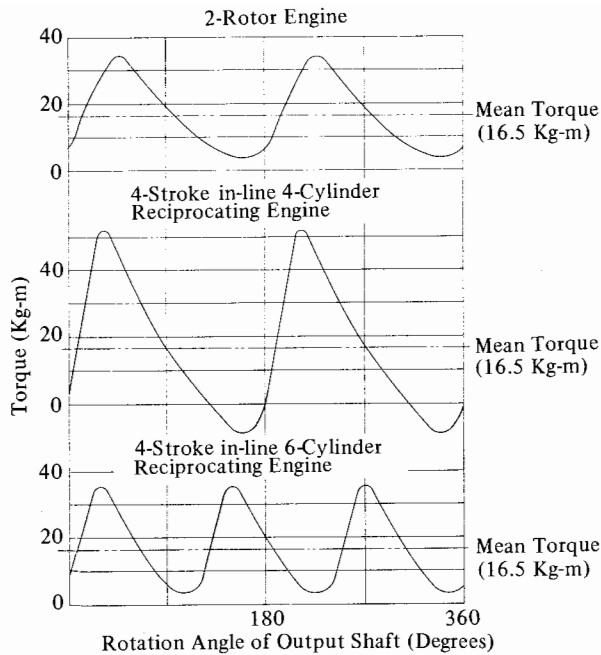


Fig. 7.7 Comparison of torque fluctuation of rotary engines and reciprocating engines

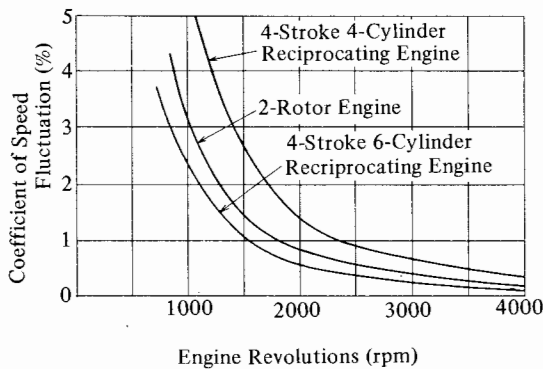


Fig. 7.8 Coefficient of speed fluctuation of reciprocating engine
(Total inertia moment $I_o = 1.5 \text{ kg.cm.sec}^2$)

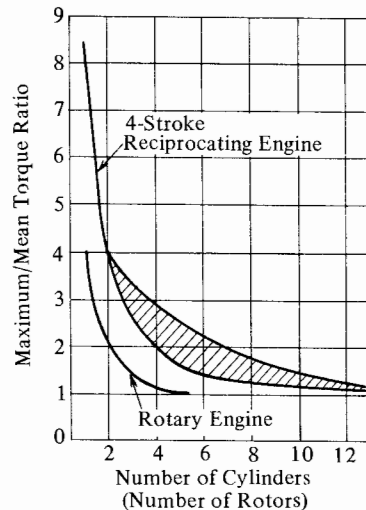


Fig. 7.9 Maximum/mean torque ratio

Illustrated in Fig. 7.9 is a comparison between a rotary engine and reciprocating engine of the maximum/mean torque ratio, necessary in designing the output shaft and drive trains. The hatched area represents the deviation resulting from change in cylinder arrangement of a reciprocating engine. As these figures show, there is much less necessity to primarily reduce the torque fluctuation in multi-rotor design than for a reciprocating engine, and therefore it is possible to reduce the length of the engine. This also results in an advantage for rotary engines in that

more rigidity can be maintained against torsional vibration on the shorter output shaft

8. IGNITION SYSTEM

8.1 Spark Plug

The number of times of ignition for a rotary engine is twice that of a conventional 4-stroke reciprocating engine for the same number of output shaft revolutions. The compression ratio of a rotary engine is far greater than that of a 2-stroke engine. These, plus the fact that a rotary engine operates under a wide range of changing loads, cause the spark plugs to be subject to a greater amount of heat than spark plugs in conventional engines.

The design of the rotary engine does not permit the spark plug electrode to stick out inside the combustion chamber. The spark plug is installed in a hole in the rotor housing. As a result, the duration of spark plug cooling by intake fuel mixture is relatively short. Therefore the heat range of the spark plug for a rotary engine is slightly higher than for a reciprocating engine (a colder plug is required), and when it is used for automobiles and the like where the load fluctuates frequently, a spark plug with a wide heat characteristic (referred to as a wide range spark plug) is required for full utilization of the output characteristics of the rotary engine.

The spark plugs developed by incorporating these points are shown in Figs. 8. 1 and 8. 2. The key point of structural design of these spark plugs is to design them so that the heat accumulated on the center electrode, porcelain insulator, side electrode, and the gas pocket is easily released to the engine block via the spark plug thread and sealing gasket to keep the electrode at an appropriate temperature for the purpose of keeping the spark plug clean and preventing preignition.

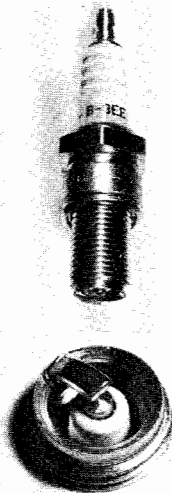


Fig. 8. 1 B-8EE spark plug
(of Nippon Tokushu Togyo Co.)

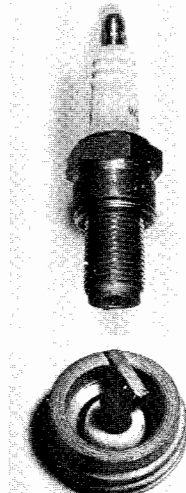


Fig. 8. 2 W25EG spark plug
(of Nippon Denso Co.)

8.2 Two-Spark Plug Arrangement and Ignition System

For a reciprocating engine, the method of using two spark plugs has been utilized as a means for improving the combustion efficiency when the combustion chamber is relatively large and the flame has to spread over a larger distance.

If the displacement of a single cylinder measures something like 500 cc, it is regarded as a large cylinder, even by present day standards, and for such a cylinder to have a perfect combustion stroke and deliver full power, it is effective to use multiple spark plugs each connected to an independent source.

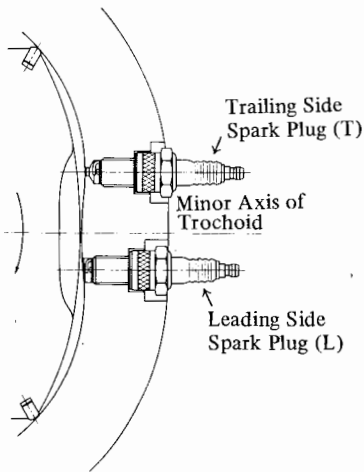


Fig. 8.3 Two-spark plug arrangement

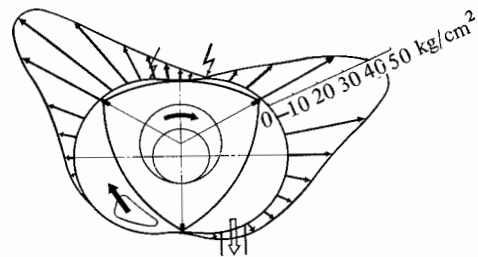
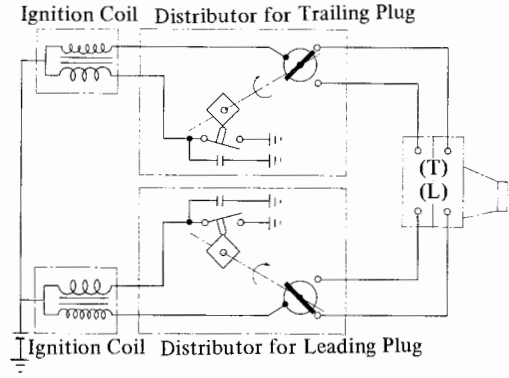


Fig. 8.4 Gas pressure difference between trailing and leading sides

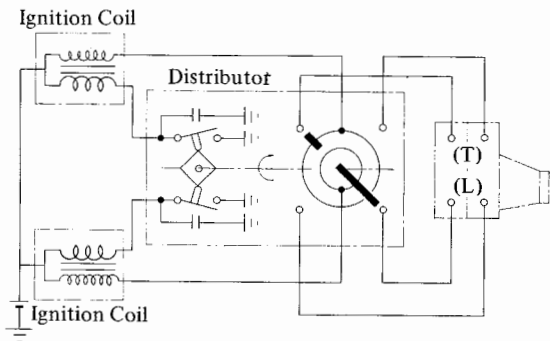
Shown in Fig. 8.3 is an example of a two-spark plug arrangement for a rotary engine. The location of each spark plug is determined primarily by the way combustion gas flows, which is largely affected by the shape of the combustion chamber. Normally, one is installed at the leading side and the other one at the trailing side.

The size of the spark hole between ignition chamber and combustion chamber is not the same for the two spark plugs. The reason for this is the pressure differential that will develop between the two adjacent working chambers formed on both sides of the apex seal. At the instant the apex seal passes across the spark hole, gas leaks through the spark hole. The pressure differential is almost zero near the spark plug hole on the leading side, whereas it increases as the apex draws nearer to the trailing side, as shown in Fig. 8.4. Therefore, in order to prevent leakage, the spark hole at the trailing side is made smaller. As a result, the spark plug at the trailing side suffers the disadvantage of difficulty in keeping the electrode clean and getting a good spark when operating under a light load at a low speed, while it has the advantage of providing fast combustion along the direction of rotor

revolution when operating under a heavy load. On the other hand, at the leading side, it is possible to have a larger spark plug hole and the electrodes are brought closer to the inside surface of the rotor housing. It, therefore, helps provide smooth idling and better starting when cold.



(a) 2-ignition coil – 2-distributor system



(b) 2-ignition coil – 1-distributor system

Fig. 8. 5 Two-spark plug ignition system

Fig. 8. 5 shows typical examples of two spark plug systems where each spark plug is provided with an independent ignition coil. System (a) is wired so that each spark plug has an ignition coil and distributor of its own and each operates with an advance angle set independent from the other, whereas system (b) is wired in such a way that the ignition coils are shared by the two spark plugs and the ignition timing is adjusted the same for both spark plugs.

8.3 Trend of Future Ignition Systems

Automobiles are going to be required to operate at extremely low speeds more frequently in urban areas, and with the progress being made in the construction of highway networks there will be more and more long distance driving at high speeds. Therefore, in the future, the heat range required for automotive spark plugs will become even wider. It, therefore, is necessary to improve not only the materials, but also the structural design, of both the spark plug and ignition power sources to

meet the requirements for wider heat range.

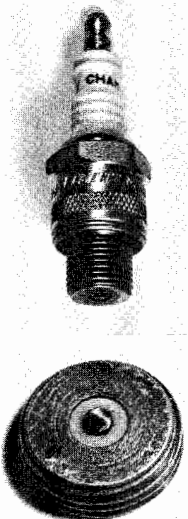


Fig. 8. 6 Surface discharge spark plug

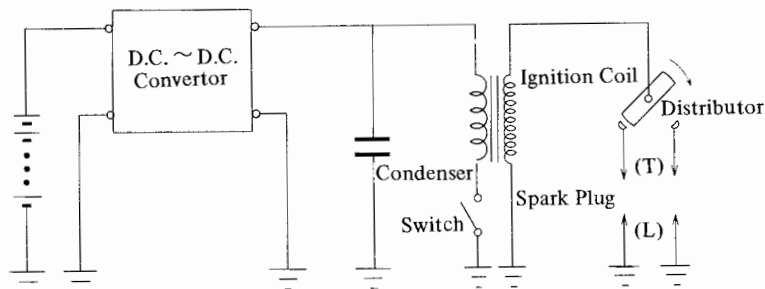


Fig. 8. 7 Condenser discharge igniter

One solution of the problem of wider heat range is the combination of the surface discharge spark plug, shown in Fig. 8. 6 and the condenser discharge igniter shown in Fig. 8. 7. This combination shows great promise for the future.

Some of the advantages of the surface discharge spark plug are, the heat range is high and therefore prevents pre-ignition ; it does not require too high a voltage, so the electrode does not wear out as fast because of sparking along the porcelain surface ; and because of its flat end, it can be mounted closer to the inner surface of the rotor housing to help improve ignition.

A spark plug used for a rotary engine is in an environment quite different from that of reciprocating engines. The many advantages of the surface discharge spark plug make it a very hopeful aspirant for use as a specialized spark plug for rotary engines.

The condenser discharge igniter takes DC voltage from a battery and boosts it up from several hundred to one thousand volts with a DC-DC convertor. The high tension electricity is then stored in the condenser. The condenser then is tripped by a timing signal from the distributor to discharge quickly through the primary winding of the ignition coil, causing high tension voltage with a short rise time to generate in the secondary winding. It then causes the spark plug to spark. The short rise time of the secondary voltage means that a strong spark will result, even when the spark plug is fouled with carbon or lead. Another advantage of this ignition system is that, unlike a conventional ignition system, the breaker points act only to provide a timing signal and have nothing to do with supplying electricity to the ignition coil. Therefore, this system is free from capacity declining at high speeds and is capable of supplying a high voltage output at any speeds specified, whereas with a conventional battery-coil system, the output drops at high speeds as the input through the breaker points decreases.

9. ENGINE PERFORMANCE · COMBUSTION

9.1 Power Generated by Engine

One side of the triangle rotor and the two-lobe peritrochoid wall of the rotor housing form an working chamber, whose volume changes between a minimum and maximum as the function of sine. It completes distinctly identifiable processes of intake, compression, combustion and exhaust for one rotation of the rotor (3 rotations of the output shaft = 1,080°), and it has one combustion process for every 1/3 rotation of the rotor (1 rotation of the output shaft = 360°). The performance of this NSU-Wankel type rotary engine is evaluated by the method shown in Table 9. 1.

Table 9. 1 Equation for calculating output of an NSU-Wankel type rotary engine

Method of delivering effective output	Eccentric shaft n : Revolution of eccentric shaft (rpm)
Total displacement $V(l)$	$V = zV_H$ z : V_H :
Indicated mean effective pressure $P_{mi}(\text{Kg/cm}^2)$	$P_{mi} = \frac{1}{V_H} \int_{\theta=0^\circ}^{\theta=1080^\circ}$ P : Working chamber gas pressure (Kg/cm ²) θ : Angle of rotation of eccentric shaft V_θ : Single working chamber volume (ℓ) when the angle of rotation of the eccentric shaft is θ .
Indicated horsepower $N_i(\text{PS})$	$N_i = P_{mi} \frac{V_n}{75 \times 60} = P_{mi} \frac{V_n}{450}$ PS : 75Kg · m/sec
Brake horsepower $N_i(\text{PS})$	$N = \eta_m, N_i = \eta_m, P_{mi} \frac{V_n}{450} = P_{mi} \frac{V_n}{450}$ η_m : Mechanical efficiency
Brake mean effective pressure $P_{mi}(\text{Kg/cm}^2)$	$P_{mi} = \eta_m, P_{mi} = \frac{450 \cdot N_e}{V_n}$

9.2 Engine Performance

(1) Friction losses

A number of engines, including prototype rotary engines, were test-driven to determine engine friction losses. The results are shown in Fig. 9. 1. The simplicity of rotary engine design is reflected in their smaller friction losses. There is less friction from major moving parts of the engine since there are fewer parts, and there is also less loss from pumping and driving other secondary mechanisms such as intake and exhaust valves. The rate of increase of friction losses against the increase of engine speed for the rotary engine is not as high as that for conventional engines. This is an indication of the possibility of introducing high speed versions of the current design rotary engine.

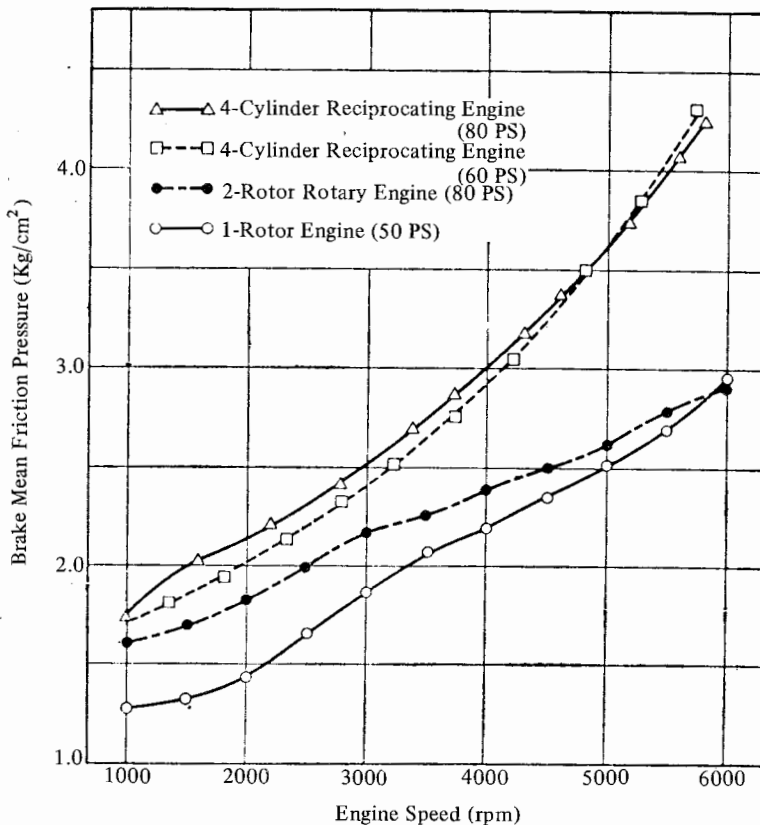


Fig. 9. 1 Comparison of brake mean friction pressure

Shown in Fig. 9. 2 is one example of a breakdown of engine friction. For introduction of a high speed model, it is obviously necessary to concentrate on reducing friction losses due to oil seals, which account for almost half of the total friction losses. In seal structure, seal location, and length of the sliding trace of

seals, proper selection of the various basic specifications of the trochoid is important. These are for example the trochoid constant R/e and the ratio of trochoid axis R/b .

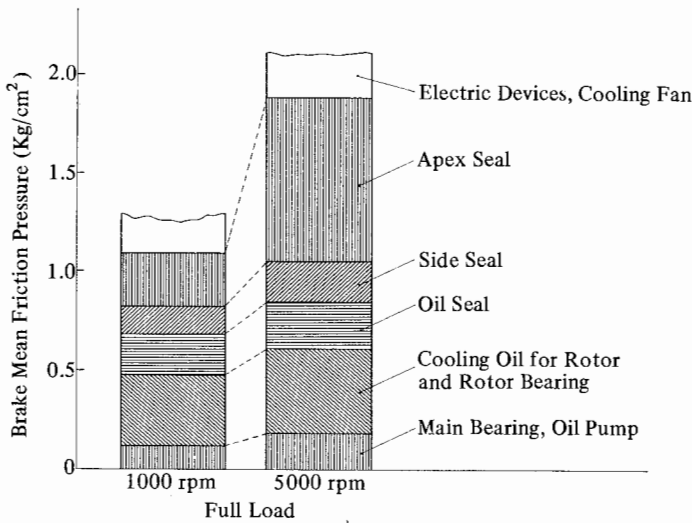


Fig. 9. 2 Friction losses of engine parts

(2) Gas seal

From a PV Indicator Diagram, the adiabatic curve for gas can be drawn in reference to the ideal adiabatic compression cycle, which follows a curve of $PV^n = a$ constant polytrope factor. It is also helpful in estimating the qualitative trend of the overall compression cycle, including gas leakage losses. Fig. 9. 3 is a dual logarithmic presentation of the indicator diagram for wide open throttle, and it shows changes against engine speed increase. The gas leakage through the apex seal is greatest at both axial ends. The relation between the clearance, at axial end, and the brake torque of the output shaft of a one-piece apex seal is illustrated in Fig. 9. 4.

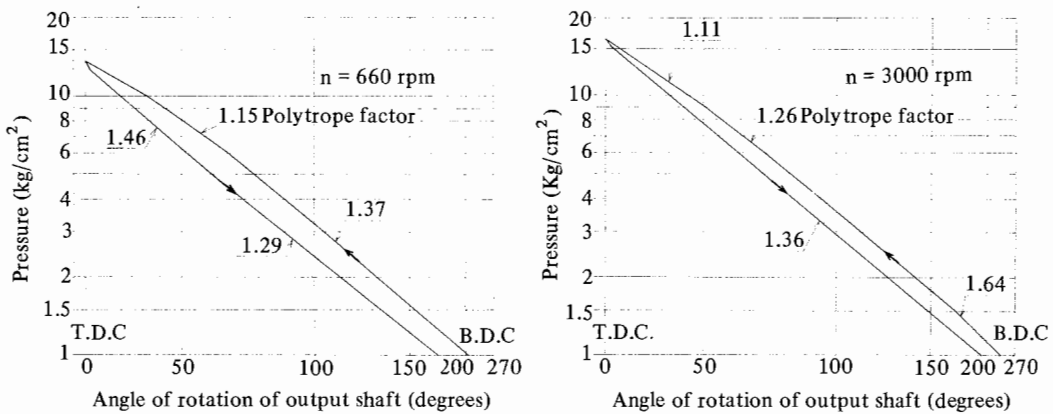


Fig. 9. 3 Motoring indicator diagram (compression ratio : 9.0)

A three-piece apex seal, composed of one trapezium piece in the middle flanked by two triangular pieces, is used to help reduce leakage. The three-piece apex seal is especially effective for low speed operation. Fig. 9. 5 shows an effectiveness comparison of the three-piece apex seal and the one-piece seal.

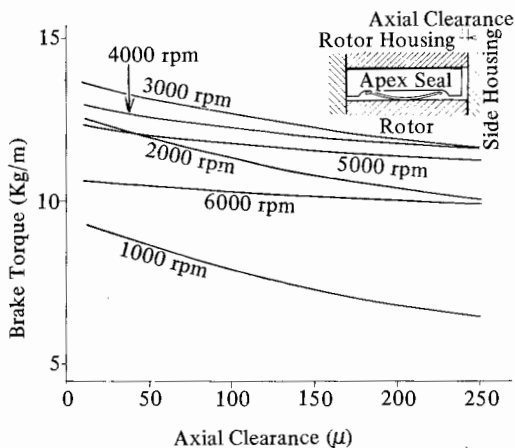


Fig. 9. 4 Relationship between axial clearance of apex seal and output

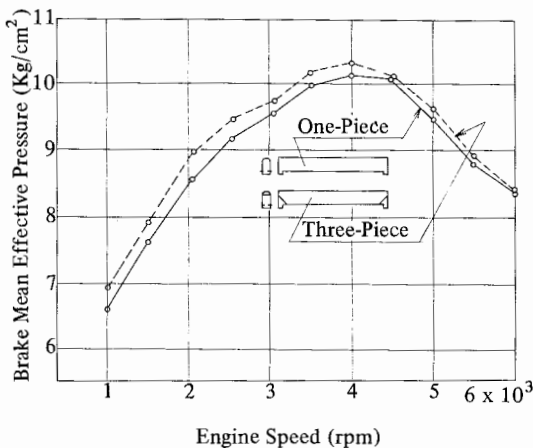


Fig. 9. 5 Comparison of one-piece and three-piece apex seals

The gas leakage through the side seal is mostly unburned gas. Therefore, it is suspected that the gas leakage occurs when the inertia force applied to the seal and the gas pressure balance in the compression cycle. When they balance, the part of the seal contacting the sealing groove flips partly, allowing gas to leak through. This gas leak is not necessarily always unfavorable. For instance, when lubricating the seal sliding surface by mixing a small amount of lubricating oil into the intake gas, it helps the oil to spray over the necessary surface.

Fig. 9. 6 shows a comparison on air tightness between the single and the double side seal. The double side seal improves the sealing effect by 30% to 50% because of its labyrinthine design. The leakage loss is about 1% of intake at high speed operation.

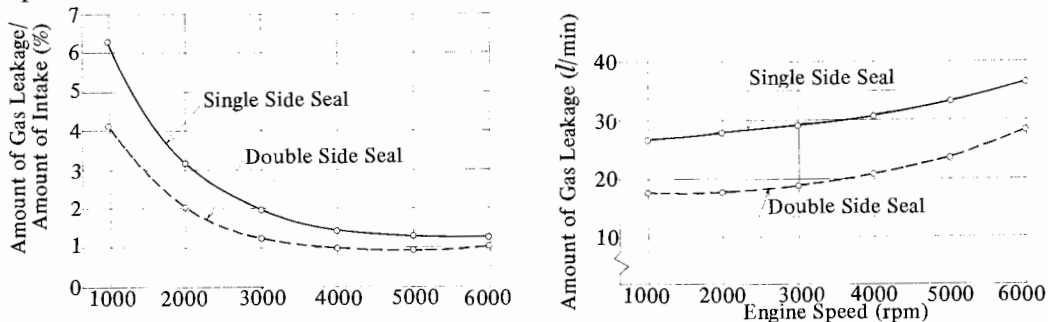


Fig. 9. 6 Effectiveness comparison of single and double side seals

Of course, in maximizing gas seal performance, it is necessary to consider both the plus factor of increased compression pressure, which is increased output ratio, and the main minus factor of increased pressure, which is increased gas leakage.

(3) Effect of intake and exhaust methods

Fig. 9. 7 compares the peripheral port, which is an intake port located right on the trochoid wall, and the side port, which is located on the side housing, in their effect on wide open throttle.

With the peripheral port, the duration of intake and exhaust overlap is longer, and it also has less intake resistance. These are basic requirements for a high-speed engine. The peripheral port however has drawbacks too, one of which is the pulsation effect of exhaust gas on the exhaust back pressure, which is liable to

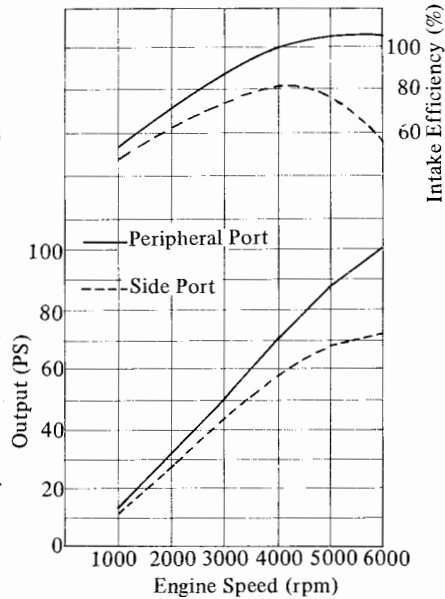


Fig. 9. 7 Types of intake ports and their influence on intake efficiency and output

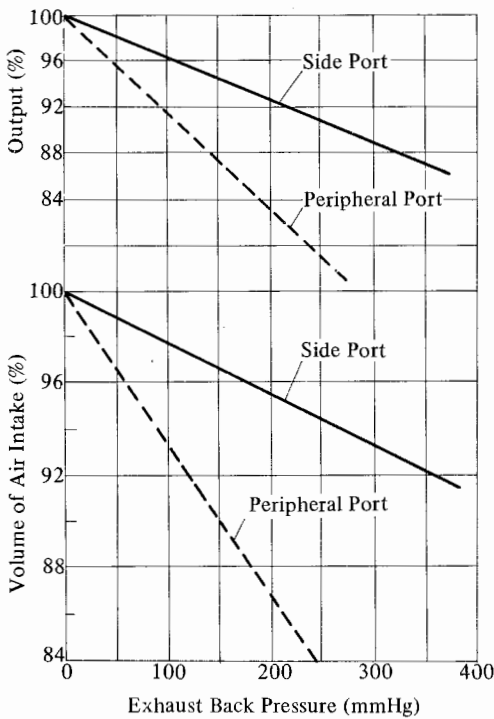


Fig. 9. 8 Effect of exhaust back pressure

reduce output. Another is unstable ignition when in partial load operation. Therefore, when using the peripheral intake port, it is necessary to give thorough consideration to the pulsation effect on the exhaust system, including the muffler, and also the inertia effect of the intake system. The degree of exhaust back pressure for each type of intake port is shown in Fig. 9. 8.

(4) Effect of timing of port opening and closing

As one example of the effect of the timing of port opening and closing on the performance of an engine, Fig. 9. 9 illustrates the relation between the timing of intake port closing and the changes of the mean effective pressure. In general, just as in reciprocating engines, relatively early closing

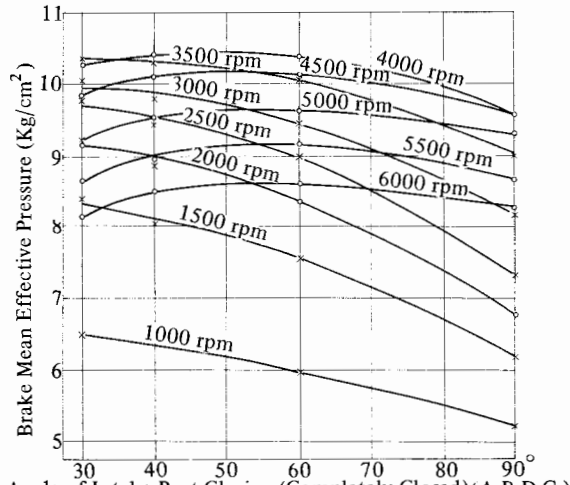


Fig. 9.9 Effect of timing of intake port closing on output

of the intake port helps the mean effective pressure to be higher, resulting in good low-speed operating, because of the inertia effect of intake gas. The timing of exhaust port opening, on the other hand, has an appreciable effect on the rate of fuel consumption. The relatively early opening of the exhaust port is helpful for high-speed operation, but it means more energy loss in low-speed operation and tends to lead to a higher fuel consumption rate and a lower output.

(5) Lean mixture operation

Shown in Fig. 9.10 is the effect of excess air in the mixture on the mean effective pressure and the rate of fuel consumption. The maximum output is obtained with a mixture of 5% less air than an ideal amount, and the most economical fuel consumption rate is attained with a mixture containing 5% to 10% excess air. Therefore, the response of a rotary engine to the change of air-to-fuel ratio is said to be about the same as for reciprocating engines.

The factors that most affect the limitations of lean mixture operation are the shape of the hollow of the rotor combustion chamber and the location of the spark plug. Generally, a spark plug provides good ignition when located on the leading side, where it provides a better chance of operating with a very lean mixture.

(6) Compression ratio

Fig. 9.11 gives the presently available experimental data showing the effect of the compression ratio on the output. The highest brake mean effective pressure is obtained for compression ratios between 9 : 1 through 11 : 1, and the specific fuel consumption reaches the minimum at the compression ratio of 9.5 : 1. The major

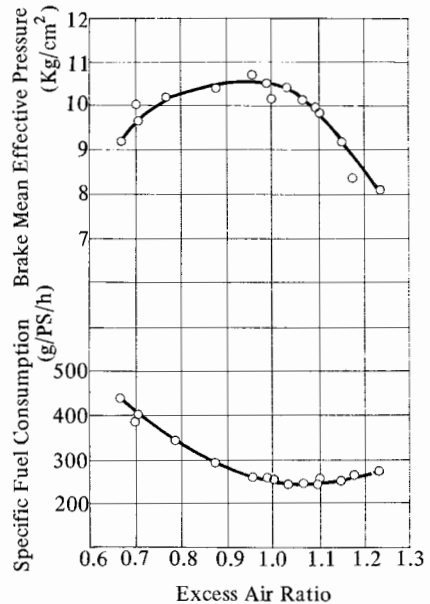


Fig.9.10 Effect of excess air mixture rate on mean effective pressure and rate of fuel consumption

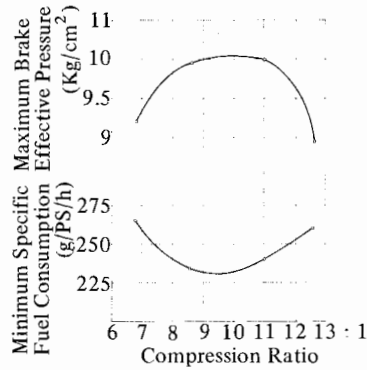


Fig. 9. 11 Relation between compression ratio and performance
(Displacement of single working chamber 250 cc)

reasons why output and specific fuel consumption deteriorate at the extremely high compression ratio of 12.6 seem to be unsatisfactory location of spark plug, sudden increase of blow-by leakage of combustion gas and compressed gas, and the fact that the displacement of the combustion chamber is too small for that high compression, resulting in poor combustion.

9.3 Heat Balance

Fig. 9. 12 shows the distribution of heat generated while the excess air ratio is in the range of 0.83 through 1.18. At 0.95, the ratio which gives maximum output, letting heat generated equal 100%, the breakdown is :

Effective heat	26%
Heat absorbed by lubrication oil	7%
Heat absorbed by cooling water	12%
Heat of exhaust gas	36%
Heat of unburned exhaust gas	16%
Heat loss through radiation and conduction	3%

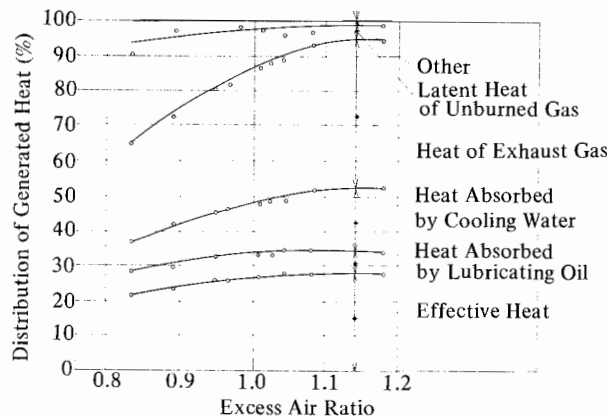


Fig. 9. 12 Relation between excess air ratio and heat distribution
(Full load : 4,000 rpm)

If the excess air ratio is raised, the temperature of combustion gas will rise, and as a result the heat loss of unburned gas will become less. At the same time, the effective heat, heat absorbed by cooling water, and heat of exhaust gas all tend to increase.

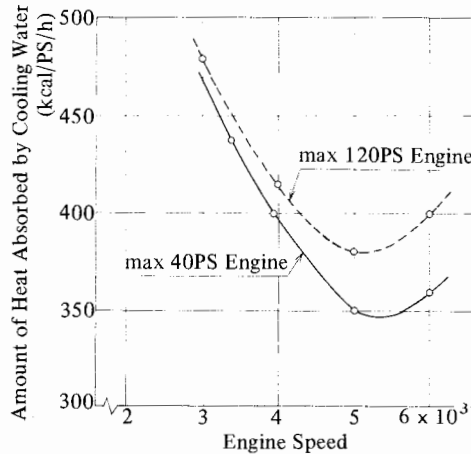


Fig. 9.13 Heat loss through cooling water under wide open throttle

Shown in Fig. 9.13 is an example of the relation between the amount of heat absorbed by cooling water and the engine speed.

9.4 Combustion

In the sense that the combustion process of a rotary engine involves the mixing of fuel and air and the ignition by sparking, it is intrinsically not different from that of a conventional 4-stroke reciprocating engine. However, it is to be expected that the progress of combustion will be considerably different because of the unique working cycle and shape of the combustion chamber. And indeed, in the course of investigation, quite a number of important factors in working conditions relating to combustion and other relevant matters have been brought to light.

(1) Flame propagation

Shown in Fig. 9.14 is a sketch of a housing specially designed and used for measuring the speed of flame travel at various positions on the trochoid wall.

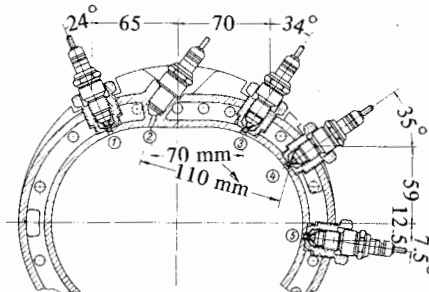


Fig. 9.14 Arrangement of ion electrodes for measuring the speed of flame travel

At arbitrarily selected spots on the trochoid wall, insulated ion electrodes are installed and a DC voltage is applied between the electrodes and the ground. When the flame reaches an electrode, ion current will flow through the electrode and the housing, thus recording the time when the flame reaches an electrode. At the same time of course, the time of ignition is also recorded. By comparing these two, the speed of the flame travel can be calculated.

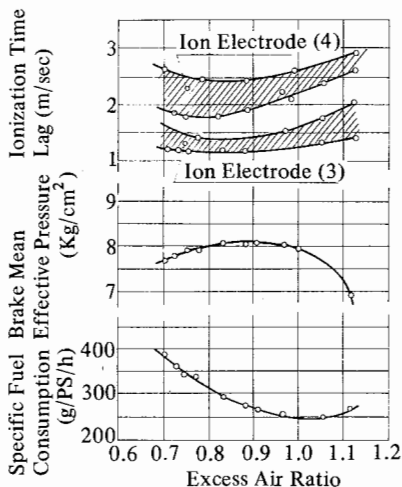


Fig. 9. 15 Relation between the time required for flame to reach ion electrode and the air-fuel ratio (Compression ratio : 7.9 ; Engine speed : 5,000 rpm)

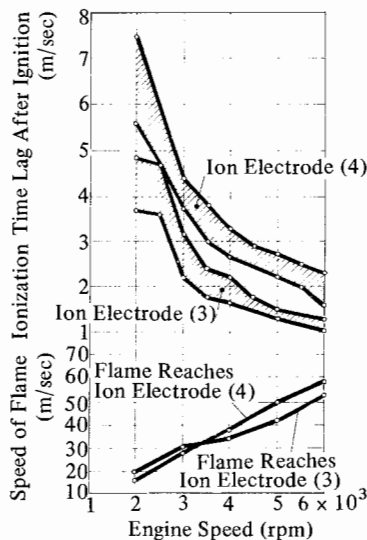


Fig. 9. 16 Speed of flame travel under full load operation (Compression ratio : 7.9 ; Excess air ratio : 0.95)

The results of the measurements are shown in Fig. 9. 15. The time lags from spark plug (2) to ion electrodes (3) and (4) are plotted in relation to the excess air ratio. We see from the Figure that maximum speed of flame travel is obtained with a lean mixture containing 15% to 20% less air than the theoretical optimum.

The speed of flame travel measured by the time lag between the ignition and ionization is plotted in Fig. 9. 16 in relation to the engine speed. The increase of flame speed by the increase of engine speed is more noticeable in a rotary engine than in a conventional engine. This is because the gas in the combustion chamber is pushed by the rotor in the direction of rotation, and at the same time, the trailing side combustion chamber functions as a squish area and generates strong compression turbulence. Thus as a result, the flame growing from the ignition electrode is pushed at very high speed, by the combination of turbulent flow and normal rotating gas, in the downstream direction to the leading side.

Shown in Fig. 9. 17 is a sketch of a few frames of a high speed movie taken of the flame travelling near the top dead center. It is clearly noticeable from the sketch that the flame moves very rapidly in the direction of rotation, reaching

a relatively long distance fairly easily. However, because of strong compression turbulence, the speed of flame travel in the opposite direction (upstream) is far slower. Furthermore, the flame tends to be quenched in the trailing side, giving an added effect of slowing down the upstream movement of the flame.

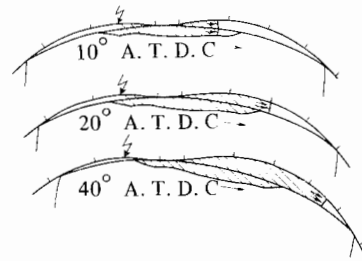
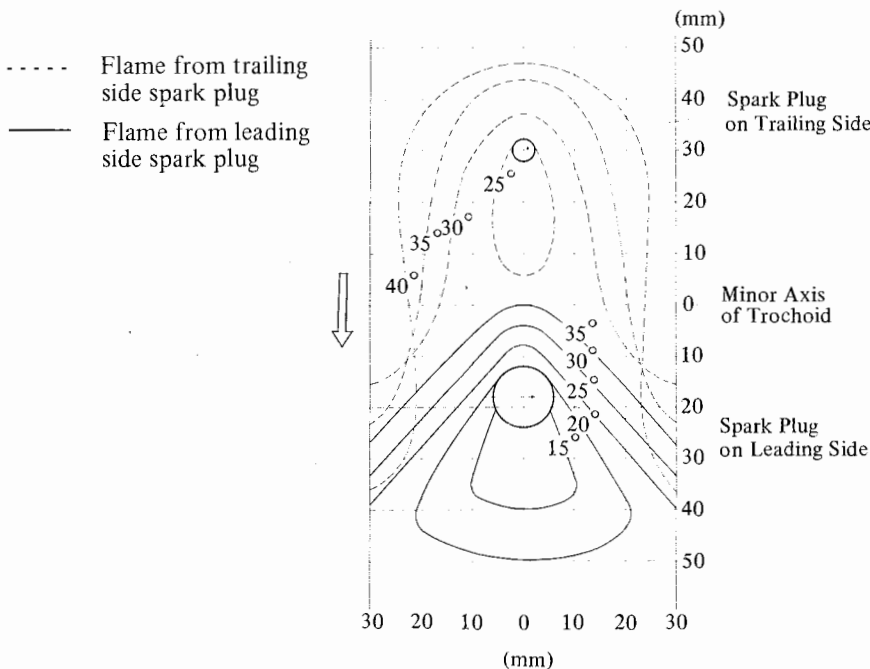


Fig. 9. 17 Flame travel near top dead center



Compression ratio	Revolutions of output shaft	Filling efficiency	Air-fuel ratio	Ignition timing	
				Trailing side	Leading side
9.3	1500 rpm	60%	16	B.T.D.C 20°	B.T.D.C 30°

Fig. 9. 18 Flame travel in the direction of the axis of the trochoid

Fig. 9. 18 shows flame travel along the trochoid wall. The time lags from time of ignition to ionization are plotted in relation to the engine speed.

(2) Effect of spark plug location

Generally speaking, in order to improve combustion by shortening combustion time, it is helpful to use the dual spark plug system, where one spark plug is installed on the trailing side and the other one on the leading side.

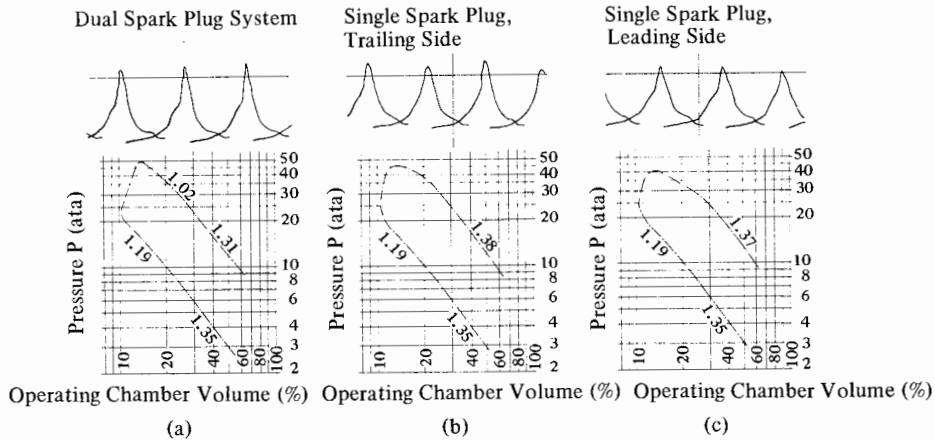


Fig. 9. 19 Indicator diagram (wide open throttle; 3,400 rpm)

Table 9. 2 Single spark plug and dual spark plug systems and their influence on engine performance.

	Location of spark plug	Ignition timing (B.T.D.C deg)		Mean effective pressure (kg/cm ²)	Excess air ratio	Filling efficiency (%)	Rate of pressure rise (kg/cm ² /deg)
		Trailing side	Leading side				
(a)	Dual spark plug system	12	17	9.07	0.83	103	0.82 ~ 1.46
(b)	Single spark plug system on trailing side	29	—	8.83	0.78	103	0.79 ~ 1.14
(c)	Single spark plug system on leading side	—	20	8.54	0.79	104	0.69 ~ 1.0

Fig. 9. 19 and Table 9. 2 show the results of a study conducted about the effect of the number and location of spark plugs. Comparison is made at the ignition advance which gives a maximum torque.

With a single spark plug at the trailing side, even with the timing advanced quite a bit from a dual spark plug system, the pressure does not seem to want to go up very much, and the combustion tends to take place at almost constant pressure.

When a spark plug is installed on the leading side, there is a clear tendency toward two-stage combustion because the mixture of gas upstream from the spark plug will not burn until it comes across the minor axis of the trochoid. The pressure rise in this system is the least of all systems.

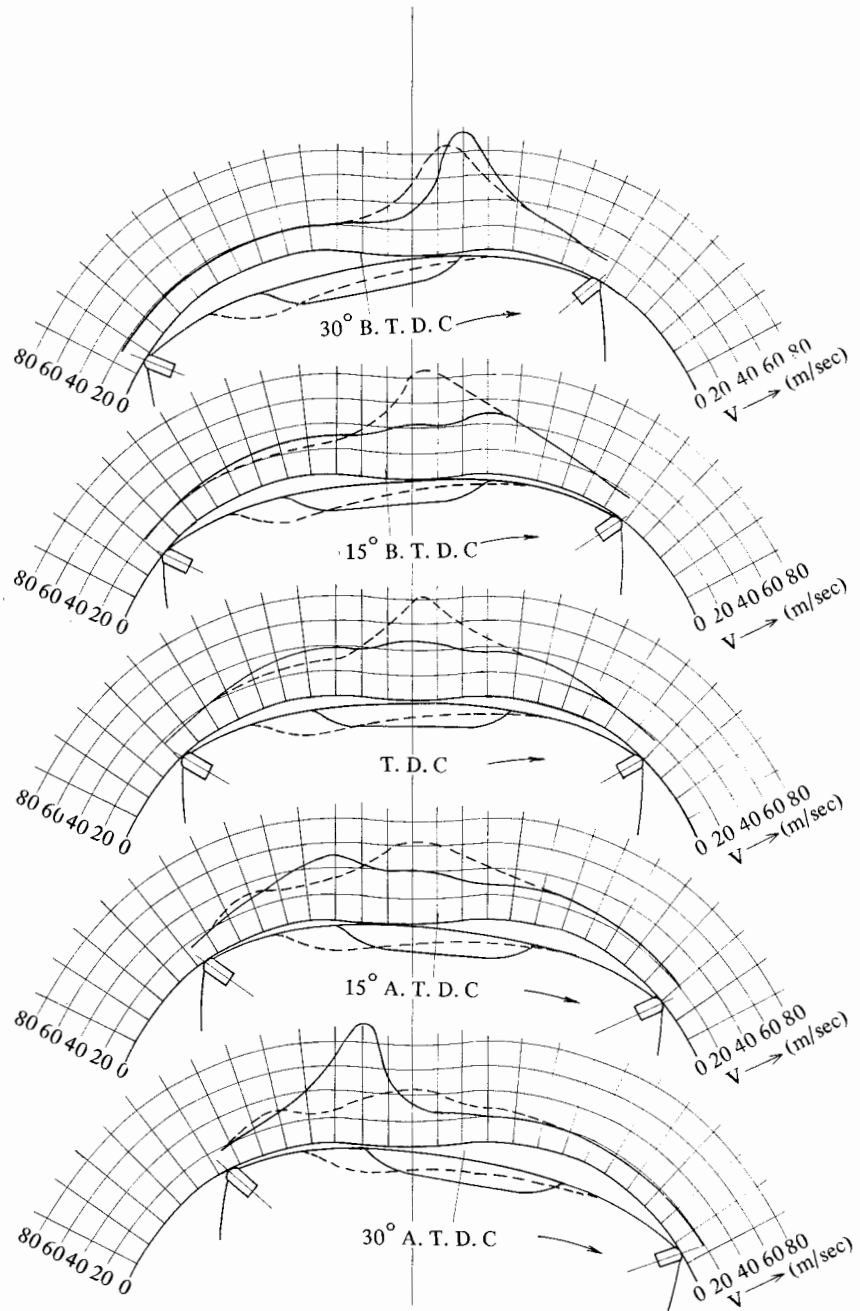


Fig. 9. 20 Speed of gas flow near top dead center for two different combustion chambers

(3) Effect of rotor combustion chamber

The location and shape of the hollow combustion chamber of the rotor are interrelated with the efficiency and quietness of combustion and the required octane value, and they have a substantial influence on general engine performance.

Fig. 9. 20 shows an example of the effect of compressing to generate turbulence, and the effect of forming a quenching area to prevent abnormal combustion, calculated for their influence on the speed of gas flow in different types of combustion chambers.

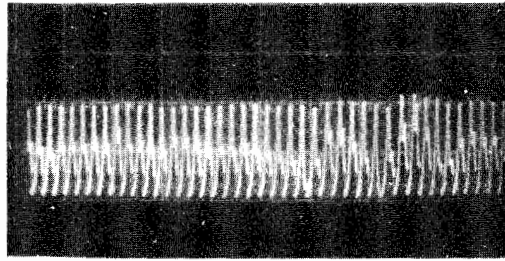
In terms of the ratio of the combustion chamber surface area to the volume of the combustion chamber at top dead center (s/v), the rotary engine is intrinsically disadvantageous compared to the reciprocating engine with an equivalent displacement and compression ratio. On the other hand, with a rotary engine, it is easy to generate a turbulent flow, whose speed is far greater than the speed of combustion, and the trailing side of the rotor forms a quenching area to reduce the temperature of end gas. These factors contribute to a unique combustion mechanism for the rotary engine which is relatively uncritical to the kind of fuel, and provides superior anti-knocking characteristics.

(4) Effect of type of intake port

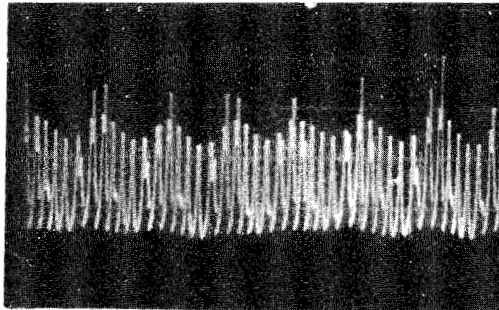
Under near-full load conditions, the change in charging efficiency caused by the dynamic effect of intake flow affects the brake mean effective pressure and specific fuel consumption to a certain extent, but not as much as the effect of spark plug location on combustion characteristics. The type of intake port, however, has a noticeable effect on combustion at idling or under light load, when the amount of residue exhaust gas suddenly jumps to a sizeable level, as compared to fresh mixture taken into the engine.

The combined port arrangement (see Figure 3. 3 (d)) provides a geometrically longer overlap of exhaust and intake port opening, and its secondary air system from the carburetor throttle valve through the trochoid, together with the hollow of the combustion chamber, serves to retain a part of the exhaust gas. An engine equipped with a combination port, therefore, is liable to dilute fresh intake gas in low-speed and low-load operation more than engines with other port arrangements. The effect of the port valve on an engine equipped with a combination port arrangement was studied in terms of pressure fluctuation at idling, and the results are shown in Fig. 9. 21.

The way in which the pressure changes in the combined port arrangement while the port valve is fully closed seems to follow almost the same pattern as in the side port arrangement, because of the location and arrangement of the port. However, when the port valve is fully opened, the amount of fresh intake is so small that before the mixture reaches a combustible level and combustion takes place, it has gone through several purging cycles, resulting in misfiring and unstable combustion.



(a) Port valve closed



(b) Port valve fully open

Fig. 9. 21 Port valve effect at idling

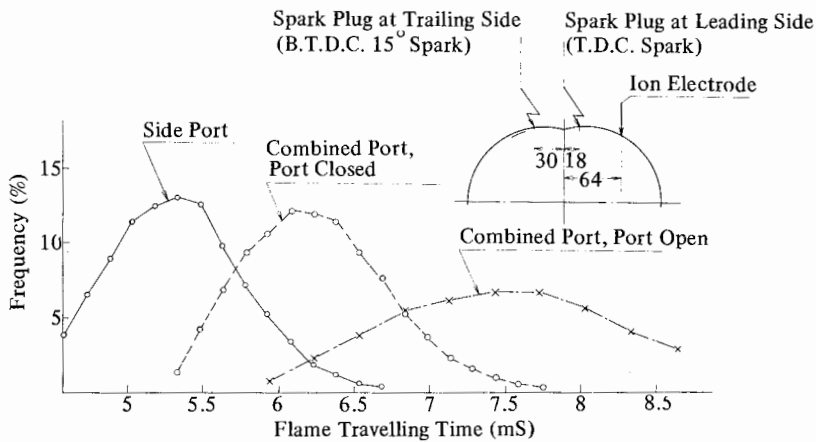


Fig. 9. 22 Distribution of flame travelling time (1,000 rpm ; brake mean effective pressure 1.3 kg/cm²)

Fig. 9. 22 shows fluctuation of combustion at light load operation. Distribution of time lags for flames to reach the ion electrode from the spark plug on the trailing side over several cycles of engine operation was plotted by digital representation, showing the comparison between the effect of the combined port arrangement and that of the side port arrangement. It is clearly seen from the figure that when the port valve is opened, the maximum value of the frequency drops, and at

the same time, the distribution curve becomes wider at its bottom, indicating that combustion becomes unstable.

Reference Materials

- 1) E. W. Huber : Thermodynamische Untersuchungen an der Kreiskolbenmaschine. VDI Berichte, Nr. 45 (1960).
- 2) F. Sisto : Comparison of Some Rotary Piston Engines. SAE Paper 770B, Oct. (1963).
- 3) Felix Wankel : Rotary Piston Engine Performance Criteria. Automobile Engineer, September (1964).
- 4) G. Bobbert : Brennkammerauswahl und Winkelmarkierung bei Messungen am Kreiskolbenmotor. MTZ, 27/1 (1966).
- 5) K. Yamamoto : Experiment Relating to Combustion of NSU-Wankel Type Rotary Engine. Mechanical Engineers Association of Japan Publications. Volume 70 Issue No. 581 (1967).
- 6) M. Shimoji : Flame Propagation of Spark Plug Ignition NSU-Wankel Engine Internal Combustion Engine Volume 7 Issue 71 (1968).
- 7) Walter Froede : NSU-Wankel Engine Automobile Engineer. July (1963).
- 8) Walter Froede : Forward with Wankel. Motor, 12 February (1966).

10. MULTI-ROTOR ENGINES

10.1 Significance of Multi-Rotor Engines

In reciprocating engines, to improve the output without increasing mechanical or thermal loading conditions on component parts, the following two techniques have been general practice :

- (i) To make an engine of similar design with increased total displacement (working chamber volume).
- (ii) To increase allowable engine speed by decreasing reciprocating inertia mass and rate of torque fluctuation by means of increasing the number of cylinders.

These techniques, however, tend to be limited by various factors such as sharp increase in overall dimensions and weight, and increasing complexity of intake and exhaust valve mechanism. They also involve many secondary problems such as torque harmonics. Thus, improving the output of reciprocating engines has never been a simple matter, and the general opinion is that in the future it will become ever more difficult.

The rotary engine, on the contrary, has neither reciprocating inertia mass nor valve moving mechanism. Add to this its small rate of torque fluctuation, and it becomes clear that the rotary engine inherently has great possibility of increasing the engine speed. Also, it is possible to greatly increase working chamber volume with relatively little increase in dimensions, because the total engine size increases at a lower rate than the rate in which the single chamber capacity is increased, as shown in Fig. 10. 1.

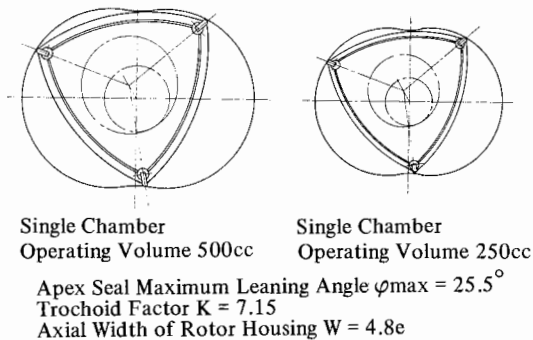


Fig. 10. 1 Increase of dimensions in engines of similar design

This means that increase in output by means of increase in working chamber volume can be accomplished rather easily. Therefore, the necessity of providing multiple rotors (corresponding to increase in number of cylinders) is not so high as compared to the reciprocating engine.

The aim of adopting the multi-rotor type in rotary engines is not only to improve power output and to reduce engine noise level, but also to improve specific

power in relation to engine weight, overall dimensions and volume. Also, multi-rotors reduce engine unit size, meaning higher bearing load, and increased loading limit of gas and oil seal pieces relative to sliding speed, thereby permitting allowable engine speed range to be increased to attain greater power.

10.2 Operation of Multi-Rotor Engines

Fig. 10. 2 shows the basic layout of multi-rotor engines, with engine units arranged in tandem. In this case, engine units (a_1) and (a_2) are installed on an eccentric shaft (k) serving as output shaft. Rotors (b_1) and (b_2), which are set at 180° of rotation apart to insure equal intervals of ignition and operation, and static balance. The arrangement of rotor journals in this case can be considered the same as for the journal pins in a in-line 2-cylinder reciprocating engine.

Front and rear rotors and rotor journals, which constitute dynamic unbalanced weights, are counter-balanced by two balance weights (f_1) and (f_2) attached to the ends of the eccentric shaft. These ensure complete balance of inertia forces and moment acting on the eccentric shaft, as described in 7. 1.

Intake ports (c_1) and (c_2) and exhaust ports (d_1) and (d_2) are respectively in the same phase, and each unit is connected to carburetor (g) common to two units, intake manifold (h) and exhaust manifold (i), to simplify the engine construction.

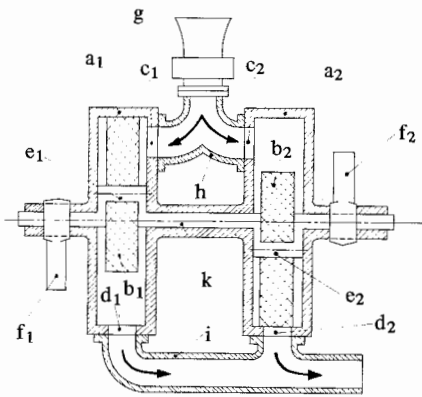


Fig. 10. 2 Fundamental structure of 2-rotor engine

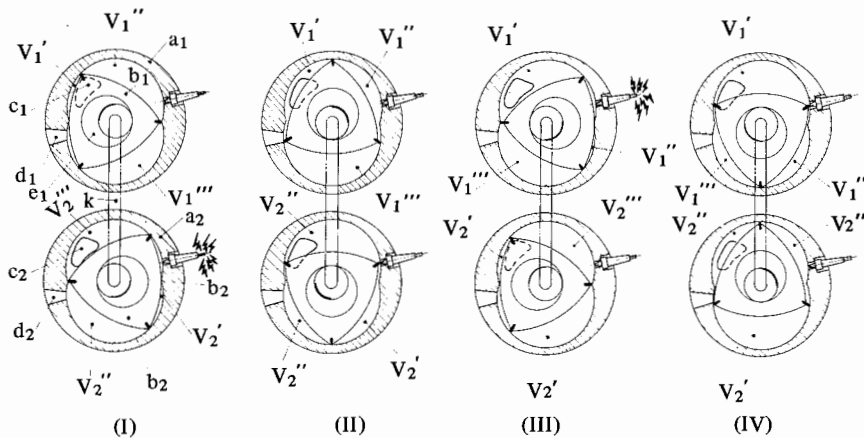


Fig. 10. 3 Working principle of 2-rotor engine

Fig. 10. 3 shows the working cycle of a 2-rotor engine with engine units (a_1) and (a_2) shown in parallel arrangement for convenience of explanation. Working chambers V_1 and V_2 of engine units (a_1) and (a_2) operate at equal interval phase difference, 180° in eccentric shaft rotation angle.

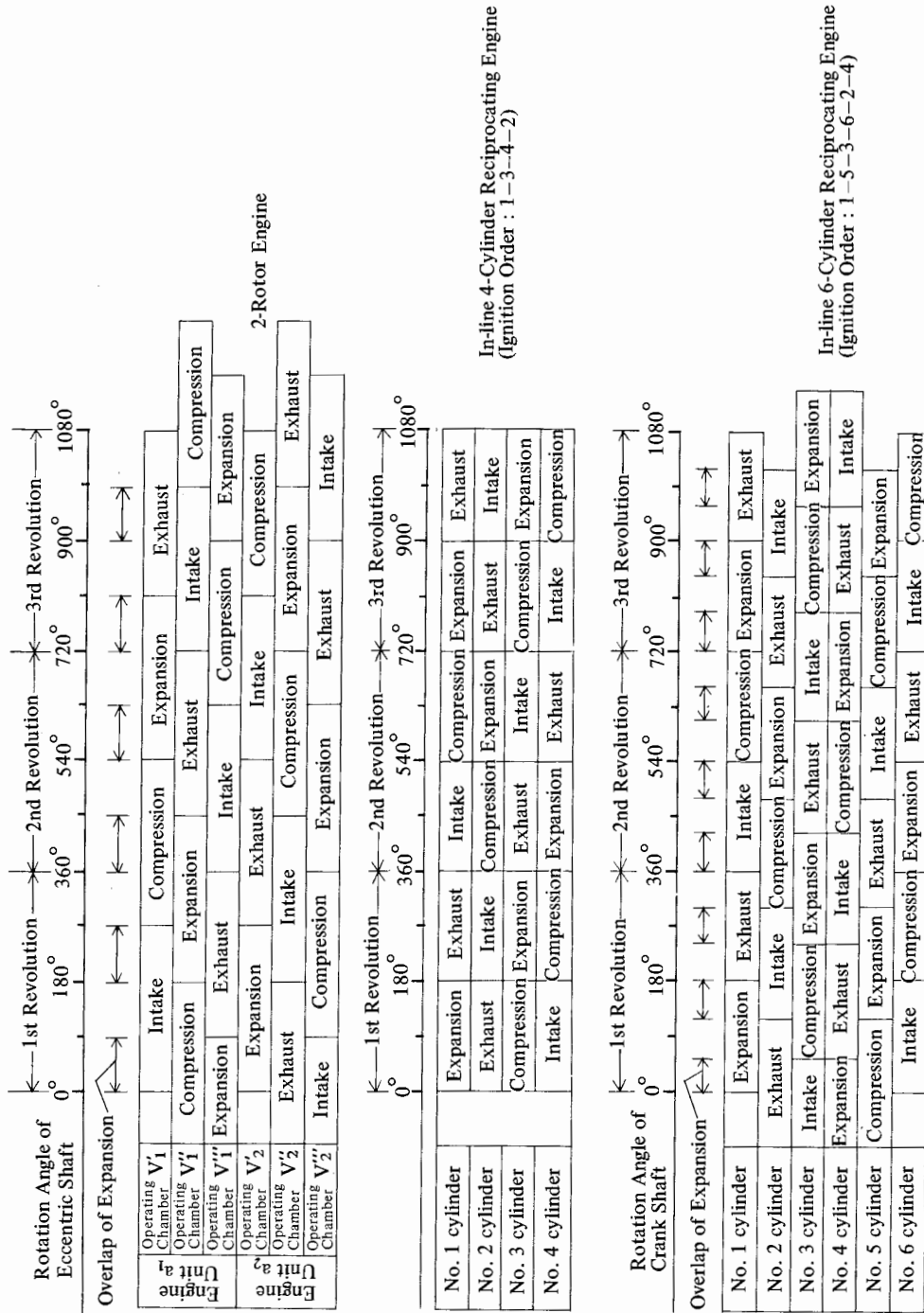


Fig. 10. 4 Comparison of engine working conditions

Fig. 10. 4 compares operating conditions of a 2-rotor engine and reciprocating engines. Although the ignition interval of the 2-rotor engine is the same as that of a 4-cylinder reciprocating engine, it has the advantage that the total sum of explosion/expansion periods is comparable to that of a 6-cylinder reciprocating engine. The effect of increasing the number of cylinders in a rotary engine will, therefore, be much greater than in a reciprocating engine.

The number of rotors can easily be increased to in-line 3-rotor or 4-rotor by arranging the rotor journals at 120° or 90° angular distance interval. In a 4-rotor engine, it is even possible to achieve a journal arrangement requiring no balancing weight at all.

10.3 Performance Possibility of Multi-Rotor Engines

Up to now, most research work on multi-rotor arrangements in rotary engines has been concentrated on 2-rotor, 3-rotor or 4-rotor engines, with rotors arranged in series (straight). The results confirmed that from the structural standpoint, there is no factor which discourages increasing the number of rotors, and that power output directly proportional to the number of engine units can thereby be obtained.

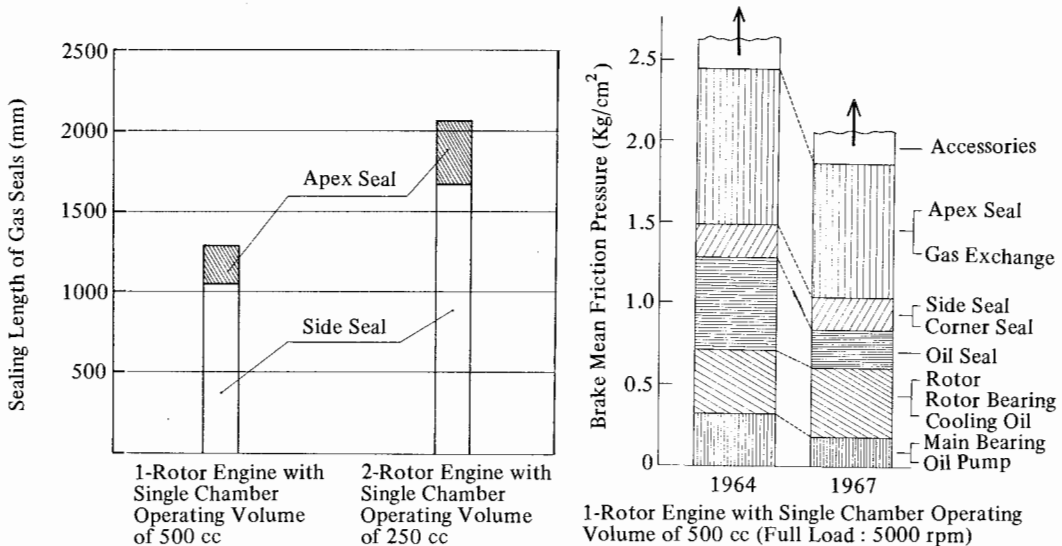


Fig. 10. 5 Comparison of sealing lengths of gas seals. Fig. 10. 6 Comparison of friction loss

However, care must be taken in planning multi-rotor arrangements to avoid loss in mechanical efficiency due to increase in the number of parts, as in the case of planning multi-cylinder arrangements in reciprocating engines. Special care must be paid to higher friction loss and pumping loss due to longer total length of sealing lines as the number of rotors increases, as shown in **Fig. 10. 5**. Recent remark-

able improvements in construction, however, have noticeably decreased friction losses, as shown in Fig. 10. 6.

There are still many problems of mechanical efficiency in multi-rotor arrangements to be solved in the future, but it is safe to say that major problems have been solved to a reasonably adequate level to date.

If we consider the apex seal speed in the rotary engine as corresponding to the piston speed in a reciprocating engine, relative tendencies between their mean speeds and brake mean effective pressures are shown in Fig. 10. 7. Hatched areas

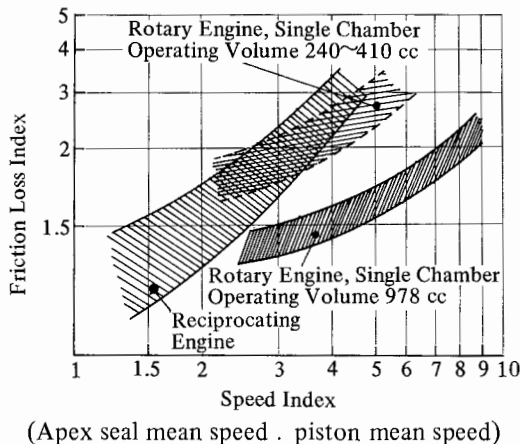


Fig. 10. 7 Comparison of tendencies for increase of friction loss

show the variation range of index values due to difference of engine specifications and test conditions. It should be noted here that brake mean friction pressure of rotary engines does not increase as sharply as that of reciprocating engines. This might serve as an example suggesting that the structure of presently used engines has a large potential for higher speeds.

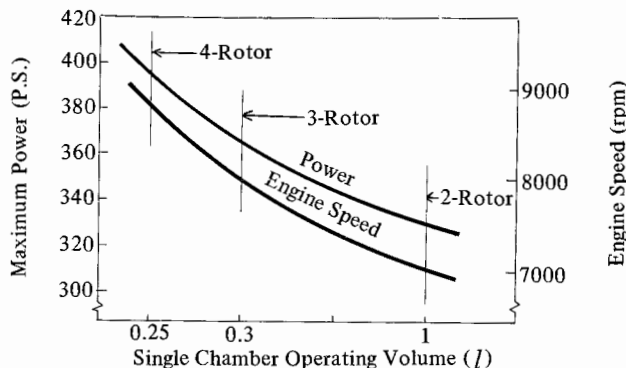


Fig. 10. 8 Example calculation of effect of increased number of rotors

As to the effect of the multi-rotor arrangement on maximum power output and increase in engine speed, an indication as shown in Fig. 10. 8 has been obtained. Total displacement and apex seal critical speed are assumed to be of fixed value in this calculation.

Besides these advantages, engine speed will be increased by adopting light-weight rotors. Also, friction loss can be held down by increasing rotor width, which substantially reduces the total length of seals required. High-speed type intake and exhaust systems can also be expected to give good results. All in all, the outlook for multi-rotor arrangements is bright indeed.

10.4 Examples of Multi-Rotor Engine Construction

Fig. 10. 9 shows a longitudinal section of a 2-rotor engine and the single-rotor engine (single chamber working volume : 978 cc) that it is based on. Both engines use the same rotors and rotor housings.

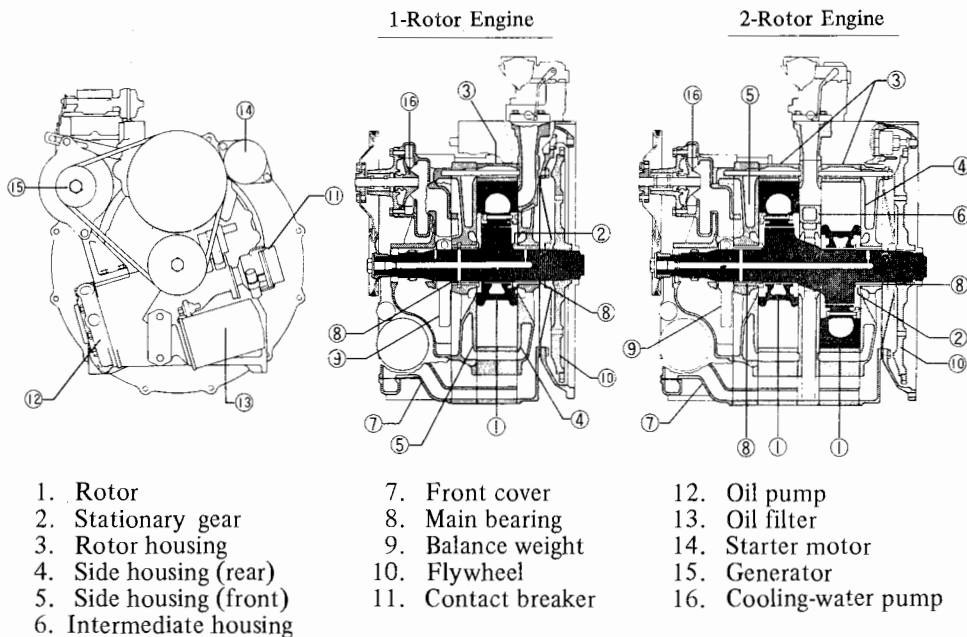
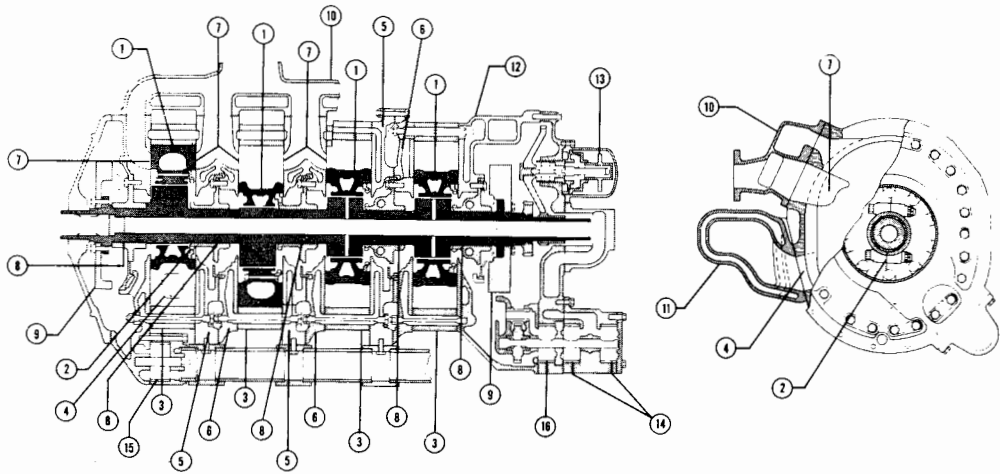


Fig. 10. 9 An example of engine unit constitution

The major advantage of the 2-rotor engine lies in the shape of the eccentric shaft and the arrangement of the main bearing, which are much simpler than the crank shaft of a reciprocating engine of the same power class. Especially important is the fact that only two main bearings are required, front and rear, the same number as for a single-rotor engine.

Further, multi-rotor engines with three or more rotors can be easily realized when engine unit output shaft has enough extra strength. However, engines with four or more rotors are in very small demand because of the output characteristics, operating qualities, etc. Engines with three or more rotors are remarkable in the set-up of the output shaft, fixed gears and main bearings. These peculiarities arise from structural needs to attach the fixed gear to an engine unit located between



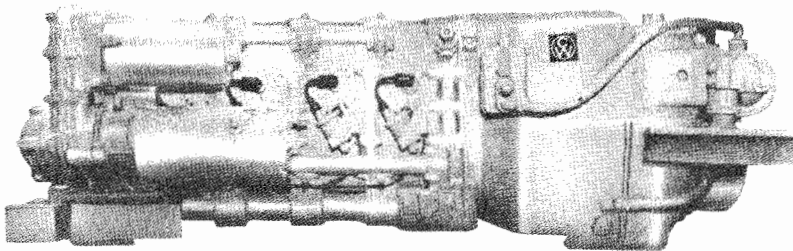
- | | | |
|--|---------------------------------|--------------------------------|
| 1. Rotor | 7. Intake port (dual side port) | 12. Accessory gear box housing |
| 2. Split stationary gear with main bearing | 8. Main bearing | 13. Ignition contact breakers |
| 3. Rotor housing | 9. Flywheel (balance weight) | 14. Oil pressure pump |
| 4. Exhaust port | 10. Intake manifold | 15. Oil scavenge pump (rear) |
| 5. Side housing (drive side) | 11. Exhaust manifold | 16. Oil scavenge pump (front) |
| 6. Side housing (anti-drive side) | | |

Fig. 10. 10 4-rotor engine with split fixed gear

front and rear units, and to provide the main bearing on the middle of the output shaft. There are two ways to meet these requirements :

- (i) Split the stationary gear including the main bearing and fit them onto integral one-piece output shaft.
- (ii) Divide the main journal of the output shaft, and each piece is put together with integral one-piece stationary gear and main bearing.

While the former can be adopted in relatively large-sized engines, the latter is used mostly in engines where the importance is put on simplicity of construction.



Single chamber working volume 1000 cc

Maximum output 425 PS/6500 rpm

Fig. 10. 11 Outside view of the Curtiss-Wright 4 RC 6 4-rotor engine

Fig. 10. 10 shows an example of a 4-rotor engine with split stationary gears and main bearings, and Fig. 10. 11 shows an outside view of the same engine from the spark plug side.

Similarly, Daimler Benz announced in 1969 and 1970 its test car C-111 mounting either 3-rotor or 4-rotor engines. Fig. 10. 12 shows an example with a 4-rotor engine.

Fig. 10. 12 is a schematic diagram of a 4-rotor engine with its output shaft divided and integrated with concentric toothed coupling. Fig. 10. 13 shows the exterior view of a trial engine of this design.

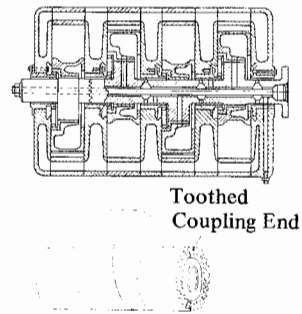


Fig. 10. 12 4-rotor engine with assembled output shaft

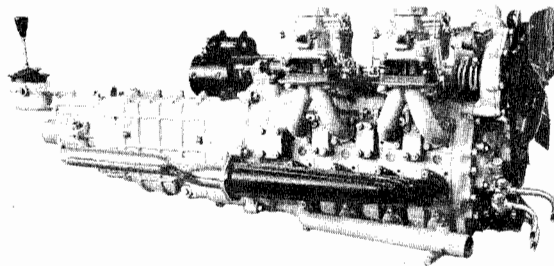


Fig. 10. 13 4-rotor trial engine (Toyo Kogyo)

11. MANUFACTURING METHODS

11.1 Machining the Trochoidal Curve

The surface of the trochoid is generally given some kind of case hardening treatment. Before this treatment it is machined and after the treatment polished with abrasives. Either of the following machining methods can be used in principle :

(1) Trochoid curve generation method

The two-lobe epitrochoid or peritrochoid is a curve generated by rolling around the circumference of a base circle without slip, either a circumscribed circle having a radius ratio of 2 : 1 or an inscribed circle with a radius ratio of 2 : 3 to the base circle. To machine a trochoid surface, reproduce this trochoid generating motion by gear-and-link mechanisms in a machine tool. And the cutting point is provided at a certain point on the rolling circle which generates the locus of a trochoid. The inscribed circle combination is generally used for this machining in consideration of machine space and the rigidity of linking mechanisms which support the cutting head.

This method may be divided into the following three categories corresponding to the type of rotary engine function.

- (i) The method where the eccentric shaft and rotor rotate around a stationary gear (KKM System)
- (ii) The method where the rotor and housing rotate around a stationary eccentric shaft (DKM System)
- (iii) The method where the eccentric shaft and rotor housing rotate with a rotor fixed.

In all cases, the cutting point is provided at the top of the apex seal. This generating mechanism has the following characteristics :

- (a) The normal direction to trochoid at cutting point varies with the sliding angle.
- (b) The tangential velocity of the trochoid generating motion at the cutting point varies.

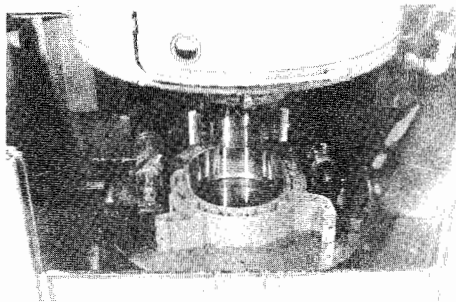


Fig. 11. 1 Internal trochoidal face honing machine

While (i) and (ii) are used with vertical turning mills and similar machine tools, their cutting efficiency is limited due to variation in cutting angle, rake angle and cutting speed.

In a honing machine, hones having the same shape as the apex seal are pressed against the trochoid surface by hydraulic, air or spring pressure. Only the position

of the abrasive varies according to the change of the leaning angle. The honing machine is primarily used for improving the finish, so it is not effective in improving the accuracy of form or straightness. For this reason it is usually used after the grinder finishing. Fig. 11. 1 is a vertical internal honing machine. (iii) can be applied to an internal grinding machine or milling machine. The cutter axis is placed on a normal line to the trochoid at the contact point between the apex seal and trochoid surface, and both the cutter axis and the workpiece are rotated, and then the trochoid generating motion should only be developed between the two. In this case, interference between locus of the outer orbit of the cutter and trochoid curve must be avoided by making the radius of hone or cutter (bit) smaller than that of the radius of the curvature of the trochoid's inner surface.

These methods for obtaining trochoid surface by direct generation of the trochoid can increase the rigidity of the trochoid-generating mechanism, but on the other hand, the precision of the trochoid surface is affected directly by play in the trochoid generating mechanism, such as the backlash of gearing and excessive clearance in linkages.

(2) Model profiling method

A tracer mounted coaxial with cutting axis, e. g., a profiling roller, is made to contact and follow the model (or template) which has a trochoid curve or a parallel curve to it. When this follower is made to trace the contour of a template with the cutter spindle revolving, the shape of the template is transcribed in the inner face of the housing, to produce a parallel surface curve to the trochoid.

If the contacting surfaces of both template and follower are tapered as shown in Fig. 11. 2, continuous feed of cutter as well as automatic compensation for wear of cutter can be achieved by continuous shifting of the contact point between the template and the follower faces. Since the required accuracy of the trochoid curve in this system is easily affected by the profiling characteristics in this mechanism and the contact surfaces of the template and the profiling roller, it is required to increase the wear resistance of the template and to maintain its precision.

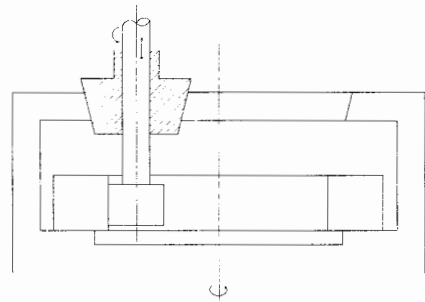


Fig. 11. 2 Concept of model profiling and cutter feed

The template is generally ground by a high-precision, high-performance trochoid generating mechanism. Correction by hand-finishing is sometimes made to reduce the error of the generating mechanism.

Fig. 11. 3 shows an example of the internal grinder with the mechanism of (1) and (2) combined.

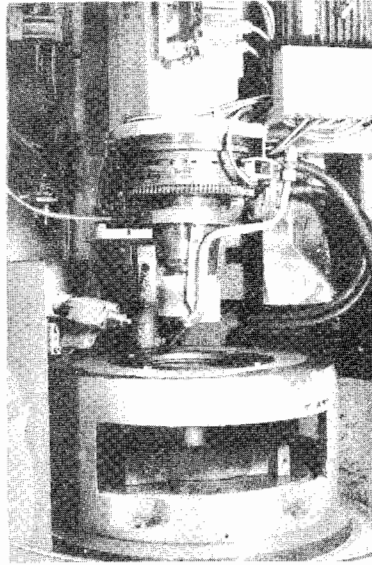


Fig. 11.3 Internal trochoid grinder

(3) Machining by numerical control method

In this method, a trochoid curve is divided into a series of X and Y values of rectangular coordinates and recorded on tape. Input of these coordinate values actuates the operating circuits of the numerical control system and they are transformed into displacements in the mechanical drive system. For instance, the feed screw is driven by a pulse motor to the amount corresponding to the pulse transmitted from the signal system. As the feeds of the table are restricted to either one direction of X or Y at one time, the displacement of cutter relative to workpiece follows a step-shaped locus. However, the finished surface becomes a continuous curve, since the machined surface is gotten as the external envelope of the orbit of the cutter.

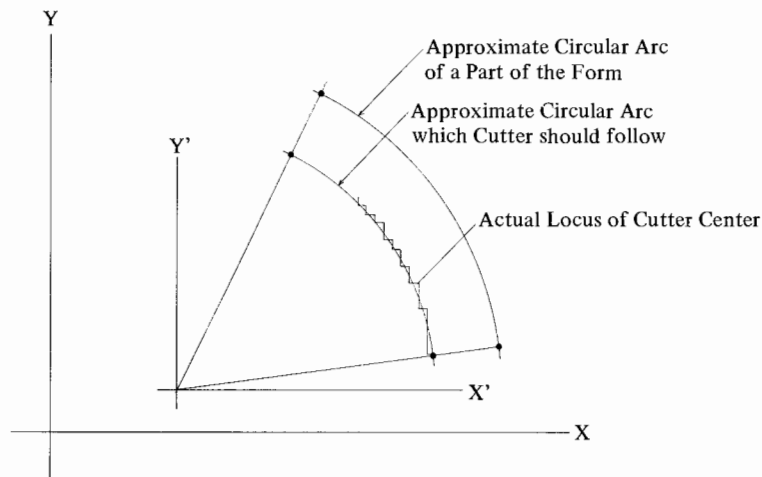


Fig. 11.4 The 2-point approximation method

Since the control tape will become excessively long if the coordinates are finely divided to obtain the required precision, an approximation method is sometimes used, where the trochoidal curve is approximated by a circular arc which overlaps the two points, obtained by dividing the curve.

In this method the locus of the cutter center is automatically offset by designating the cutter radius. Therefore, there is no need of changing controlling numbers since, even if the cutter radius changes by regrinding, it will automatically be corrected.

This system is generally applied to two-dimensional numerically controlled milling machines, and is used in cutting various trochoid surfaces having different generating parameters, such as work on trial models or production of a small quantity of different models. This method is suitable for the so-called "tool-room" system.

(4) Cutting by formed cutter method

In the case of mass-production, it is theoretically possible to employ drawing forming by cutters already formed to the desired contours, such as broach cutters. In such a case, several workpieces for preliminary machining prior to the case hardening process may be stacked for machining in one operation. This method, however, has some drawbacks such as difficulties in the manufacture of cutters meeting the accuracies required for the trochoid.

11.2 Inspection of Trochoid

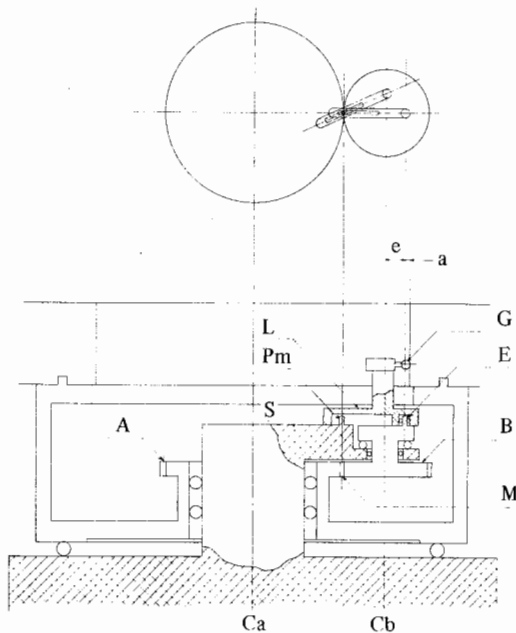


Fig. 11.5 Concept of a trochoid form inspecting device

Peritrochoidal curve can be obtained by tracing a certain point on either circumscribed or inscribed circles. However, on trochoid form testers, generating epitrochoid by tracing a point on a circumscribed circle is generally used to simplify the mechanical construction. To generate a two-lobe epitrochoid, a couple of gears on base circle (A) and rolling circle (B) in Fig. 11.5 are chosen at gear ratio 2 : 1. Shaft (Ca) of base circle (A), shaft (Cb) of rolling circle (B) and a fixed pin (Pm) located at point of contact (M) between (A) and (B) are fixed on support (S). Pin (E) is located on (B) at the distance of an

eccentricity 'e' from (Ca). A swing arm (L) with rolling center (E) and guided by pin (Pm) is provided. Since the directions of center line of swing arm (L) always coincide with the direction of a line connecting point of contact (Pm) between gears (A) and (B) and point (E) on the generating curve, the swing arm (L) is in the direction normal to the epitrochoid. An indicator (G) is mounted on the swing arm (L).

The housing to be inspected is fixed on mount (F) which makes the same rotation as the base circle gear (A) and when it rotates, the hand of indicator (G) will show deviations of the workpiece surface from true trochoid or a curve parallel to it. The actual shape of the trochoid curve to be tested can be obtained by recording the values of deviation according to the rotation of base circle gear (A).

Besides the above, there is another method where the distance to the curved surface from the hypothetical center can be obtained by the combination of a dividing plate and length measuring instrument. This method increases the measurement accuracy but will require more time, and its use, therefore, may be limited to precision inspection in template making, etc.

11.3 Machining of Inner Envelope

The arc-shaped profile of the rotor is formed by the inner envelope of a two-lobe epitrochoid or peritrochoid. The following machining methods can generally be considered :

(1) Model profiling

This method can be applied to turning mills, milling machines, cylindrical grinders, etc. In profile turning mills, the desired shape of rotors can be machined

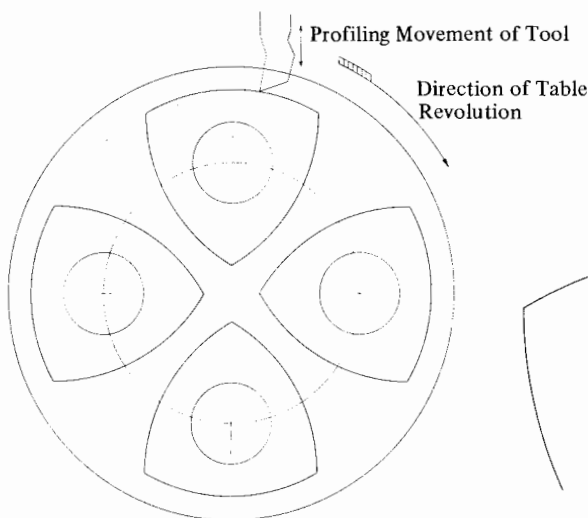


Fig. 11.6 Rotor profile cutting in turning mill

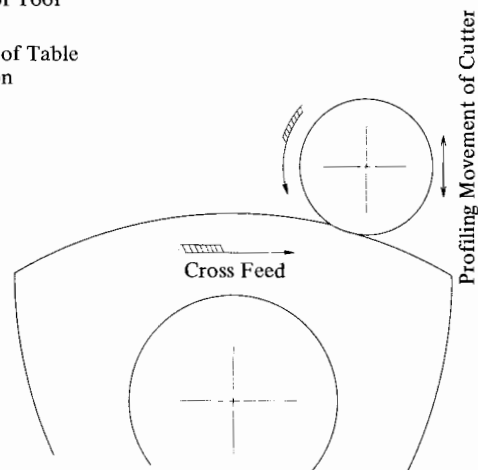


Fig. 11.7 Rotor profile cutting in profile milling machine

by turning the table fitted with rotors and feeding it into the tool which is moved relative to rotor surfaces by means of a profiling mechanism. In most cases, three to four rotors are machined simultaneously. Upon completion of one arc-shaped segment of each rotor, each rotor is turned 120° on the table to finish the next segment.

Either vertical or horizontal type profile milling machines can be used, and the milling cutter is rotated by having its spindle placed parallel to the rotor shaft. In the case of the vertical milling machine, the table will be fed transversely, while the milling cutter is being moved longitudinally along the profiling model.

The profile cylindrical grinder is a combination of a cylindrical grinder and profile modeling mechanism. As a tolerance of 0.5 mm is provided between the trochoid surface and the profile of the arc-shaped segments of the rotor, the finished segment profile does not require a high degree of accuracy. The subsequent grinding finish of the arc-shaped segment, however, allows the precision of the preceding profiling process to be rough.

(2) Approximation by circular arcs

An arc-shaped segment of the rotor can be approximated by two or three circular arcs, and those circular arcs can be machined by a turning mill which does not have a profiling mechanism. Afterward, the remaining portions are machined by having the rotor attachment position displaced. Further, another method of approximation by circular arcs that can be considered is the drawing forming, as explained in (4) of paragraph 10. 1.

(3) Machining by numerical control

The arc-shaped rotor profile is expressed in numerals and the table carrying the rotor is moved respectively along X and Y axes. While this method is, so to speak, the "tool-room" system, as in the case of trochoid surface cutting in rotor housings. The two-dimensional numerically controlled milling machine can often be commonly utilized for machining of the arc-shaped rotor segment as well as machining of the combustion chamber recess of the rotor and trochoid surface of the rotor housing.

Reference Materials

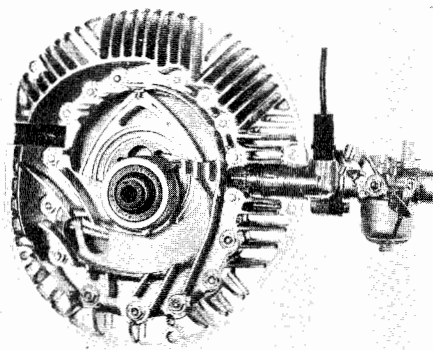
- 1) D. Scott : NSU Foresees Mass Production of Wankel Engine Part I, II. Automotive Industries, Feb. 15, March 1 (1965).
- 2) D. Scott : Tooling for Volume Production of Wankel Automotive Industries, August 15 (1966).
- 3) P. von Manteuffel : Ausgewählte Fertigungsverfahren des Kreiskolbenmotors Bauart NSU-Wankel. MTZ, 28/6 (1967).

12. EXAMPLES OF ROTARY ENGINE APPLICATIONS

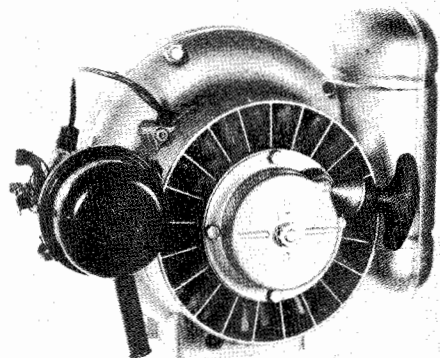
Steady progress has been made in research over a wide variety of applications of the intrinsic features of the rotary engine. Some of them have passed the stage of development and have moved on to actual application. Especially the automotive engines and the small multi-purpose engines, both of which are now available commercially from mass production lines, are drawing a great deal of attention as test cases by which to judge the future of the rotary engine. For both of these applications, new models have been introduced in rapid succession, and the use of the rotary engine is growing accordingly. In this chapter, we will present some examples of applications as multi-purpose engines, automotive engines, motorboat engines, and airplane engines.

12.1 Multi-Purpose Engine

The Fichtel and Sachs' Model 37 air-cooled engine is a typical example of the small multi-purpose engine, for which compactness and lightness are a must.

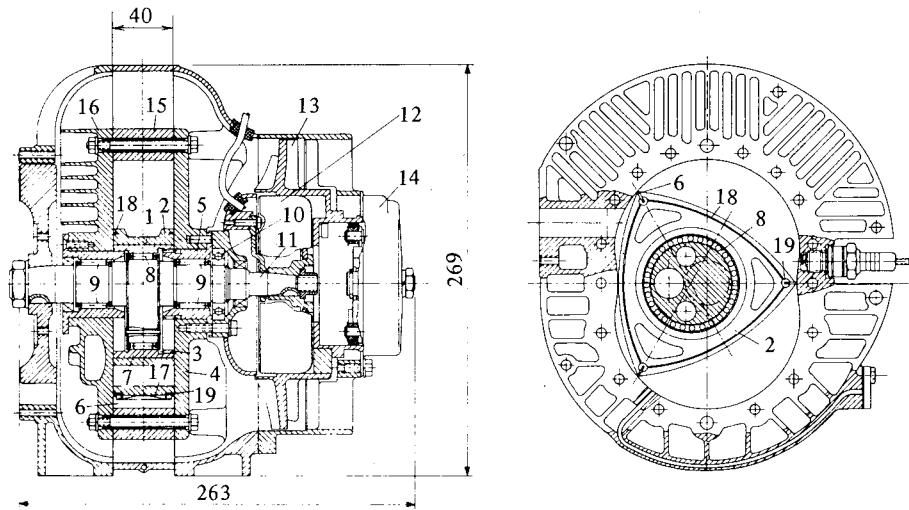


(a) Sectional view to show construction



(b) External appearance
(Displacement of single working chamber-108 cc ; Compression ratio-8.5 : 1 ; weight-15.5 kg)

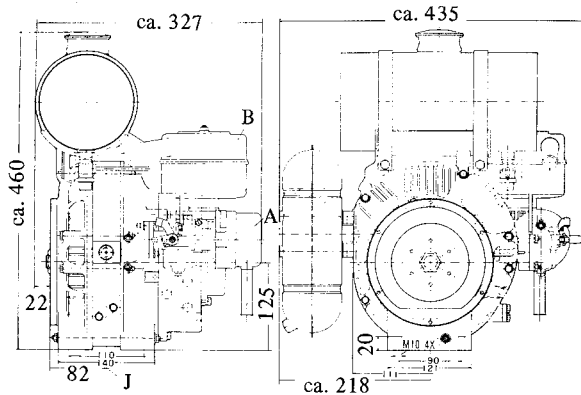
Fig. 12.1 Single-rotor air-cooled engine, Fichtel and Sachs' model KM37



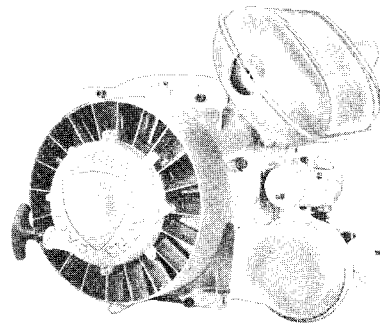
- | | | |
|-------------------------|------------------------|-------------------------|
| 1. Bearing sleeve hole | 8. Rotor bearing | 15. Rotor housing |
| 2. Rotor | 9. Main bearing | 16. Side housing (rear) |
| 3. Rotor gear | 10. Thrust bearing | 17. Apex seal spring |
| 4. Side housing (front) | 11. Eccentric shaft | 18. Side seal |
| 5. Stationary gear | 12. Magneto dynamo | 19. Corner seal |
| 6. Apex seal | 13. Axial flow fan | |
| 7. Rotor bearing sleeve | 14. Rope starter cover | |

(Displacement of single working chamber - 160 cc ; compression ratio - 8.5 : 1 ; weight - 17 kg)

Fig. 12. 2 Fichtel and Sachs' model KM 48 single-rotor air-cooled engine

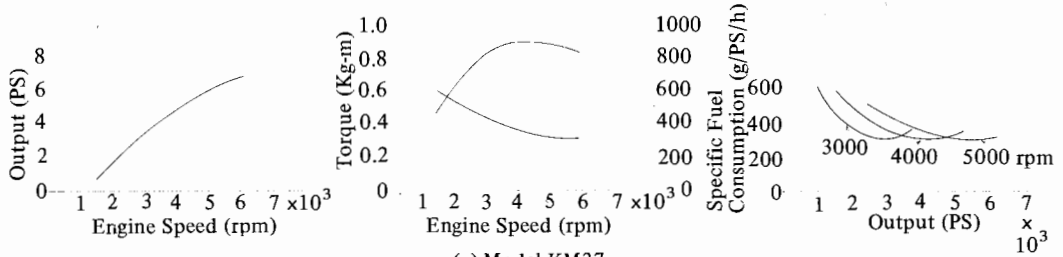


(a) Model KM 48 single-rotor air-cooled engine



(b) Model KM 914A single-rotor air-cooled engine
(Displacement of single working chamber - 300 cc ; compression ratio - 8 : 1 ; weight - 32 kg)

Fig. 12. 3 Fichtel and Sachs' multi-purpose engines



(a) Model KM37

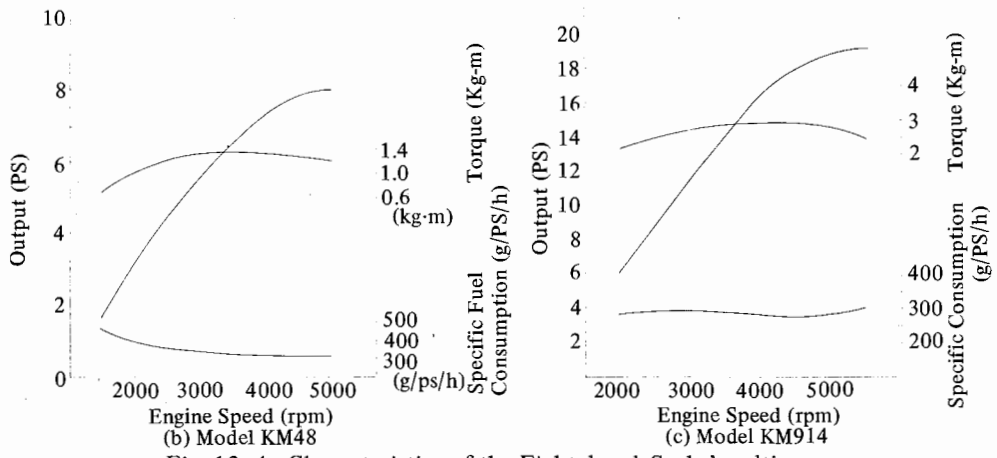
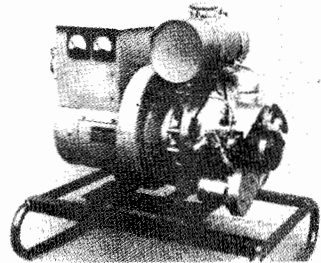
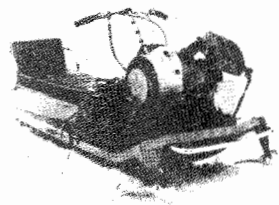


Fig. 12. 4 Characteristics of the Fichtel and Sachs' multi-purpose single-rotor air-cooled engine



(a) Portable generator with F & S KM37 engine



(b) Snowmobile with F & S KM914 engine

Fig. 12. 5 Examples of small air-cooled engine application

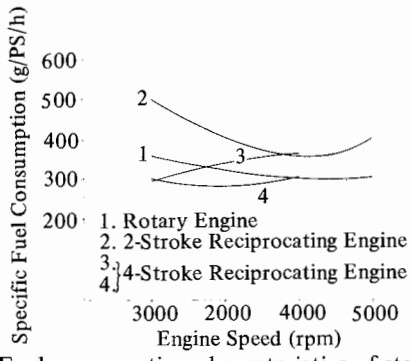


Fig. 12. 6 Fuel consumption characteristics of stationary engine

Shown in Fig. 12. 1 are the inside and outside appearance of model KM37 engine (6. 5 PS at 6,500 rpm). Mass production of this model started in 1964. Recently, mass production has begun on similar models, the KM48 (8. 5 PS at 5,000 rpm), KM914 (18. 5 PS at 5,500 rpm) and KM914A (16 PS at 4,500 rpm). Its sectional views are shown in Fig. 12. 2.

Fig. 12. 3 shows the external appearance of these engines. They are designed to circulate intake gas containing 50 : 1 ratio of fuel/oil mixture through the engine to cool the rotor and lubricate the engine internally.

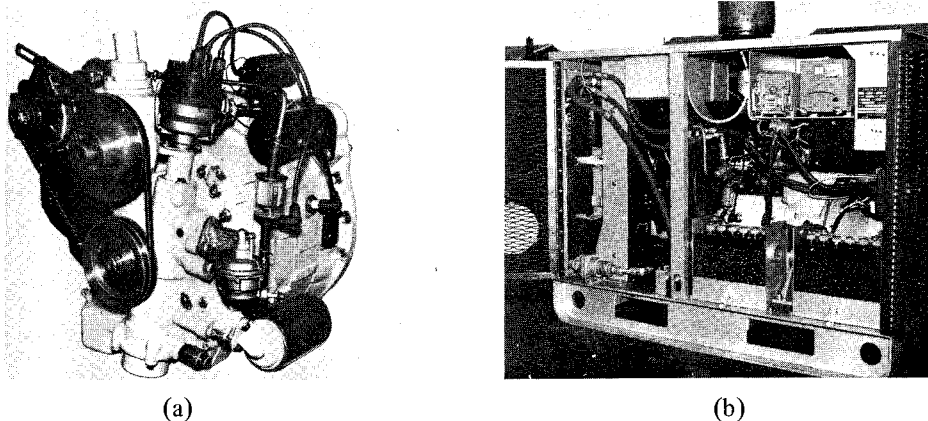


Fig. 12. 7 Curtiss-Wright RC 2-60 water-cooled engine (a) used with a 60 kW generator (b)

Table 12. 1 Comparison of various types of engine used with a 60 kW generator

	2-Rotor engine	Gas turbine	Reciprocating diesel engine	Reciprocating gasoline engine
Weight (kg)	490	442	2132	658
Length (mm)	1257	2065	2360	1830
Width (mm)	864	914	914	1142
Height (mm)	940	686	1500	1142
Total volume (m ³)	1.02	1.275	3.23	2.38

The housing is cooled by air from the axial flow fan, and therefore, the output characteristics shown in Fig. 12. 4 seem to be kept down. These engines are applied to a wide variety of uses. Because of the fact that the rotary engine is better than other types of engine in terms of vibration, it is well suited for agricultural machinery such as hand tractors. Some of the stationary applications are portable generators and well pumps. Recently special applications such as in snowmobiles have been attempted. The fuel consumption characteristics of a small air-cooled rotary

engine compared in Fig. 12. 6 with a comparable size (5 to 7 PS) stationary-use reciprocating engine show it is sufficiently competitive with conventional engines from the viewpoint of economy.

The development of a water-cooled engine is also being pursued very actively. The example shown in Fig. 12. 7 is a Curtiss-Wright model RC 2-60 engine (displacement of single working chamber : 978 cc, 2-rotors) combined with a 60 kW generator. It is showing good performance in terms of generator operation conditions, vibration and resulting stress, and flexibility in coping with load changes. Table 12. 1 shows a comparison of the 60 kW generator equipped with a rotary engine and the same generator equipped with a conventional engine.

12.2 Automotive Engines

The development of the automotive engine has been pursued continuously, and the production models evolved thus far are the KKM502 single-rotor engine, and the KKM612 2-rotor engine, both manufactured by NSU, and model 0813 2-rotor engine for the MAZDA 110S model, and model 0820 2-rotor engine for the MAZDA R100 (Coupé and Sedan), 2-rotor engine for the MAZDA RX-2 which are manufactured by Toyo Kogyo. In 1970 Citroen had a limited number of customers use the M35 powered by a single-rotor engine supplied by Comotor. The specifications of these engines are shown in Table 12. 2, and their output characteristics are shown in Fig. 12. 12.

The construction of the single-rotor engine is shown in Fig. 12. 13, and the 2-rotor engines are shown in Figs. 12. 13 and 12. 14. The difference between these two 2-rotor engines is found in the location of the spark plugs, the method of circulating cooling water through the engine housing, and the method of sealing lubricating oil in the rotor. As examples of 3-rotor and 4-rotor vehicles, there are the C-111s announced by Daimler Benz in 1969 and 1970. The 4-rotor engine, each rotor having a displacement of 600 cc, is said to develop 350 PS at 7000 rpm.

The specific output of a rotary engine for automobiles is compared with reciprocating engines in Table 12. 3. Note that the rotary engine tends to become increasingly compact for larger output.

Fig. 12. 16 shows an experiment where a 200-PS rotary engine is installed in a commercially available truck. This experiment served to illustrate graphically the shorter length of the engine.

The result of noise level measurement inside a passenger car equipped with a rotary engine is compared with that for other engines in Fig. 12. 17. Fig. 12. 18 compares the full-throttle acceleration characteristics of a rotary engine with those of other engines. In both comparisons, the rotary engine shows its effectiveness at

high speeds.

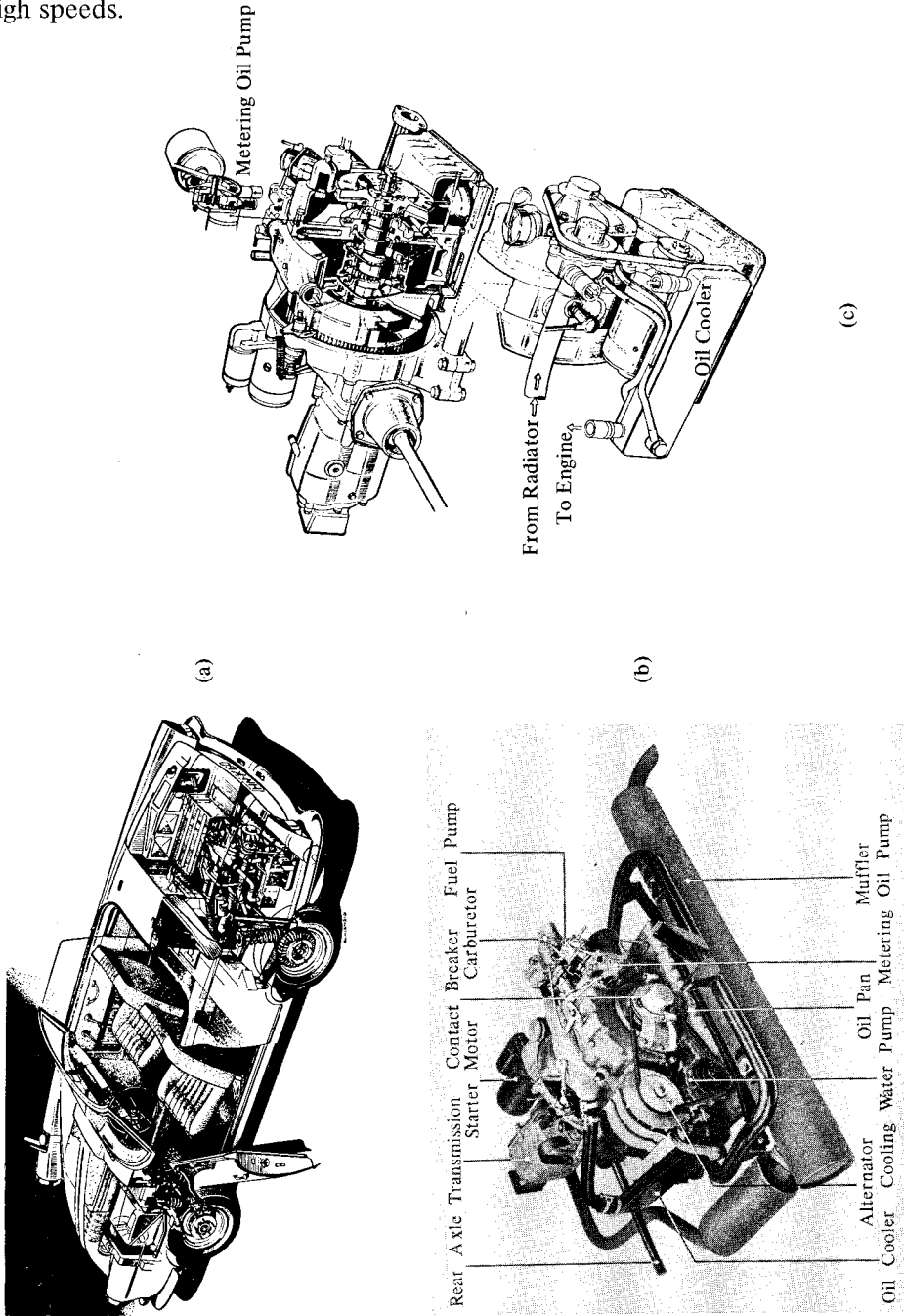
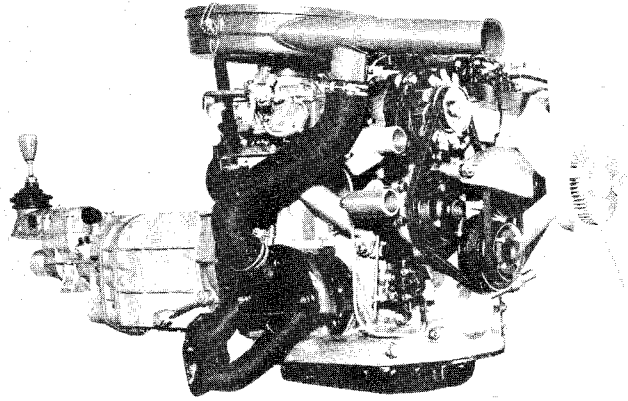
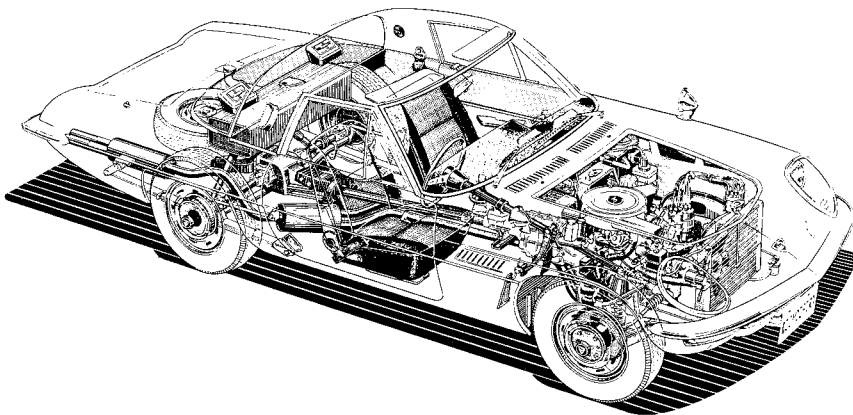


Fig. 12. 8 NSU-Spider and KKM 502 single-rotor water-cooled engine

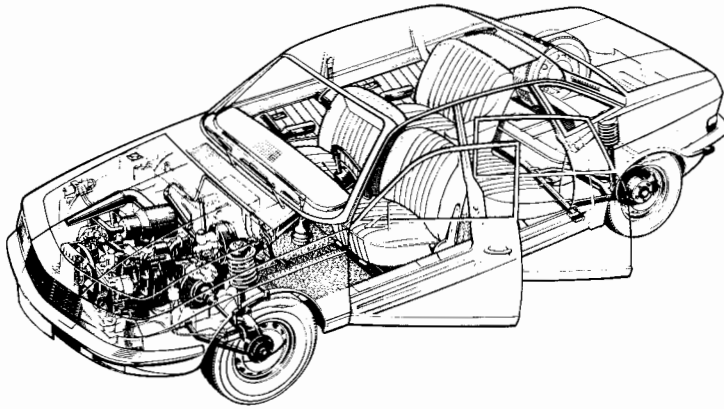


(a)

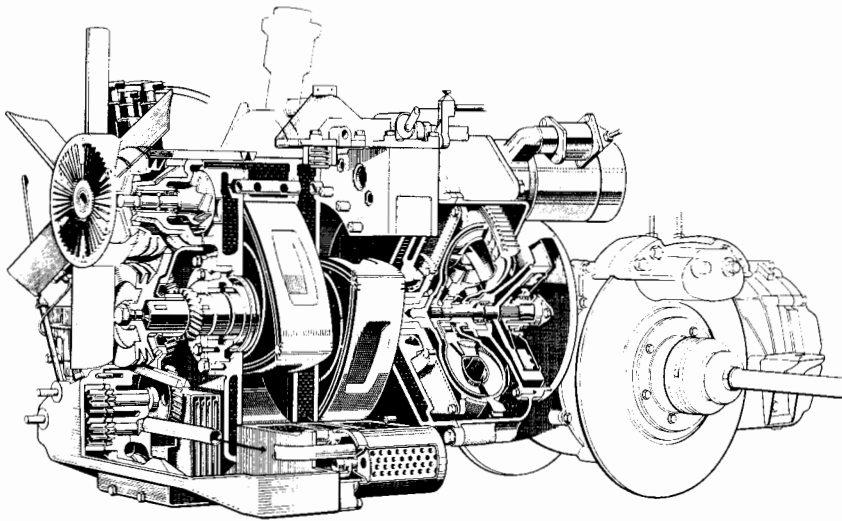


(b)

Fig. 12.9 Toyo Kogyo model 0813 2-rotor engine
(a) and the MAZDA 110S model (b)
(Production started in 1967)

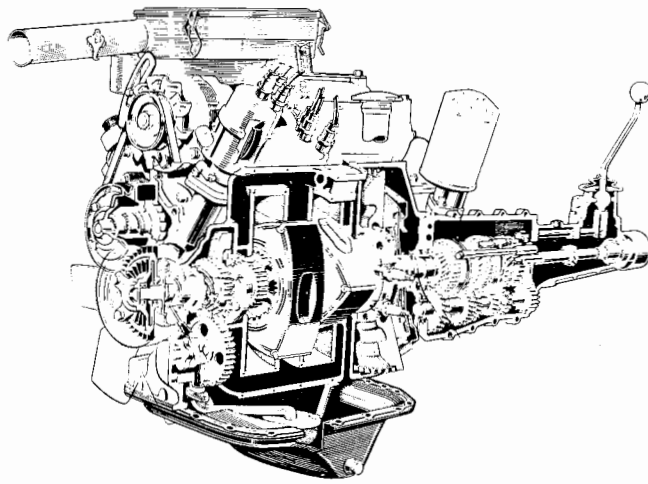


(a)



(b)

Fig. 12. 10 NSU-RO 80 and KKM 612 2-rotor engine (Production started in 1967)



(a)

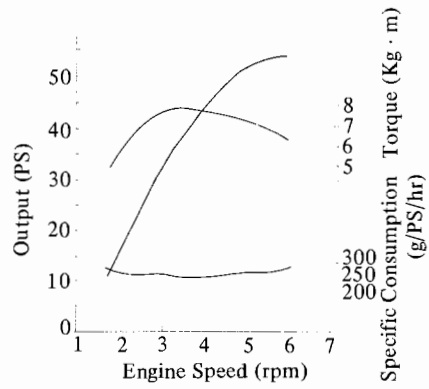


(b)

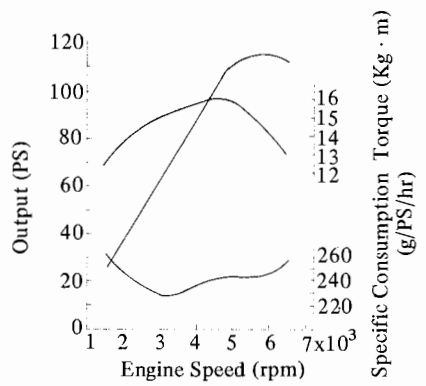
Fig. 12. 11 "MAZDA R100 Coupé" equipped with
Toyo Kogyo 0820 2-rotor engine
(Production started in 1968)

Table 12. 2 Engine specifications

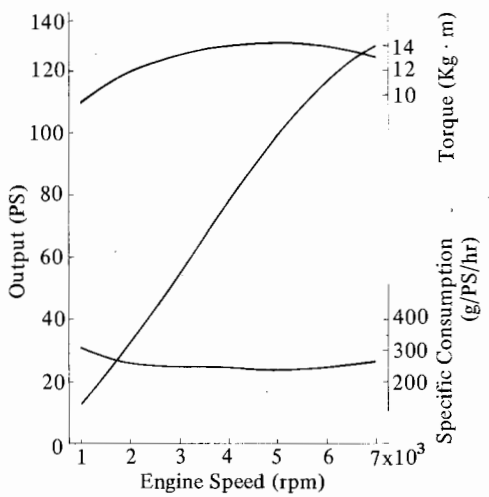
Model		NSU Model KKM502	NSU Model KKM612	Toyco Kogyo Model 0813	Toyco Kogyo Model 0820
Specifications					
Rotor arrangement		Single-rotor water-cooled	2-rotor water-cooled		
Displacement of single working chamber (cc)		497.5		491	
Compression ratio		8.6 : 1	9.0 : 1	9.4 : 1	
Maximum output (PS/rpm)		54/6 000	115/5 500	128/7 000	110/7 000
Maximum torque (kg.m/rpm)		7.9/3 500	16.2/4 500	14.2/5 000	13.5/3 500
Minimum specific consumption under full load (g/PS/hr)		230/3 300	225/3 000	235/5 000	230/4 000
Engine dimensions (length x width x height mm)			407 x 432 x 458	655 x 575 x 610	625 x 575 x 630
Total weight of engine (kg)		72.5	129	102	122
Trochoid	Generating Radius (mm)	100		101	
	Eccentricity (mm)	14		15	
	Equidistance (mm)	2		4	
	Axial width (mm)	67		60	
Arrangement of intake port		Peripheral port		Dual side ports, peripheral port	
Arrangement of exhaust port		Peripheral port			
Port timing	Intake open (deg.)	108 (B. T. D. C)		25 (A. T. D. C)	32 (A. T. D. C)
	Intake closed (deg.)	40 (A. B. D. C)		45 (A. B. D. C)	40 (A. B. D. C)
	Exhaust open (deg.)	63 (B. B. D. C)		75 (B. B. D. C)	
	Exhaust closed (deg.)	71 (A. T. D. C)		42 (A. T. D. C)	32 (A. T. D. C)
Port area (intake) (cm ²)		8	16	29	28
Port area (exhaust) (cm ²)		7	14	12	8
Carburetor		Side draft 2-stage solex type	Side draft 2-stage solex type (dual)	Down draft 2-stage Stromberg type 4-barrel	
Gas valve diameter (mm)		18 x 32		26 x 30	
Lubricating system		Full flow with a metering oil pump			
Viscosity of lubricating oil		SAE 10 W/30		SAE 10 W/30	
Method of cooling		Pressurized, circular flow		Pressurized, axial flow	
Ignition system		12 volt con- denser discharge system	2-spark plug, 12-volt battery coil system		



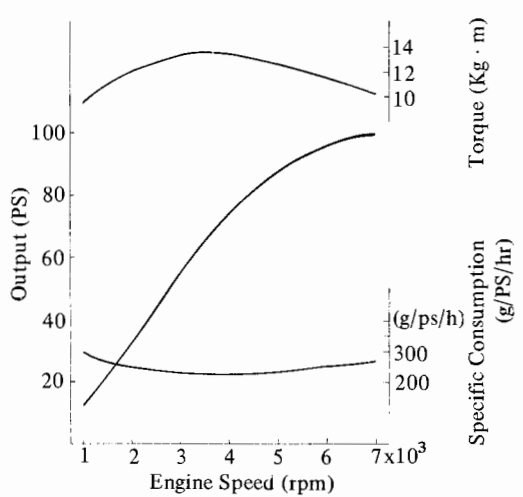
(a) NSU model KKM 502



(b) NSU model KKM 612



(c) Toyo Kogyo model 0813



(d) Toyo Kogyo model 0820

Fig. 12.12 Output characteristics under full load

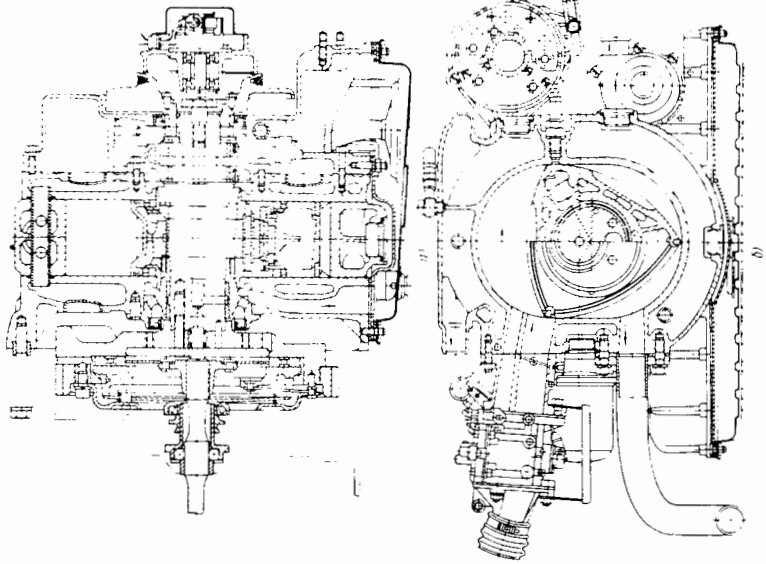


Fig. 12.13 Sectional drawing of NSU model KKM 502 single-rotor engine

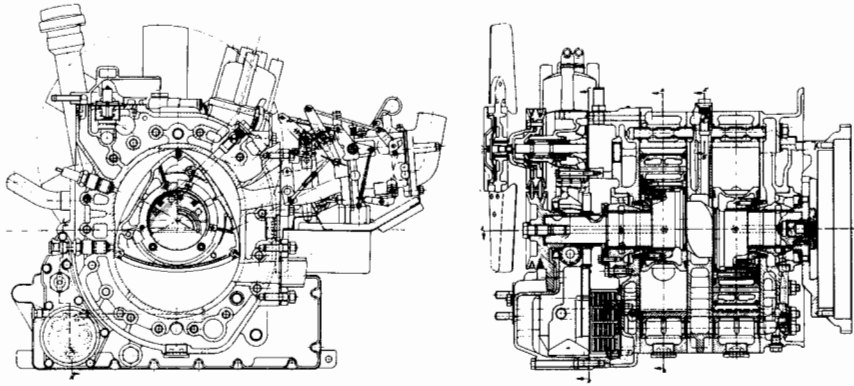


Fig. 12. 14 Sectional drawing of NSU model KKM 612 2-rotor engine

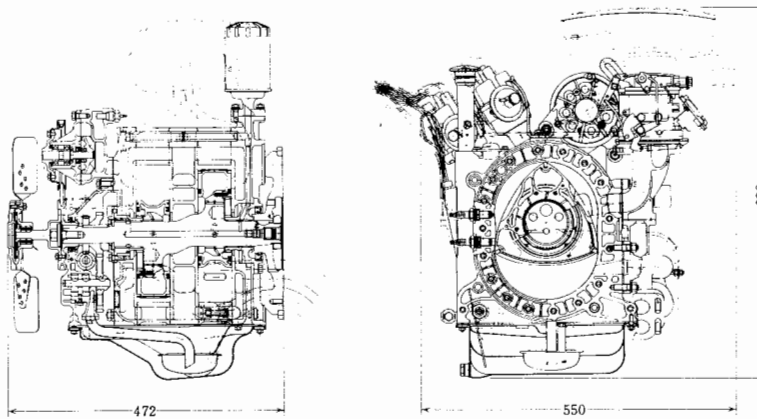


Fig. 12. 15 Sectional drawing of Toyo Kogyo model 0820 2-rotor engine

Table 12. 3 Specific output comparison of automotive engines

	2-rotor engine	V-8 gasoline engine (reciprocating)	2-rotor engine	In-line 4-cylinder gasoline engine (reciprocating)	In-line 6-cylinder gasoline engine (reciprocating)
Output (PS)	190	200	110	100	110
Weight of engine/output (kg/PS)	0.5	1.4	0.9	1.8	1.7
Engine length x width x height/output (cm ³ /PS)	70	215	122	288	327

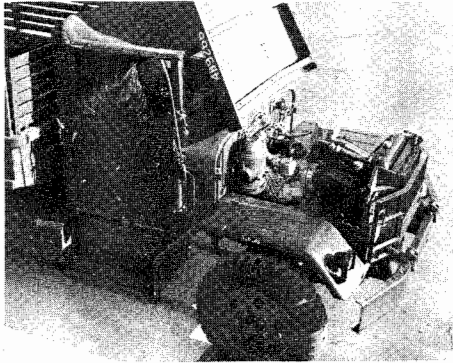


Fig. 12. 16 Experimental truck equipped with a 200 PS 2-rotor engine

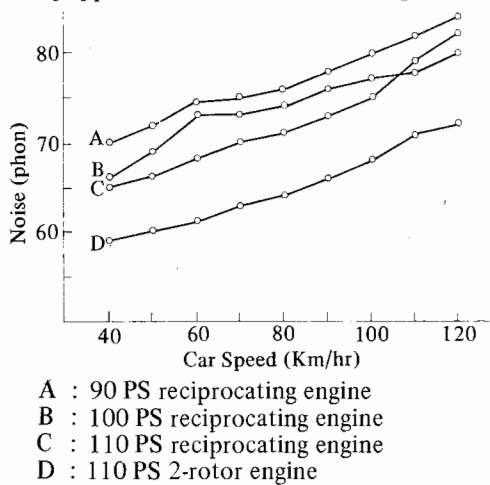


Fig. 12. 17 Comparison of interior noise levels (A-scale)

The use of rotary engines in cars has far-reaching impact, not only in improving performance because of high specific output but also by providing more flexibility for designing a larger passenger space and wider view for the driver, and because of its effect on the styling and construction of the body.

12. 3 Marine Engine

The use of the rotary engine for boats is drawing a lot of attention because a fuel saving of approximately 20% over the 2-cycle engine is anticipated and the noise level at high speeds is low.

In 1969 Yammar Diesel put on the market the world's first rotary outboard motor. This engine is water-cooled with the output shaft arranged perpendicularly, and uses a gasoline mixed with oil at the ratio of 100 : 1.

Fig. 12. 19 shows a rotary engine used for a water ski craft. The output shaft in vertical position, and the oil tank at the bottom of the engine, are exposed

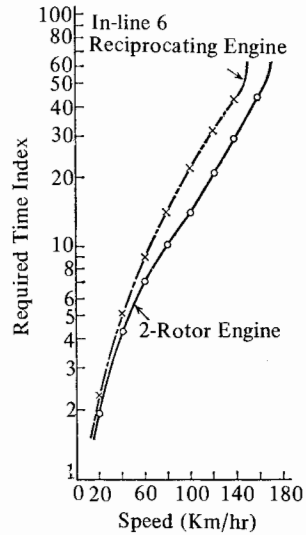
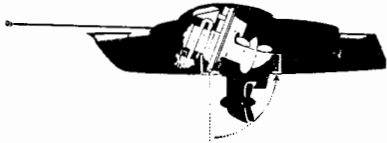
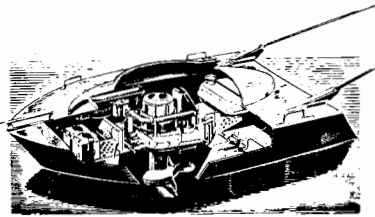
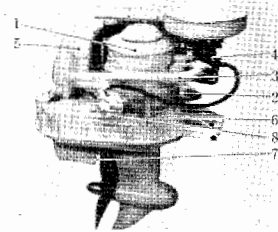


Fig. 12. 18 Full throttle acceleration performance



(a) Installation of a single-rotor engine



- | | |
|-------------------|------------------------|
| 1. Starter dynamo | 5. Exhaust muffler |
| 2. Engine casing | 6. Oil tank |
| 3. Intake tube | 7. Cooling water inlet |
| 4. Carburetor | 8. Fuel pump |

(b) Single-rotor engine (single working chamber displacement 150 cc)

Fig. 12. 19 Water ski craft

to the water serving as an oil cooler. The carburetor is located in the front toward the direction of travel. It is equipped with an extended intake tube, which is designed to utilize the pulsation effect. The maximum speed of this craft, shown in action in Fig. 12. 20, is reported to be 40 km/hr.

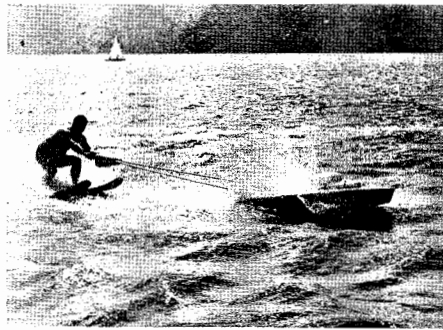


Fig. 12. 20 Water ski craft in action

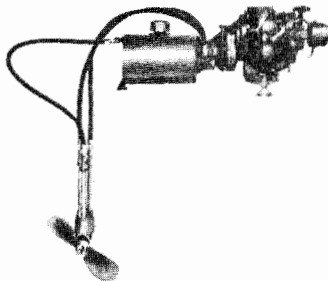


Fig. 12. 21 Combination of hydraulic drive system and single-rotor air-cooled engine



Fig. 12. 22 Combination of jet propulsion system with single-rotor air-cooled engine

Shown in Fig. 12. 21 is an example of an air-cooled 7 PS engine combined with hydraulic drive for use as an auxiliary engine for a sailboat. It provides a lot of flexibility for mounting.

Fig. 12. 22 shows a jet propulsion system equipped with a 10 PS air-cooled single-rotor engine.

Other examples of inboard applications are shown in Fig. 12. 23 where 115 PS water-cooled engines are installed in parallel, and Fig. 12. 24 where a 200 PS water-cooled engine is used. Fig. 12. 25 shows one of these boats in action.

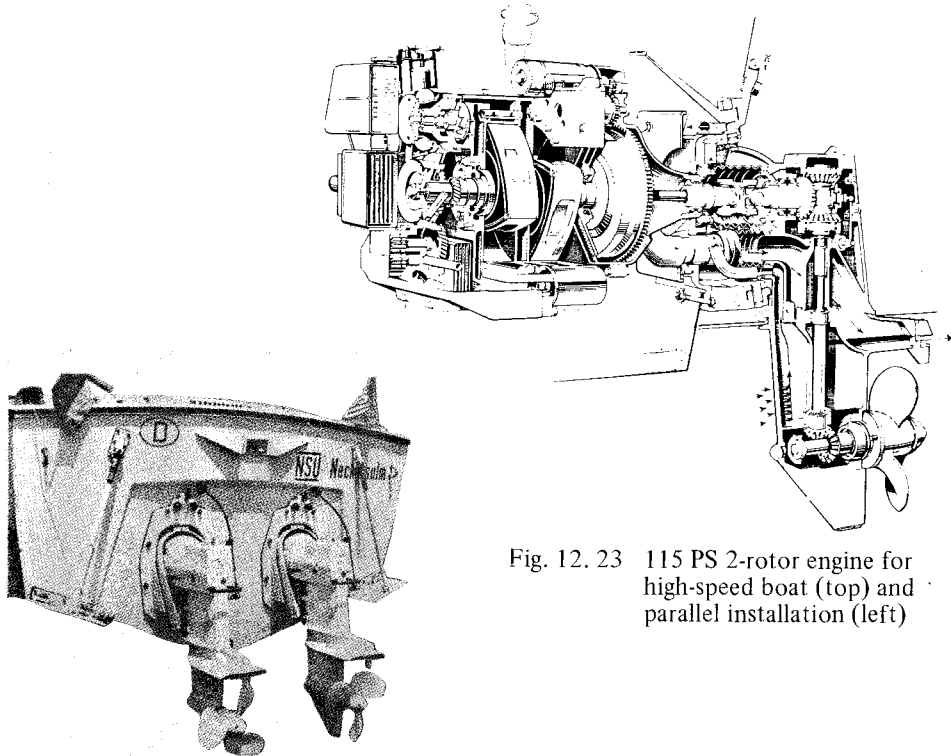


Fig. 12. 23 115 PS 2-rotor engine for high-speed boat (top) and parallel installation (left)

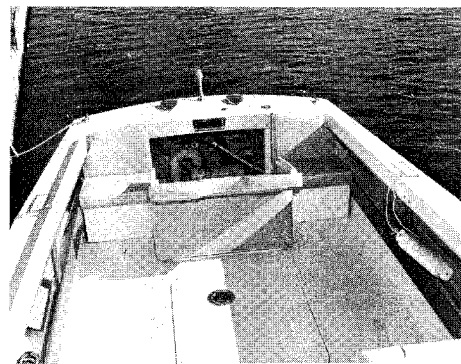
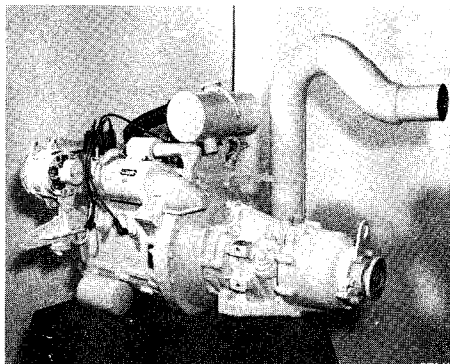


Fig. 12. 24 Installation of 200 PS 2-rotor engine



Fig. 12. 25 High-speed boat with rotary engine in action

12. 4 Aircraft Engine

In view of the rotary engine's features of light weight, compactness and smoothness with fuel consumption and initial cost being comparable to reciprocating engines, study is being made to use it as a light aircraft powerplant.

Reference Materials

- 1) Max Bentele : Curtiss-Wrights Entwicklungen an Rotationsverbrennungs-motoren. MTZ, 22/6 (1961).
- 2) O. Herterich : Magirus-Tragkraftspritze mit NSU-Wankelmotor. MTZ 24/4 (1963).
- 3) Charles Jones : The Curtiss-Wright Rotating Combustion Engines Today. SAE Paper 886D (1964).
- 4) Helmut Keller : Ein luftgekühlter Wankelmotor. MTZ, 26/4 (1965).
- 5) Charles Jones : New Rotating Combustion Powerplant Development. SAE Paper 650723 (1965).
- 6) Walter Froede : The Rotary Engine of the NSU Spider. SAE Paper 650722 (1965).
- 7) R. F. Ansdale : Wankel Progress. Autocar, 1 July (1966).
- 8) Charles Jones : The Rotating Combustion Engine Compact, Lightweight Power for Aircraft. SAE Paper 670194 (1966).
- 9) H. Brockhaus, R. M. Strobel : Ro 80 ein neuer NSU Mittelklasse Wagen mit Kreiskolbenmotor. ATZ, September (1967).
- 10) NSU Ro 80. Autocar, 1 February (1968).
- 11) Kenichi Yamamoto : Model 10A Engine for Mazda Familia Rotary Coupe, Internal Combustion Engine, Volume 7, No. 75, (1968).
- 12) Familia Rotary Coupe, Motor Fan, Volume 22, No. 10 (1968)
- 13) F. J. Bomhard : Zur Entwicklung Luftgekühlter Kreiskolbenmotoren Kleiner Leistung. MTZ, 29/8 (1968).
- 14) Helmut Keller : Small Wankel Engines. SAE Paper 680572 (1968).

13. EXHAUST EMISSION OF ROTARY ENGINES

The major air-polluting materials emitted from gasoline engines are carbon monoxides (CO), oxides of nitrogen ($\text{NO}_x = \text{NO} + \text{NO}_2$), hydrocarbons (HC), lead compounds and other particulates. Rotary engine emits the same concentration of CO, a higher concentration of HC, and a lower concentration of NO_x than reciprocating engines.

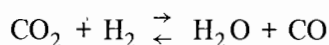
13.1 Factors Affecting Emissions

In this study, the concentration of each exhaust component is determined by a non-dispersive infrared analyzer, and HC is measured as normal hexane ($n - \text{C}_6\text{H}_{14}$).

(1) Air-fuel ratio

CO ;

Formation of CO can be generally explained by the reaction formula of H_2O gas :



When the air/fuel ratio (A/F) of the mixture is higher than the stoichiometric air/fuel ratio, the four kinds of gases, CO_2 , H_2 , H_2O and CO, are in the above equilibrium condition due to the inadequate supply of oxygen.

In this equilibrium condition, when temperature rises the reaction proceeds to the right side ; when temperature drops, it proceeds to the left side.

Fig. 13. 1 shows an example of CO percentage plotted against air/fuel ratio.

Around the stoichiometric air/fuel ratio of 14.75 : 1, CO level is slightly higher than the theoretical value. This shows that the mixture is not homogeneous in the combustion chamber, apparently causing incomplete utilization of excess oxygen in an extremely lean part of the mixture.

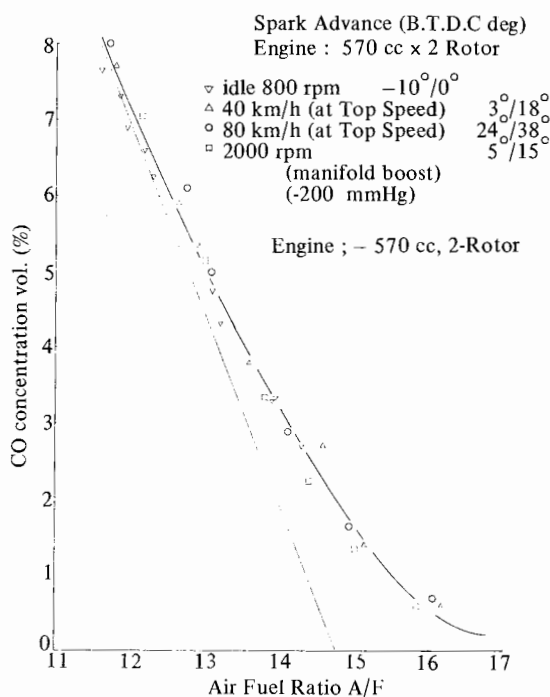


Fig. 13. 1 Characteristics of CO emission by U. S. A. regular gasoline

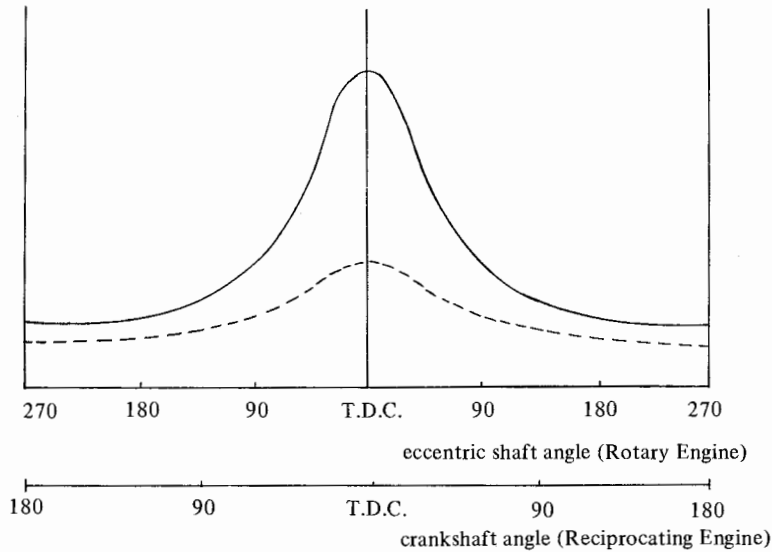


Fig. 13. 2 Surface/volume of reciprocating engine and rotary engine

HC ;

Generally the most important factor in emission of HC is the quenching of the combustion flame at some part of the combustion chamber. It is clear that the surface/volume ratio (S/V ratio) of the rotary engine is far higher than that of the reciprocating engine, as shown in Fig. 13. 2, due to the shape of the combustion chamber. In the trailing side of the combustion chamber, especially, the S/V ratio becomes locally very high and the mixture flows from the trailing side to the leading side in a very rapid flow when the rotor passes the top dead center.

This may not permit the combustion flame to reach the trailing corner, which might be partially responsible for the high concentration of unburned HC in this portion. This unburned HC will be exhausted into the atmosphere through the exhaust port around the apex and side seals. This means that HC is emitted mainly toward the end of the exhaust stroke. Fig. 13.3 shows an example of an experiment to prove this fact.

This experiment was performed by providing a sampling valve in the exhaust port to sample the HC concentration for each position of the rotor. It shows that the highest concentration of HC is emitted around the top dead center of the exhaust stroke.

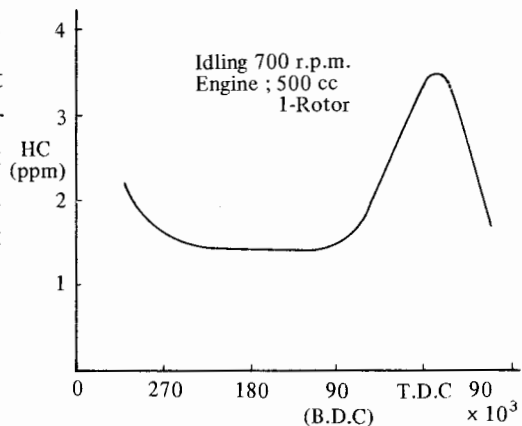


Fig. 13. 3 Shaft degree and HC concentration

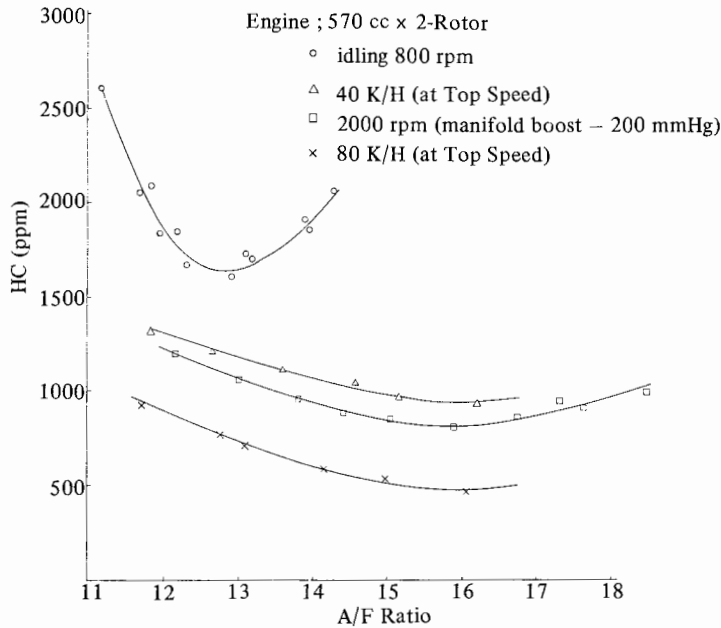


Fig. 13.4 Characteristics of HC emission

A study on the characteristics of HC concentration vs A/F ratio shows that there is an A/F point where HC level is minimum, and when the mixture is richer or leaner, HC level becomes higher. The reason for the increase of HC on the richer side seems to be that the combustion of the gas mixture is obstructed due to lack of oxygen, thus causing increase of uncombusted portion. On the leaner side it is due to the increase of misfiring.

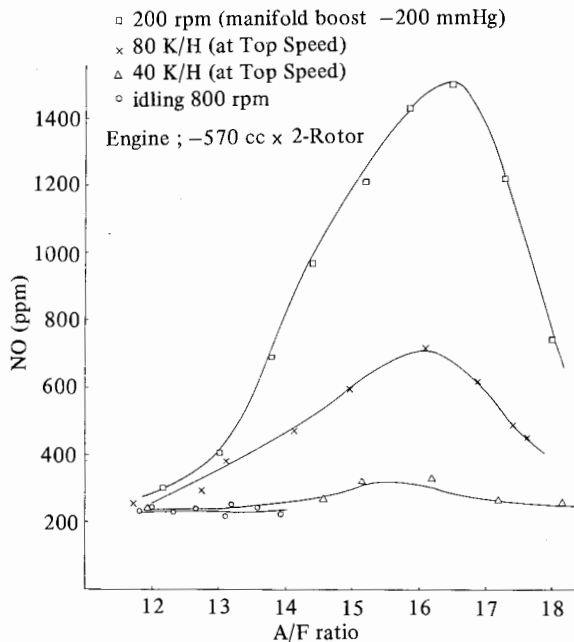


Fig. 13.5 Characteristics of NO emission

NO_x ;

According to reports by K \ddot{u} hl and others, the generating mechanism of NO is known to be controlled by the maximum temperature of the combustion gas and the concentration of residual oxygen in the combustion gas. As noted from Fig. 13.5, NO level is largely affected by the A/F ratio, showing a maximum value around A/F \doteq 16 to 17.

(2) Ignition timing
CO ;

As shown in Fig. 13. 6, CO content is almost unaffected by ignition timing. However, there is an indirect effect of ignition timing because, as mentioned in next item, the decrease of HC concentration by retarding ignition timing means a higher fuel utilization rate, which in turn may increase CO within the limit of λ (excess air coefficient) < 1 . In actual practice, however, CO formation is small enough to be considered negligible. For example, 1000 ppm decrease of HC will correspond to 0.06% increase of CO.

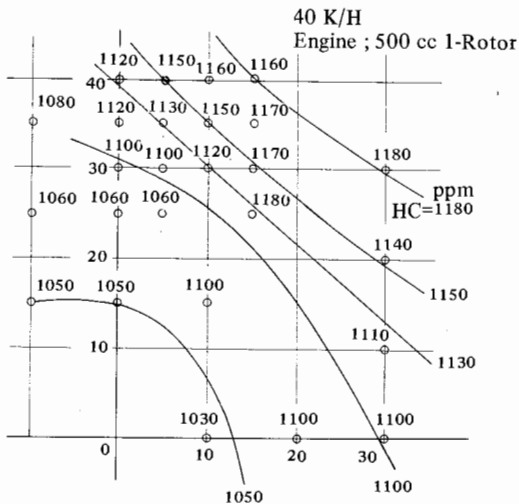


Fig. 13. 7 Effect of ignition timing on HC content

Fig. 13. 8 shows a comparison of two-spark plug ignition and leading plug ignition only.

The reason for this decrease in HC level seems to be that if ignition is provided by the leading plug only, the unburned mixture in the trailing corner increases and as the S/V ratio in the trailing corner becomes comparatively low when the rotor comes to the position shown by the dotted line in Fig. 13. 9, the unburned HC is thereby sufficiently "after-burned".

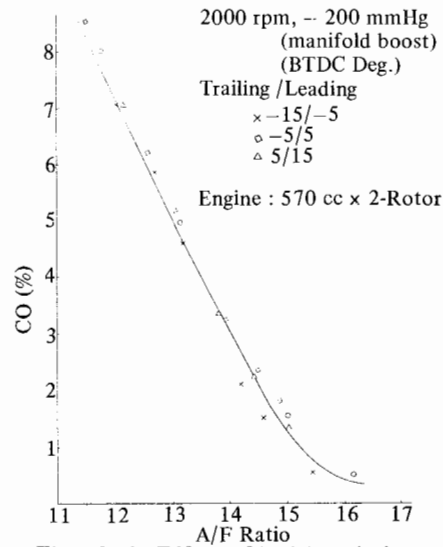


Fig. 13. 6 Effect of ignition timing on CO content

HC ;

HC content is generally liable to be affected by variation in ignition timing. As shown in Fig. 13. 7, HC level shows clear evidence of being affected by both leading and trailing ignition timings. Especially notable is the fact that the HC level can be lowered by retarding the trailing timing to such an extreme extent as causing ignition to take place almost entirely at the leading side or by having ignition at the leading side only, with the trailing spark plug disconnected.

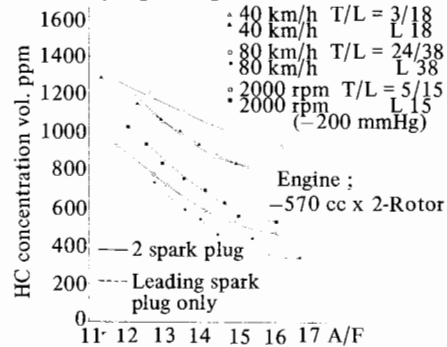


Fig. 13. 8 Effects of L only ignition system on HC emission by U.S. regular gasoline

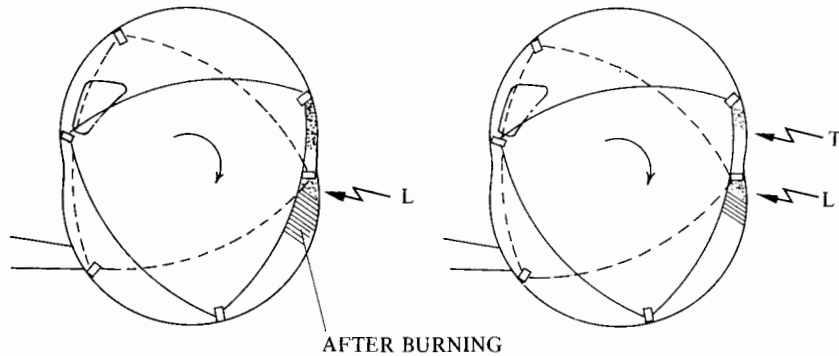


Fig. 13.9 Position of spark plug and "after-burning"

On the other hand, if normal ignition is provided on the trailing side, flame propagation will be improved and will result in a smaller amount of unburned gas. Under these conditions, even when the rotor comes to the position shown by the dotted line, with the S/V ratio favorably reduced for "after-burning". Unburned HC sticking to the wall will be emitted, because oxygen and heat are insufficient to effect after-burning.

NO_x ;

NO_x concentration generally will increase as ignition timing is advanced, but this effect becomes very small under light load, as shown in Fig. 13. 10. On the contrary, when load is heavy, noticeable effect of ignition timing is seen especially on the lean mixture side.

(3) Effect of load and engine speed
HC and CO ;

Study of constant-concentration curves revealed the results shown in Figs. 13. 11 and 13. 12. Very marked effects of engine speed on HC concentration are shown, but the load has relatively little effect on HC.

In general, HC concentration decreases rapidly as the engine speed increases, but in the very light load region high level of HC is maintained even at high engine speeds. There are several possible reasons for this peculiar phenomenon : 1) increase in misfiring due to excessive dilution by exhaust gas, 2) fuel in the gas mixture cannot reach the leading side of the combustion chamber due to the effect of its

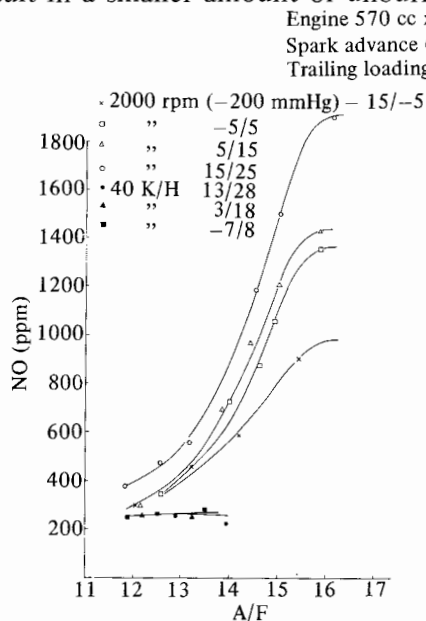


Fig. 13. 10 Effect of ignition timing on NO_x concentration

inertia, resulting in an extremely high A/F ratio in this portion, which in turn leads to misfiring.

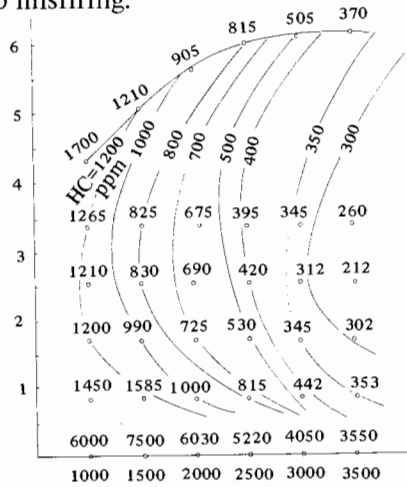


Fig. 13. 11 Constant-concentration curves of HC

NO ;

As shown in Fig. 13. 13, load has a marked effect on NO concentration especially in the region of high A/F ratio, namely the region of richer oxygen. Reasons considered for this are : 1) combustion pressure increases as a result of higher intake pressure, which results in higher maximum combustion temperature. 2) when the intake pressure is low, there is an increase in the dilution rate by exhaust gas carried over through clearance volume, and further increase is brought about through the intake-exhaust overlapping.

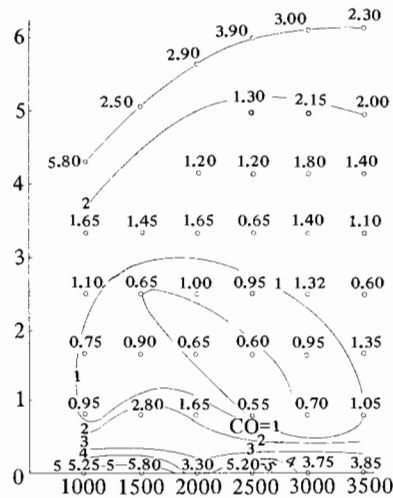


Fig. 13. 12 Constant-concentration curves of CO

(4) Shape of combustion chamber

It is obvious that the quenching effect due to S/V ratio, which is one of the basic controlling conditions of HC concentration, is dependent upon the shape of the combustion chamber. Therefore an investigation was attempted of the relation of the shape of the combustion chamber to HC level. Three kinds of rotor profiles (Fig. 13. 14) were chosen for this purpose, with special attention focussed on the locations of recesses.

The three types were compared with ignition timing for each type chosen at maximum performance points, and under various air/fuel ratios, to obtain the results shown in Fig. 13. 15.

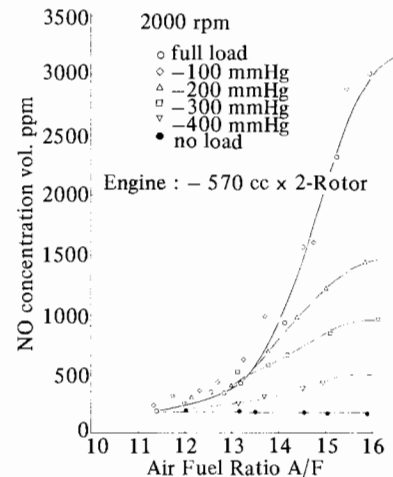


Fig. 13. 13 Influence of boost pressure on NO emission

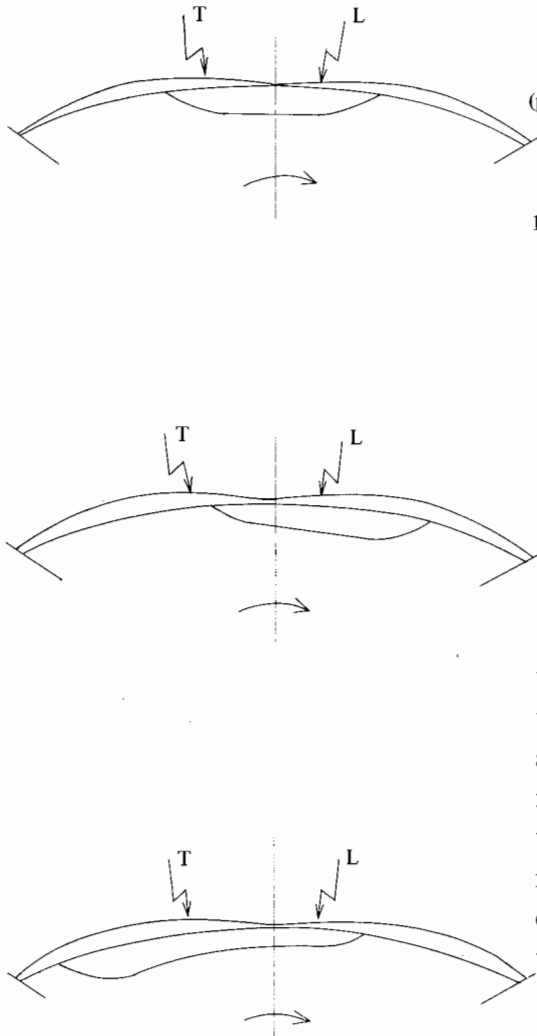


Fig. 13. 14 Rotor profiles

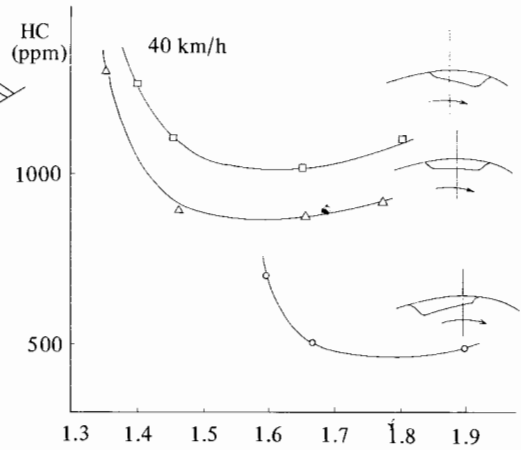


Fig. 13. 15 Rotor profiles and HC concentration

It is evident from this result that the combustion recess positioned toward the trailing side has a smaller S/V ratio at the trailing portion and tends to be more effective in reducing the HC level there, and the HC level tends to increase in accordance with the change of the combustion recess from the trailing side to the leading side.

13.2 Secondary Air Injection System

Concentration of CO and HC emitted from the engine may be further reduced by means of oxidation reaction in a thermal reactor provided in the exhaust system with so-called secondary air blown in by an air pump. This system is called the "Air Injection with Reactor (A. I. R.) system". The fundamental concept of this A. I. R. system is to make the exhaust gas react with the secondary air under the condition of the rich mixture, thus reducing the HC and CO levels. Fig. 13. 16 shows reduction of the HC level.

Calculation of the amount of secondary air :

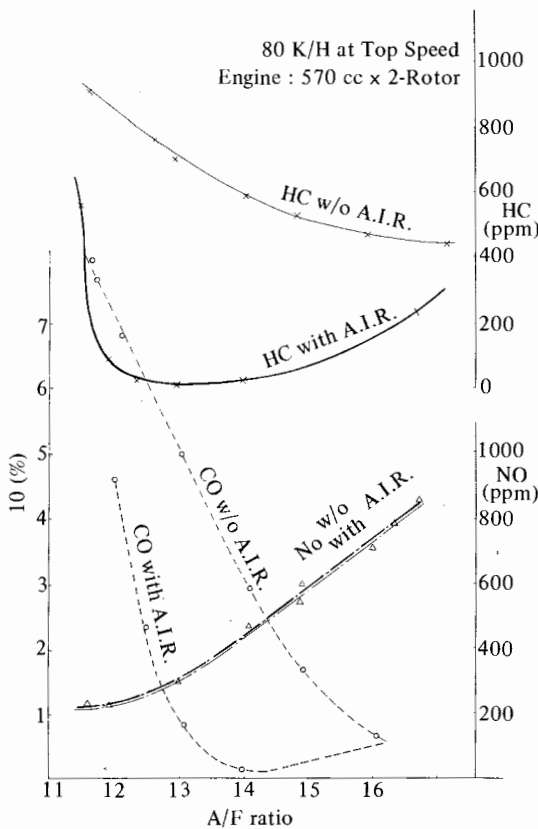
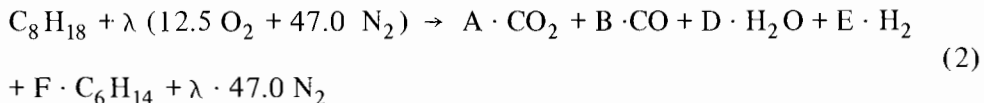


Fig. 13. 16 Effect of A. I. R. system

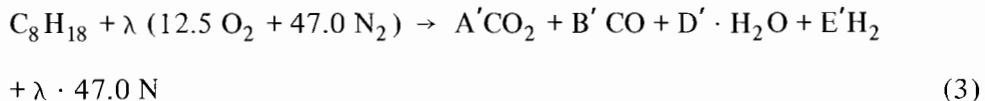


where : C_8H_{18} = average composition of gasoline

λ = excess air coefficient

C_6H_{14} = average composition of unburned gas (hexane)

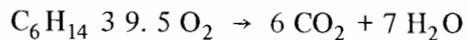
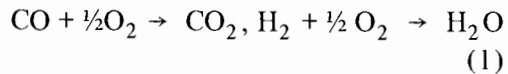
Now when we consider complete oxidation of C_6H_{14} in (2) above :



Assuming the volume of exhaust gas generated by formula (2) to be V and the volumetric percentage of C_6H_{14} in exhaust gas to be y , the absolute volume of C_6H_{14} in the exhaust will become

$$v \times \frac{y}{100}$$

Let us obtain the amount of secondary air necessary for oxidizing unburned gas in the thermal reactor. The amount of oxygen necessary for oxidation of CO , H_2 and C_6H_{14} (hexane), which are generally involved in oxidation, can be obtained from the following reaction formulas :



and amount of air for each reaction can be derived from the above.

Volumetric concentration of CO , H_2 and C_6H_{14} in exhaust gas can be determined by actual measurements.

However, to obtain their absolute amounts, the total amount of exhaust gas must be obtained.

To calculate the amount of exhaust gas :

Firstly, combustion of gasoline in an engine can be explained as

According to formula (3), C_6H_{14} is converted to gases such as CO, CO_2 , H_2O , H_2 , etc. in the following manner :



where : $a + b = 6$, $d + e = 7$ or $a + b + d + e = 13$

(a, b, c, d, m are constants)

Therefore, C_6H_{14} of $V \cdot \frac{y}{100}$ is converted into mixed gas of $13 : V : \frac{y}{100}$. Then, the volume of exhaust gas in formula (3) becomes :

$$V - V \frac{y}{100} + 13 V \frac{y}{100} = V \left(1 + \frac{12}{100} y \right) \quad (5)$$

On the other hand, as the following relations

$$A' + B' = 8 \text{ and } D' + E' = 9$$

are established by formula (3), $(17 + 47 \lambda)$ mole of exhaust gas is generated when 1 mole of C_8H_{18} burns.

Therefore, combining the above with formula (5), we obtain :

$$17 + 47 \lambda = V \left(1 + \frac{12}{100} y \right)$$

$$\therefore V = \frac{17 + 47 \lambda}{1 + 0.12 y} \quad (6)$$

As a result of the above calculation from formula (2), $\left(\frac{17 - 47 \lambda}{1 - 0.12 y} \right)$ mole of exhaust gas is generated from 1 mole of C_8H_{18} . Fig. 13. 17 shows an example of the volume of secondary air obtained by the above calculation based on actual concentration of CO, H_2 , C_6H_{14} , etc.

Thermal reactor :

A thermal reactor generally requires ability to purify CO and HC and durability.

To improve purifying capability, the following conditions must be satisfied :

- (1) Sufficiently long resident time of exhaust gas in the reactor.
- (2) Sufficient heat insulation to maintain high internal temperature.
- (3) Adequate mixing of the secondary air and exhaust gas.

Resident time is a function of both volume and exhaust gas flow path arrangement in the reactor. The effect of volume was first investigated. In experiments with

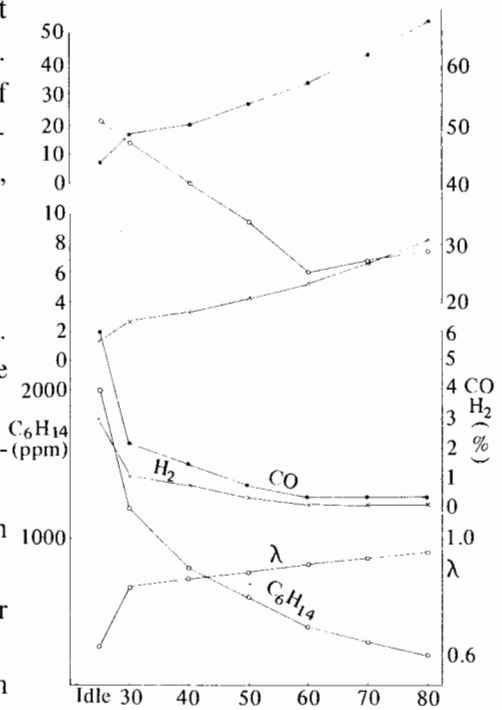


Fig. 13. 17 Theoretical secondary air volume

three reactors of different volumes, warm-up characteristics showed considerable improvement with increase of volume, as indicated in Fig. 13. 18.

This is due to the effective action of both reduced space velocity (h^{-1}) of gas flow due to increased volume, and improvement in warming-up performance, which is related to reduction of S/V ratio.

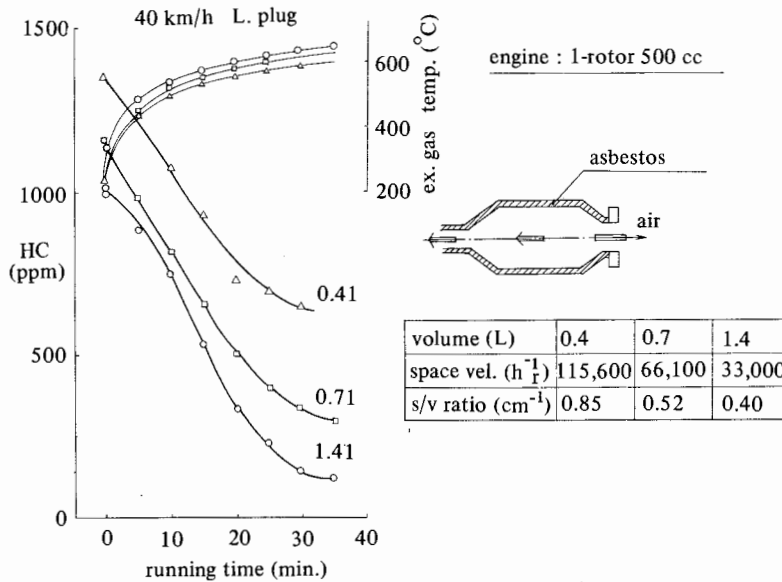


Fig. 13. 18 Effect of reactor volume

Next, experiments were conducted with two types of reactors, one with a single shell and the other with double shell as shown in Fig. 13. 19, and single shell, double shell, and no reactor results were compared.

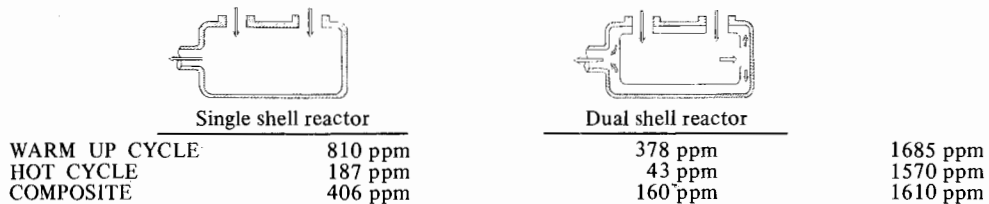


Fig. 13. 19 Reactor structure and HC purifying efficiency

The test results showed a considerable difference between the two types, as shown in the illustration. The values were determined in accordance with the test method described in U. S. Emission Control Test Mode - F. T. P. (Federal Test Procedure in U. S. A.).

This difference is considered due not only to the increase of resident time owing to the return passage of gas, but

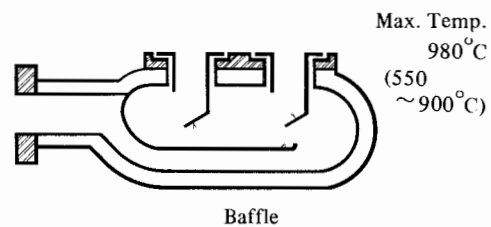


Fig. 13. 20 Schematic illustration of thermal reactor

also to an improvement of the heat-keeping effect on the inner chamber, and improvement of the mixing between the secondary air and exhaust gas by mixed gas flow reflexion.

To conclude, it may be said that more than ninety percent of the unburned gas in the exhaust can be purified in a thermal reactor. Fig. 13. 20 shows an example of the basic thermal reactor construction.

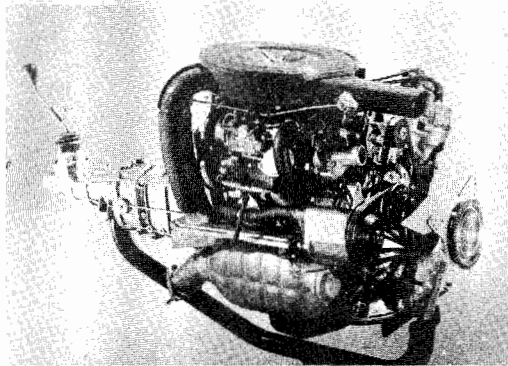


Fig. 13. 21 shows an example of a rotary engine equipped with the A. I. R. system.

